2015

Three essays on crop yield, crop insurance and climate change

Lisha Li
Iowa State University

Three essays on crop yield, crop insurance and climate change

by

Lisha Li

A dissertation submitted to the graduate faculty

in partial fulfillment of the requirements for the degree of

DOCTOR OF PHILOSOPHY

Major: Economics

Program of Study Committee:
Dermot Hayes, Co-Major Professor
Chad Hart, Co-Major Professor
Christopher Anderson
Bruce Babcock
Cindy Yu

Iowa State University

Ames, Iowa

2015

TABLE OF CONTENTS

Page

Page

LIST OF FIGURES

Page

Page

LIST OF TABLES

Page

ACKNOWLEDGEMENTS

I would like to take this opportunity to express the deepest gratitude to my advisors Dr. Dermot Hayes and Dr. Chad Hart, for their excellent guidance and unlimited supply of time and patience throughout the course of this research. Their insights and words of encouragement always inspired me to complete my research. I would never have been able to finish my dissertation without their guidance.

I would like to thank my committee members Dr. Christopher Anderson, Dr. Bruce Babcock and Dr. Cindy Yu, for their constructive comments to the dissertation and making themselves available every time I needed their help and advice.

I would also like to thank my friend Dr. Yongjie Ji for his invaluable suggestions to the dissertation. I have been benefited a lot from the discussion with him about the dissertation. I would like to thank the faculty and staff of the Center for Agricultural and Rural Development and Economics Department for the help I received during my graduate education.

Finally, I would like to give my special thanks to my family for their encouragement, understanding and love.

ABSTRACT

The main subject of this dissertation includes the study of the impact of weather on crop yields and developing crop revenue insurance product. The dissertation limits its analysis to the state of Iowa because it's a critical corn production area in the United States. Chapter 2 introduced a dynamic linear model to measure weather-adjusted trends in Iowa corn yields. The weather factors consist of the amount of rainfall, temperature and a measurement of soil moisture. Results show a significant improved yield growth in the 1990s, controlling for the impact of weather. Results also indicate that the critical temperature varies across the state of Iowa. The critical temperature is higher in the areas of the state with higher soil quality and is most suitable to grow corn. Chapter 3 develops a long-term corn revenue insurance product that provides crop growers with yield or revenue protection for as long as five years into the future. The premium rates are calculated at both county and farm level. Chapter 4 estimates the impact of projected climate change on Iowa corn yield. The climate projection indicates a significant increase in the daily maximum temperature in July, whereas a significant increment trend is not found in the amount of rainfall during June to August. Controlling for the uncertainty in yield projection, results indicate that projected climate change will cause a statewide reduction of corn yield by 10% at the end of this century. Controlling for uncertainty in climate projection and allowing for uncertainty in yield projections, results show that projected climate change reduces Iowa corn yield by 9%.

CHAPTER 1. OVERVIEW

Both the 4th and 5th Intergovernmental Panel on Climate Change (IPCC) reports find evidence that the global average near-surface temperatures have increased since the nineteenth century. These studies also suggest a warmer environment in the future. Agriculture sector critically depends on weather factors such as temperature, the amount of rainfall and drought. Corn is the major feed grain in the United States and around half of the corn production has been used as feedstock to ethanol production since the biofuel boom in last decade. As the world's largest corn producer and exporter, the United States exports around fifteen percent of annual corn production. If future climate change causes damages to corn production, the resulting cost to society will be significant. Since the state of Iowa is the major corn produce area in the United States, we limit our analysis to this area.

This dissertation provides a methodology to estimate the impact of weather on corn yields and projects the impact of climate change on corn yield as well. Introducing weather variability, this dissertation also develops a long-term crop yield and revenue insurance products at both county and farm level.

The rest of this dissertation is organized as follows. Chapter 2 introduced the dynamic linear model and estimated the impact of weather factors on corn yield. The weather factors include temperature, amount of rainfall and drought. Results show that the critical temperature varies across the state, with a range of 88oF to 95oF. The district with the better soil quality has a higher critical temperature. This result suggests that the producers will have the opportunity to adjust genetics and management to offset the impact of higher

temperatures. In addition, a faster growth rate is found around mid-1990s, which is consistent with the genetic improvement.

Chapter 3 develops a long-term crop yield and revenue insurance products at both county and farm level. The long-term futures pricing model in Jin et al. (2012) is applied to compute long-term corn futures prices. We also take the weather variability into consideration and calculate the premium rates at difference coverage level.

Chapter 4 estimated the impact of climate change on Iowa corn yield. The climate projection of daily maximum temperature shows a significant increase trend. The result also indicates that the 70-year linear trend in the July daily maximum temperature during 2030 to 2099 will be almost twice as high as the 70-year linear trend during 1960 to 2029. The climate projection also suggests that the amount of rainfall in June to August will be relatively unchanged. The uncertainty of the impact of climate change may come from the uncertainty in climate projection or yield projection models. Controlling for the uncertainty in yield projection, results indicate that projected climate change will cause a reduction of corn yield by 1%–35% and with a statewide reduction of corn yield by 10% at the end of this century. Controlling for uncertainty in climate projection and allowing for uncertainty in yield projections, results show that projected climate change reduces Iowa corn yield by 9%.

CHAPTER 2. WEATHER ADJUSTED TRENDS IN IOWA CORN YIELDS

Abstract

A Bayesian dynamic linear model is used to measure weather-adjusted trends in Iowa corn yields. Estimation is done via a Bayesian Markov Chain Monte Carlo method that allows for stochastic and time-varying yield change. Explanatory variables and functional forms are chosen based on statistical significance and best-fit criteria and include critical temperature and rainfall as well as the moisture content of the soil during the growing season . Results indicate that weather events such as drought, flood and extreme heat cause considerable damage to corn yields. The results show that the critical temperature varies across the state of Iowa and is higher in areas of the state where soils are most suitable to corn. When averaged over the entire state, yields growth, measured in bushels per year, improved in the 1990s.

2.1 Introduction

In a 2009 paper, Schlenker and Roberts present results showing a steep non-linear decline in county-level corn yields at temperatures above 84°F. Results for soybeans and cotton suggest critical temperatures of 86°F and 90°F. They then use this temperature sensitivity and results from climate models to project area weighted reductions in US corn, soybean and cotton yields of 30–46% under the model with the slowest climate warming scenario and 63–82% under the model with the most rapid climate warming scenario.

Schlenker and Roberts show that the sensitivity of yields to high temperatures is robust across time and across crop growing areas of the United States. The similarity of the cross-sectional results to the time series results is used to conclude that farmers cannot adopt seed varieties or management practices to avoid this heat sensitivity. Schlenker and Roberts also show that the heat sensitivity result is robust with respect to three different functional forms of the yield-temperature relationship. In separate bilateral or trilateral tests, they also show that the key result is robust with respect to latitude, longitude, time period, the use of July versus a season average temperature, and year-fixed effects.

The discovery of a critical temperature for corn that is slightly below the average daytime temperature in Iowa in July, as well as results showing that this critical temperature is robust with respect to location, functional form, and the use of a July, rather than a season-wide average temperature, would appear to suggest that Iowa is not well suited to corn production. This result is not claimed or supported by Schlenker and Roberts because they perform their robustness tests one at a time. They do not perform tests allowing the longitude and latitude and other relevant variables to change at the same time as would be needed to claim that the results were robust for a particular state. One of the key purposes of this paper is to perform this test for Iowa. We use the same cross-sectional, time series county-level data as Schlenker and Roberts and a non-linear estimation technique to determine the critical temperature effect for all of Iowa's ninety nine counties.

Our results support Schlenker and Roberts finding of a non-linear temperature response with steep declines above a critical temperature, but the results show that this critical temperature is much higher than 84°F. In contrast to Schlenker and Roberts, our results show that this critical temperature changes across the state with higher critical temperatures

occurring in the areas with the greatest reported suitability for corn production. This cross-sectional variability suggests that producers will in fact have the opportunity to adjust genetics and management to offset the impact of higher temperatures.

Schlenker and Roberts use a 2.5 mile by 2.5 mile grid to measure weather data. We did not have access to this data and use country level data instead. This may explain differences in our results. But given the relatively flat topography of most Iowa counties and the homogeneity of management practices, temperature, and rainfall within counties, this does not seem likely to be a major factor.

A second motivation for our paper is that there is some uncertainty about whether corn yield growth is increasing, stable or decreasing. Menz and Pardey (1983) find corn yield trend had a slower increase rate during the 1970s than the previous two decades. Tannura, Irwin, and Scott (2008) cite a number of crop experts and seed companies who believe that improved technology, particularity biotechnology, has increased the rate of yield growth in corn.[1] Others have argued that climate change has slowed or even reversed the rate of yield growth (World Bank 2013).

We chose Iowa because it is an important corn producing area and because it has excellent long-term yield and weather data. We chose corn because of its economic importance and also because several biotechnological advances have been introduced into this crop. Our results indicate that there is some support for a higher statewide yield growth measured in bushels per acre in recent years. One exception to this trend is the southeastern part of the state where yield growth appears to be slowing.

---

[1] The authors show that once one adjusts for weather patterns much of the increase in yield growth disappears.

2.1.1 Previous Work

Moss and Shonkwiler (1993) use a stochastic trend model to estimate the central tendency of corn yield and find the assumption of normality is inappropriate. They use a hyperbolic sine transformation of normality for corn yield residuals and find a stochastic yield trend. Goodwin and Ker (1998) apply a nonparametric kernel density to estimate corn yield density. They use an ARIMA process to detrend corn yields, and then use the nonparametric kernel smoother to estimate the deviations of corn yields from their trends. Ardian, Harri, and Knight (2009) conclude that the rejection rate of normality depends on the selected yield trend methods, but they also find most of the counties located in the Corn Belt are more likely to be non-normally distributed and negatively skewed. These papers do not control for the effect of weather on the yield distribution.

Foote and Bean (1951) were the first to suggest that crop yield distributions should depend on weather. Kaylen and Koroma (1991) focus on temperature and rainfall during May to August using data from 1895 to 1988, and include sixteen weather variables. However, only three of the weather variables were found to be significant at the 10% level. Lobell and Asner (2003) regress corn yield trend on the observed trend in temperature and suggested that corn yield decreases by roughly 17% for each one-degree increment in temperature during the growing period. Deschênes and Greenstone (2007) also find that corn yield decreases in temperature and increases in rainfall.

As mentioned in the introduction, Schlenker and Roberts (2009) conclude that temperature has a nonlinear effect on corn yield. Corn yield increases with temperature for moderate temperatures, while temperature becomes seriously harmful when it exceeds 84°F.

Schlenker and Roberts derived the length of time each crop is exposed to each one-degree Celsius temperature interval in each day, and summed across all days of the growing season in each county. They used this data to estimate the distribution of time each crop was exposed to each one-degree Celsius interval during the growing season. They used three different functional forms to represent the heat impact: (*a*) a step function with a different growth rate in each 3°C temperature interval; (*b*) an eighth-order Chebychev polynomial; and (*c*) a piecewise linear function. All three functional forms produced similar results: corn yields increase with temperature modestly up to 84°F, and then decrease sharply. Schlenker and Roberts use a non-stochastic quadratic form for the yield trend, and although they included rainfall as an explanatory variable, they did not take the impact of drought or a drought temperature interaction into consideration. Their model assumes that the temperature effect on corn yield is additive and that corn yield is proportional to total exposure.

Yu and Babcock (2011) use a two-knot linear spline model and found that yield is concave in both temperature and rainfall. They used the county-level monthly mean temperature and rainfall from June to August as explanatory variables. Their results suggest corn yield in the state of Iowa decreases with temperatures below 72.9°F, and then decreases at a faster rate with temperatures up to 75.6°F and again for temperatures above 75.6°F. Corn yield increases when rainfall is below 3.49 inches, while it decreases sharply when rainfall is above 6.11 inches.

Elmore and Taylor (2011) discuss the agronomic reasons that link high temperatures to reduced yield. They state that very high temperatures have two impacts on corn yields: First, high temperatures induce leaf rolling and this reduces corn yields because it slows plant

development. Second, they indicate that four or more consecutive days with a maximum temperature that exceeds 93°F reduces corn yield over and above the loss computed from leaf rolling.

2.2 The Corn Yield Model

Our model considers three key weather factors: rainfall, temperature, a variable that measures the stock of accumulated rain, and interaction terms among these variables. To measure the stock of water we use the Palmer Drought Severity Index (PDSI). This is a long-term cumulative measure of water availability in the soil. The PDSI is negative if the soil is dry and positive when there is surplus water. It can therefore be used to measure both the positive and negative impacts of the quantity of water in the soil. We specify that yield follows a dynamic linear model as follows:

$$\ln y_t = \theta_t + \psi_1 d_t^2 + \psi_2 n_t^2 + \psi_3 {z_{Jun}}_t^2 + \psi_4 {z_{Jun}}_t + \psi_5 {z_{Jul}}_t^2 + \psi_6 {z_{Jul}}_t + \psi_7 {z_{Aug}}_t^2 + \psi_8 {z_{Aug}}_t + \varepsilon_t \quad (2.1)$$

$$\theta_t = \theta_{t-1} + \beta_{t-1} + \nu_t \quad (2.2)$$

$$\beta_t = \beta_{t-1} + \omega_t \quad (2.3)$$

Where t denotes time, y_t, d_t, and n_t denote corn yield, drought index , and the number of days that the maximum temperature exceeds a certain threshold, respectively. This last term is called the critical temperature in the rest of the paper. ${z_{Jun}}_t$, ${z_{Jul}}_t$, and ${z_{Aug}}_t$ represent the amount of total rainfall during the month of June to August respectively.

The logarithm of corn yield is applied to avoid potential negative projection of corn yield. A stochastic trend yield is represented by the state variables: θ_t and β_t. The stochastic

part of yield and state variables are represented by the error terms: ε_t, ν_t and η_t. We assume that the error terms are identically and independently normally distributed: $\varepsilon_t \sim N(0, \sigma_\varepsilon^2)$, $\nu_t \sim N(0, \sigma_\mu^2)$, and $\omega_t \sim N(0, \sigma_\omega^2)$. The parameters $(\psi_1, \ldots, \psi_8)$ capture weather effects. The model explains the logarithm of corn yields using this weather effect plus an unobservable stochastic trend and an error term. The model updates its information about these two state variables recursively using a Bayesian-based Kalman filter.

2.3 Estimation Method

We apply the Bayesian Markov Chain Monte Carlo (MCMC) method to estimate parameters. The MCMC method is to sequentially obtain samples from the conditional posterior distribution of the parameters using the Gibbs sampling algorithm.

2.3.1 Prior and Conditional Posteriors

We use conjugate priors for the state variables and parameters. The conjugate prior for θ_0, β_0, and ψ_i where $i = 1, \ldots, 8$ is the normal distribution $N(0,100)$. The conjugate prior for σ_ε^2, σ_μ^2, and σ_ω^2 is the uniform distribution $U(0,1000)$. In both cases, variances are chosen to create a diffuse prior.

To simplify, denote X_t as follows:

$$X_t = \psi_1 d_t^2 + \psi_2 n_t^2 + \psi_3 z_{Jun_t}^2 + \psi_4 z_{Jun_t} + \psi_5 z_{Jul_t}^2 + \psi_6 z_{Jul_t} + \psi_7 z_{Aug_t}^2 + \psi_8 z_{Aug_t} \quad (2.4)$$

Then, the likelihood function can be written as follows:

$$L(\cdot) = f(y_{1:T} | \theta_{0:T}, \beta_{0:T}, \sigma_\varepsilon^2, \sigma_\mu^2, \sigma_\omega^2, \psi_1, \ldots, \psi_8, n_{1:T}, d_{1:T}, z_{1:T})$$

$$= \prod_{t=1}^{T} f(y_t | \theta_{0:T}, \beta_{0:T}, \sigma_\varepsilon^2, \sigma_\mu^2, \sigma_\omega^2, \psi_1, \ldots, \psi_8, n_{1:T}, d_{1:T}, z_{1:T})$$

$$= (2\pi\sigma_\varepsilon^2)^{-\frac{T}{2}} \left(\prod_{t=1}^{T} y_t\right)^{-1} \exp\left(-\frac{1}{2\sigma_\varepsilon^2}\sum_{t=1}^{T} (\ln y_t - \theta_t - X_t)^2\right) \quad (2.5)$$

The conditional posterior distributions are derived according to the conjugate priors and the likelihood function. The conditional posterior distributions of the three variance parameters are as follows:

$$\sigma_\varepsilon^2 | y_{1:T}, \theta_{0:T}, \beta_{0:T}, \sigma_\mu^2, \sigma_\omega^2, X_{1:T} \sim IG\left(\frac{T}{2} - 1, \left(\frac{1}{2}\sum_{t=1}^{T} (\ln y_t - \theta_t - X_t)^2\right)^{-1}\right) \quad (2.6)$$

$$\sigma_\mu^2 | y_{1:T}, \theta_{0:T}, \beta_{0:T}, \sigma_\varepsilon^2, \sigma_\omega^2, X_{1:T} \sim IG\left(\frac{T}{2} - 1, \left(\frac{1}{2}\sum_{t=1}^{T} (\theta_t - \theta_{t-1})^2\right)^{-1}\right) \quad (2.7)$$

$$\sigma_\omega^2 | y_{1:T}, \theta_{0:T}, \beta_{0:T}, \sigma_\varepsilon^2, \sigma_\mu^2, X_{1:T} \sim IG\left(\frac{T}{2} - 1, \left(\frac{1}{2}\sum_{t=1}^{T} (\beta_t - \beta_{t-1})^2\right)^{-1}\right). \quad (2.8)$$

Using these three conditional posterior distributions, we draw samples for σ_ε^2, σ_μ^2 and σ_ω^2. Following the Baysian-Kalman filter introduced in Campagnoli et al. (2009), the conditional posterior distributions of θ_T, β_T, and ψ_i $(i = 1, \ldots, 8)$, are obtained. Then, by using the forward filtering backward sampling (FFBS) algorithm, we draw samples for θ_t, β_t $(t = 1, \ldots, T)$, and ψ_i $(i = 1, \ldots, 8)$. This FFBS method is from Carter and Kohn (1994), Frühwirth-Schnatter (1994), and Jong and Shephard (1995).

2.3.2 Gibbs Sampling Algorithm

The steps to draw samples are as follows:

- Step 1. Choose initial values for $\sigma_\varepsilon^{2[0]}$, $\sigma_\mu^{2[0]}$, and $\sigma_\omega^{2[0]}$.
- Step 2. Use the prior distribution for θ_0, β_0, and ψ_i $(i = 1, \ldots, 8)$, together with the initial values in step 1, to run the Kalman filter.
- Step 3. Use a forward filtering backward sampling (FFBS) algorithm to get the sample of $\theta_{0:T}^{[j]}$, $\beta_{0:T}^{[j]}$, and $\psi_i^{[j]}$ $(i = 1, \ldots, 8)$.

• Step 4. Calculate $X_{1:T}^{[j]}$.

• Step 5. Draw $\sigma_{\varepsilon}^{2[j]}$ using equation (2.6).

• Step 6. Draw $\sigma_{\mu}^{2[j]}$ using equation (2.7).

• Step 7. Draw $\sigma_{\omega}^{2[j]}$ using equation (2.8).

• Step 8. Substitute for the values of $\sigma_{\varepsilon}^{2[j]}$, $\sigma_{\mu}^{2[j]}$, and $\sigma_{\omega}^{2[j]}$ in step 1, and repeat steps 1–8 for 200,000 iterations.

In the first step, we chose three different initial values for $\sigma_{\varepsilon}^{2[0]}$, $\sigma_{\mu}^{2[0]}$, and $\sigma_{\omega}^{2[0]}$ so as to generate three different MCMC chains. We discard the early sample in the MCMC chains (the first 100,000) as the burn-in period. We then use Gelman-Rubin diagnostics to determine whether they all converge to the same posterior distribution. We use these subsequent samples to make Bayesian posterior inferences about the parameters.

2.4 Data Collection

Corn yield data for all 99 counties in Iowa are sourced from the National Agriculture Statistics Service (NASS) for the years 1950–2013. Therefore, $t = 1, \ldots, 64$ (1950–2013).

County-level daily temperature data for each July was collected from the National Oceanic and Atmospheric Administration (NOAA). The temperature data includes daily maximum temperature (TMAX). The number of days the maximum temperature exceeds each critical value is calculated from the collected daily temperature data. All the counties in the state of Iowa are matched with at least one weather station. For the counties with multiple stations, we use the average weather data for all stations included in the county. Where data

is missing for certain years of some counties we use the weather data collected from their neighboring counties.

The PDSI is available from NOAA at the Crop Reporting District (CRD) level, with the 99 counties in Iowa in nine CRDs.[2] The PDSI data was collected for the month of June to August. County-level total monthly precipitation (TPCP) data was also collected from NOAA. Average total monthly rainfall for the period June to August is used to estimate the effect of rainfall on corn yield.

In order to prevent county-level anomalies as well as overly long tables, results presented here are for each of Iowa's nine crop reporting districts (CRD). The county-level results are very similar and available on request. The map of CRDs in Iowa is presented in Figure 2.1. This figure also provides a measure of the suitability of the soils in each CRD to grow corn. CRDs 1,2,4,5 and 6 have the highest soil quality. While CRDs 3, 7, 8 and 9 have the lowest quality.

[2] The map of the nine CRDs for the state of Iowa is provided in Figure 2.1.

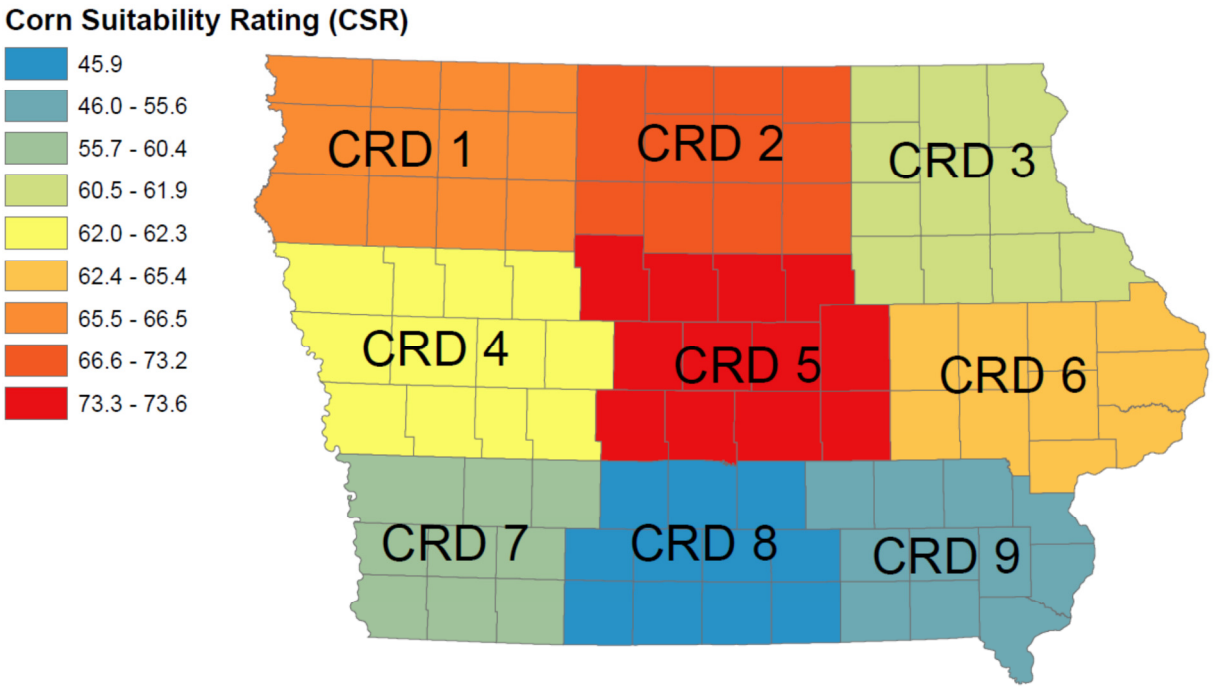

Figure 2.1: Iowa crop reporting district (CRD) map

2.5 Estimation Results

2.5.1 Results Related to Critical Temperature

Schlenker and Roberts (2009) conclude that temperature becomes seriously harmful for corn yield when it exceeds 84°F. We change the critical temperature in one degree increment up to 95°F and plot the AIC scores for these twelve models for the nine CRDs in Figure 2.2.

The Gelman-Rubin test statistics indicate that 200,000 iterations are enough for the MCMC chains to converge for all Iowa CRDs. We then use the subsequent sample to obtain Bayesian posterior inferences about the parameters. The 2.5%, 97.5%, 5.0%, and 95% quantile of posterior distributions and the posterior means of $\psi_1, \psi_2, \psi_3, \psi_4, \psi_5, \psi_6, \psi_7, \psi_8,$

σ_{ε}^2, σ_{μ}^2, and σ_{ω}^2 in the model with critical temperature selected by AIC are reported in Appendix Tables 2.1–2.9.

The results for CRDs 1, 2, and 4 show no improvement in AIC scores for any of the critical temperatures. Results for CRDs 5 and 6 show a modest improvement in AIC scores up to a critical temperature of 95°F.

The results for the CRDs with the lowest land quality show a much greater improvement in AIC scores from the inclusion of a critical temperature. The critical temperature that provides the greatest improvement in AIC score is 92°F degrees for CRD 3 and CRD 9, 90°F degrees for CRD 7, and 89°F degrees for CRD 8.

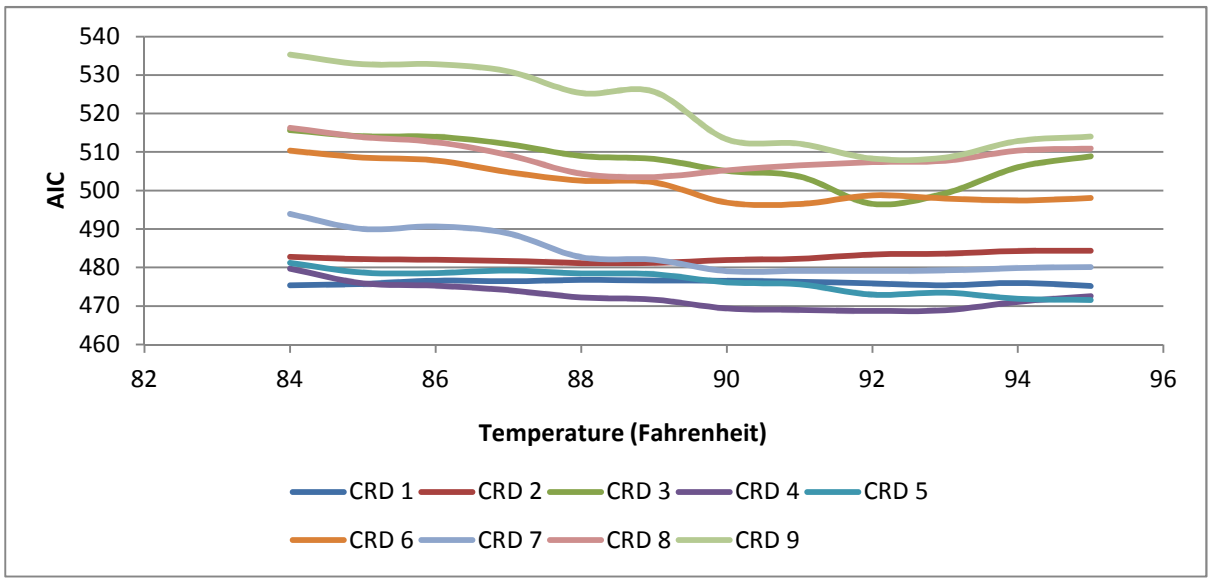

Figure 2.2: AIC scores for a range of critical temperatures for the nine CRDs

One intuitive explanation for the difference in critical temperature results across soil quality is that corn growing on high quality soils may be able to resist high temperatures

because the corn root system can source more water than in less productive soils. This suggests that the impact of global warming will be less important for areas that are most suited to corn production.

The finding that the critical temperature for corn is in a range of 89–95°F is also important. Given that the average daytime high in Iowa in July is approximately 85°F any rightward shift of the temperature distribution will dramatically increase the number of observations that are above the 84°F critical temperature reported by Schlenker and Roberts.[3] With a critical temperature in the right hand tail of the temperature distribution, a rightward shift of the temperature distribution will not result in such a dramatic increase in the projected number of time periods above the critical temperature.

There are several reasons why our critical temperature results are different from Schlenker and Roberts. Their weather data is much more disaggregated across space and time than ours. Our model selection process caused us to include a linear and quadratic terms measuring rainfall as well as a quadratic term reflecting long-term drought. Schlenker and Roberts use only a quadratic rainfall term. This means that our results control for the level of rainfall and the severity of drought; therefore they are not directly comparable to Schlenker and Roberts. Finally, as was mentioned earlier, our results are specific to Iowa, whereas Schlenker and Roberts use a national model and perform pairwise tests to determine if the results are robust across longitude and latitude.

[3] See http://www.currentresults.com/Weather/Iowa/temperature-july.php Accessed on 12/01/2014.

2.5.2 Weather Effects

Here we plot the posterior mean of corn yield against the drought index, rainfall, and the number of days that the maximum temperature exceeds critical temperature as selected by the AIC measure. To plot the posterior mean of corn yield against the drought index, we first generated 500 values of the drought index that were evenly distributed over the observed data range. We evaluated equation (1) with time $t = 63$ (the year 2012), θ_{63} and ψ_2 to ψ_8 at their posterior means, n_t, z_{Jun_t}, z_{Jul_t}, and z_{Aug_t} at their historical means. Therefore, for each generated drought index, we can obtain the posterior mean of corn yield using the MCMC chains of ψ_1. We then plotted 500 simulated posterior means of corn yield against the corresponding 500 simulated drought indexes. We used a similar method to plot the posterior mean of corn yield against rainfall and the number of the days that the maximum temperature exceeds critical temperature. We chose the four corner CRDs to illustrate the weather effects on corn yield. The plots are reported in Figures 3–7.

As shown in Table 2.1, the coefficient for the drought index ψ_1 is significant for all nine CRDs at 5% significance interval. The posterior mean of ψ_1 is negative in all CRDs. Figure 2.3 shows both drought and wetness reduce corn yield. We simulated corn yields with the 1993 and 2012 drought index data because 1993 was a flood year and 2012 was a drought year. The 2012 drought reduced corn yield by 36 bushels in CRD 1, which is around 15 percent of corn yield without drought. The 2012 drought had a smaller negative effect on corn yield in CRD 9, which reduced corn yield by 16 bushels. There was a severe flood in 1993, which put the drought index strongly in positive territory. The flood damaged corn

yield by more than 70 bushels in CRD 7 and 9. The 1993 flood caused a reduction of more than 100 bushels of corn yield in CRD 1.

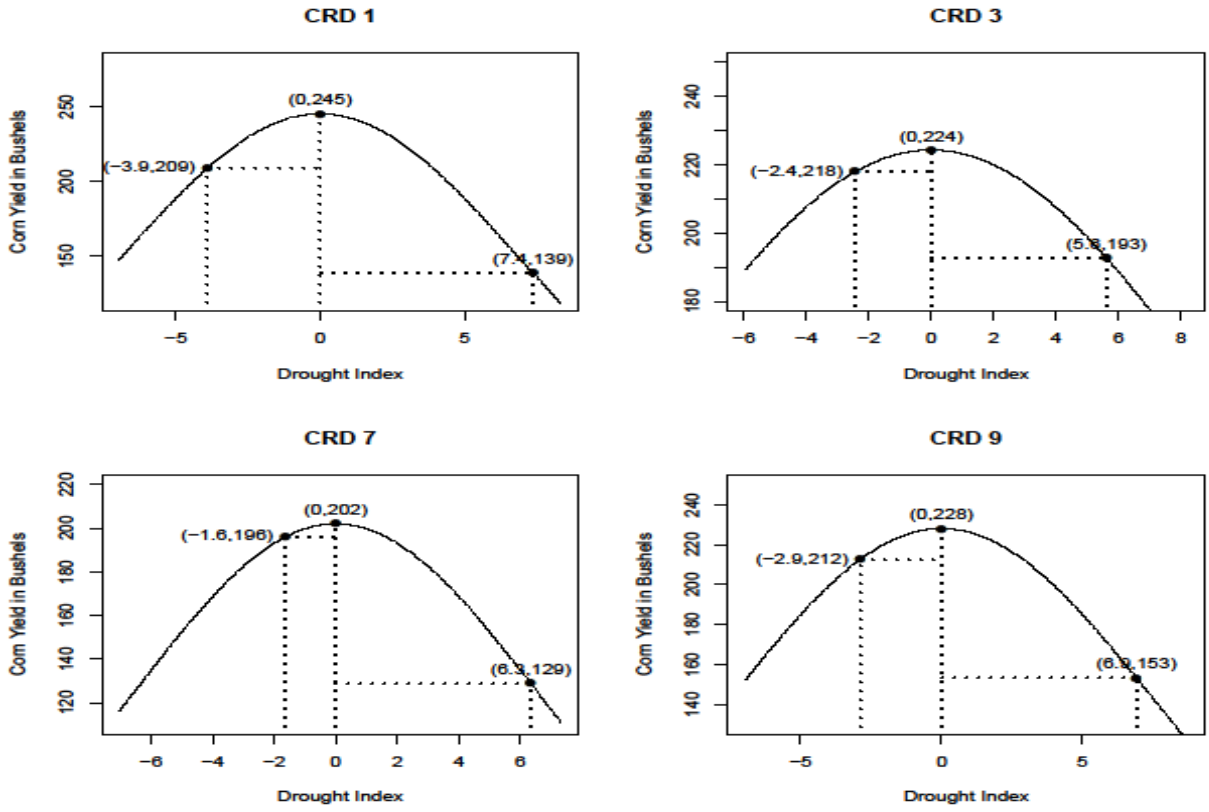

Figure 2.3: The effect of drought on corn yield

Results for models using the AIC selected critical temperature (ψ_2) are reported in Tables 2.2. The critical temperature term ψ_2 is significant for eight out of nine CRDs at a 5% significance interval.

Figure 2.4 reproduces the nonlinear relationship between temperature and corn yield estimated by Schlenker and Roberts.[4] In Figure 4, the vertical axis shows the log of yield, and a vertical difference of 0.01 between any two points indicates a 1% difference in corn yield. Schlenker and Roberts result suggests a temperature at 104°F for one twenty four hour day will reduce corn yield by around 7%.

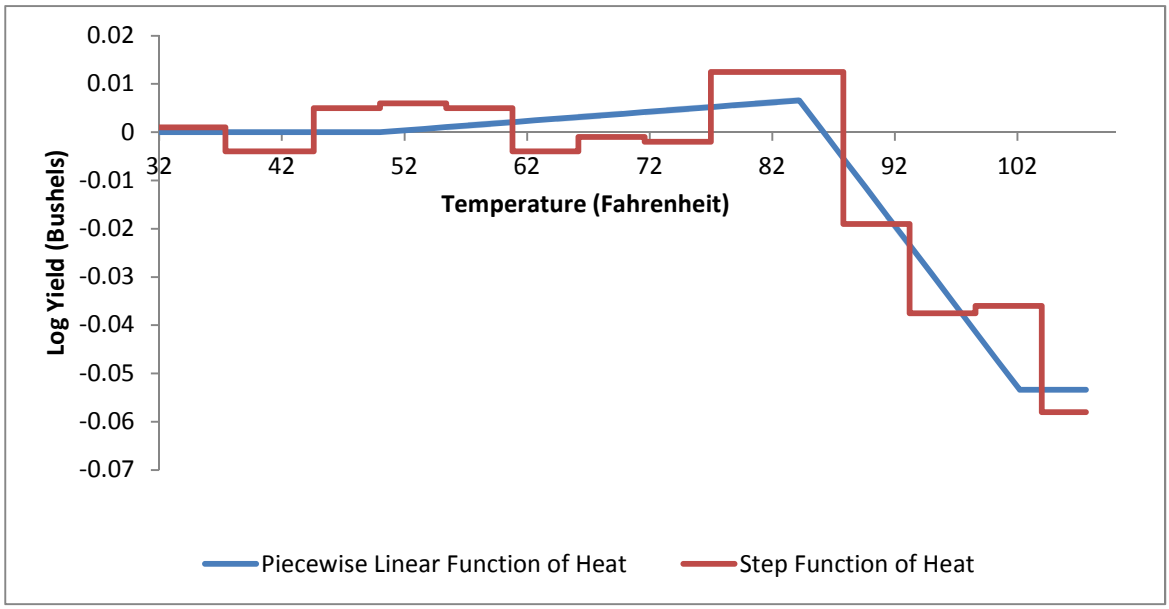

Figure 2.4: The relationship between temperature and corn yield from Schlenker and Roberts (2009)

Figure 2.5 shows the impact of temperature on corn yield in the four corner CRDs. As shown in Figure 2.6, an unusual heat wave accompanied a drought in 2012, bringing the largest number of days that the maximum temperature exceeded critical temperature for each CRD in the last twenty years. We simulated corn yields with these data of extremely hot

[4] The nonlinear relationship between temperature and corn yield estimated by Schlenker and Roberts was reproduced based on Frame A of Figure 1 in Schlenker and Roberts (2009).

days. As shown in Figure 2.5, the 2012 heat wave damaged corn yields by 31 bushels in CRD 1. The damage was even higher in CRDs 3, 7, and 9. Corn yields in CRDs 7 and 9 were reduced by more than 70 bushels, which is more than 30 percent of the corn yield without any extra heat. The 2012 heat wave had the largest impact on CRD 3, where it reduced corn yield by more than 90 bushels.

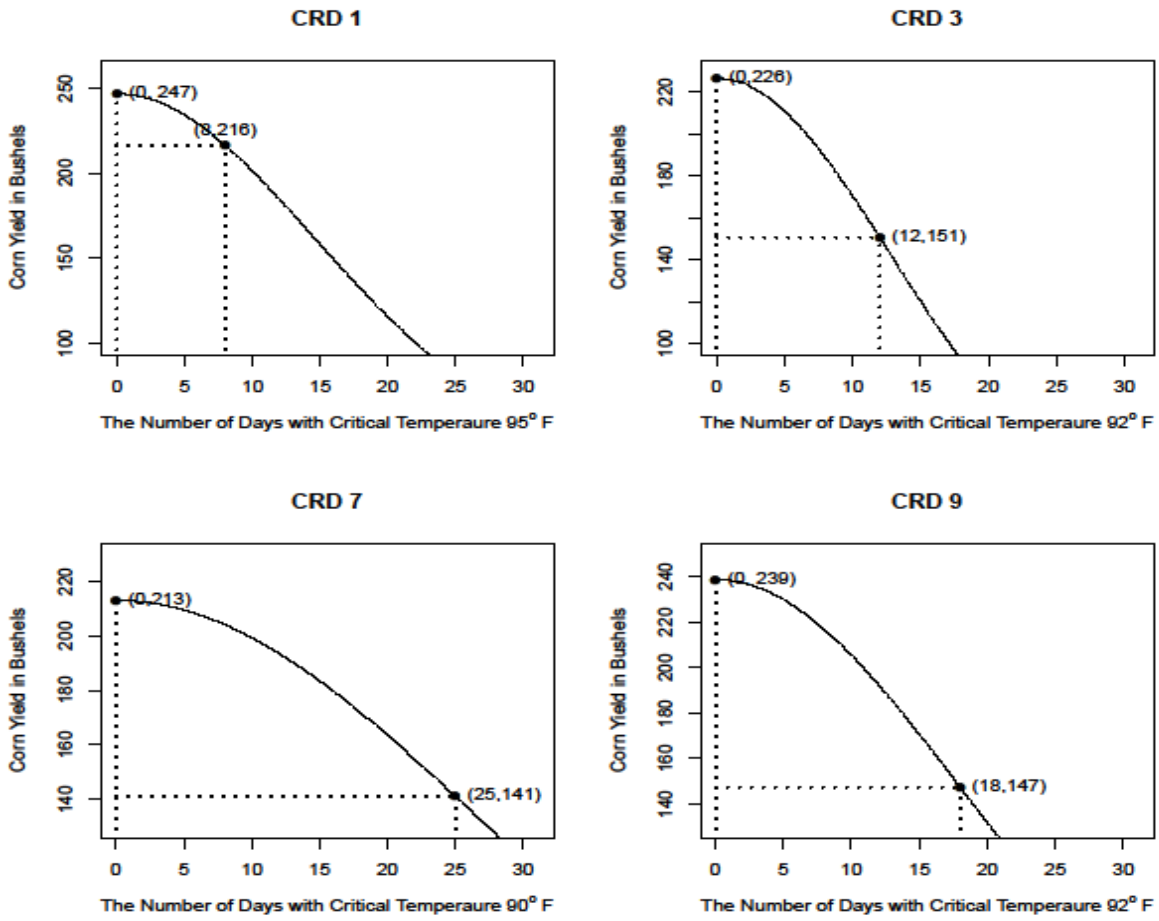

Figure 2.5: The effect of the number of days that the maximum temperature exceeds critical temperatures on corn yield

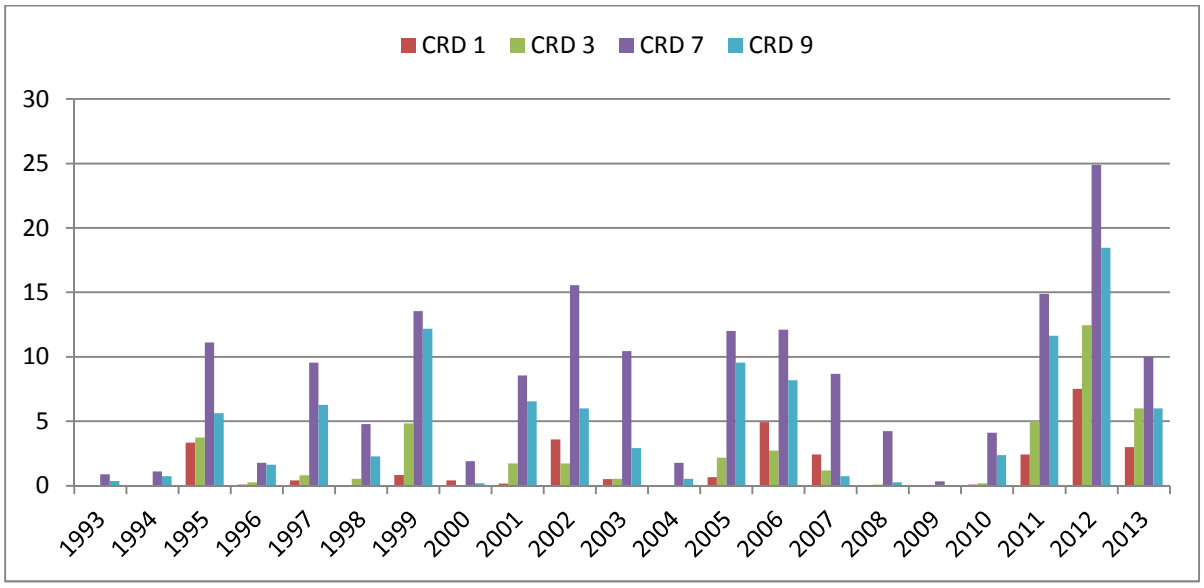

Figure 2.6: Historical data of the number of days that the maximum temperature exceeds critical temperature

Table 2.3–2.8 provide results showing that the quadratic and linear impact of rainfall (ψ_3 ,…, ψ_8). The quadratic June rainfall term ψ_3 is insignificant for all nine CRDs, while the linear June rainfall term ψ_4 is significant for only two out of nine CRDs. This indicates that if one controls for drought, the amount of rainfall in June plays a less critical role in affecting corn yield. The quadratic July rainfall term ψ_5 is significant for five out of nine CRDs and the linear term ψ_6 is significant for eight out of nine CRDs. The August rainfall terms ψ_7 and ψ_8 are significant for four out of nine CRDs. These results suggest that rainfall in July is critical for corn yield even if one controls for drought.

Figure 2.7 shows that the model-estimated "optimal" amount of rainfall in July is 6.6 inches for corn. We simulated corn yields with the 1993 and 2012 rainfall data. 2012 was a drought year with 1.03 inches of rainfall in CRD 1, 1.76 inches in CRD 3, 0.7 inches in CRD 7, and 1.19 inches in CRD 9. The lack of rainfall in 2012 reduced corn yield around 46

bushels in CRD 1, 16 bushels in CRD 3, 55 bushels in CRD 7 and 43 bushels in CRD 9. The flood in 1993 provided a tremendous amount of excess precipitation and caused considerable damage to corn yield in CRD 7. It reduced corn yield by 56 bushels in CRD 7.

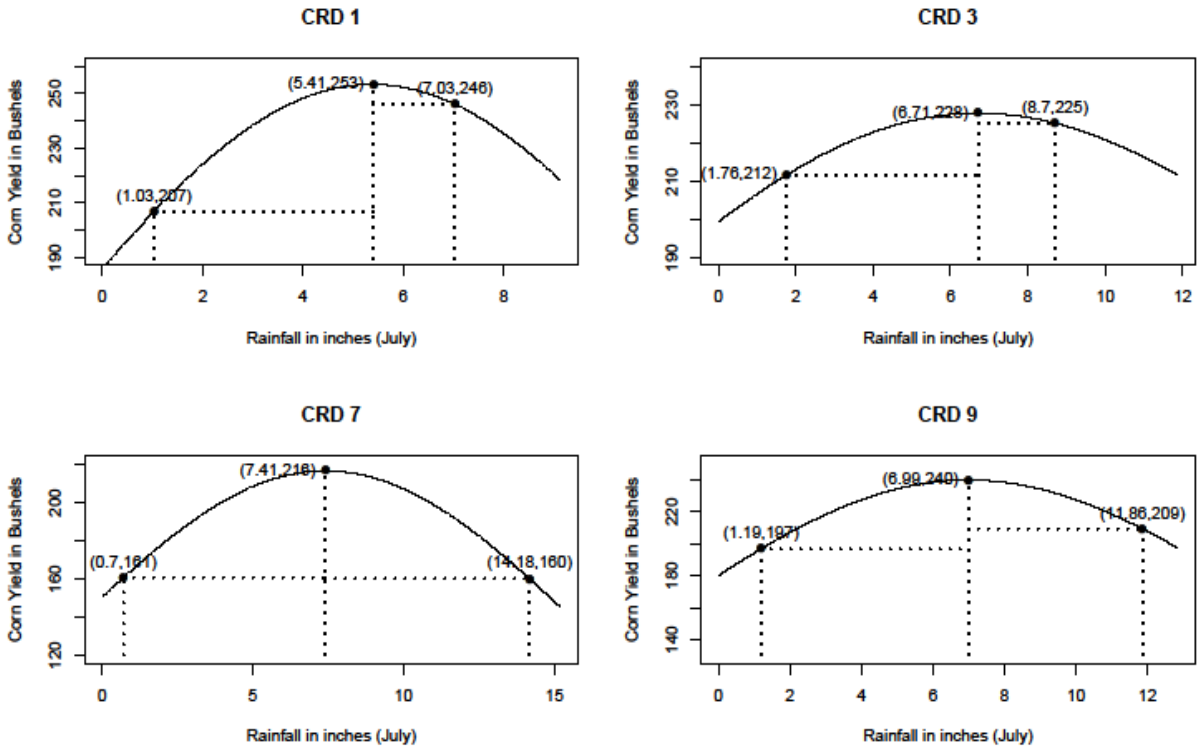

Figure 2.7: The effect of the amount of rainfall in July on corn yield

2.5.3 Trend Yields for Corn

The state variable θ_t represents the logarithm of trend yield at time t, while β_t represents the expected change in θ_t for time $t+1$. As can be seen in Table 2.9, the posterior mean of σ_μ is positive, suggesting that the logarithm of trend yield does have a stochastic trend. The

posterior mean of σ_ω is close to zero for all CRDs, which suggests that the change in the logarithm of trend yield does not fluctuate dramatically. Evaluating the drought index, the amount of rainfall and the number of days that the maximum temperature exceeds critical temperature at their historical means, the trend yield in all Iowa CRDs are reported in Figure 2.8. Figure 2.9 shows the trend yield for the state as a whole.

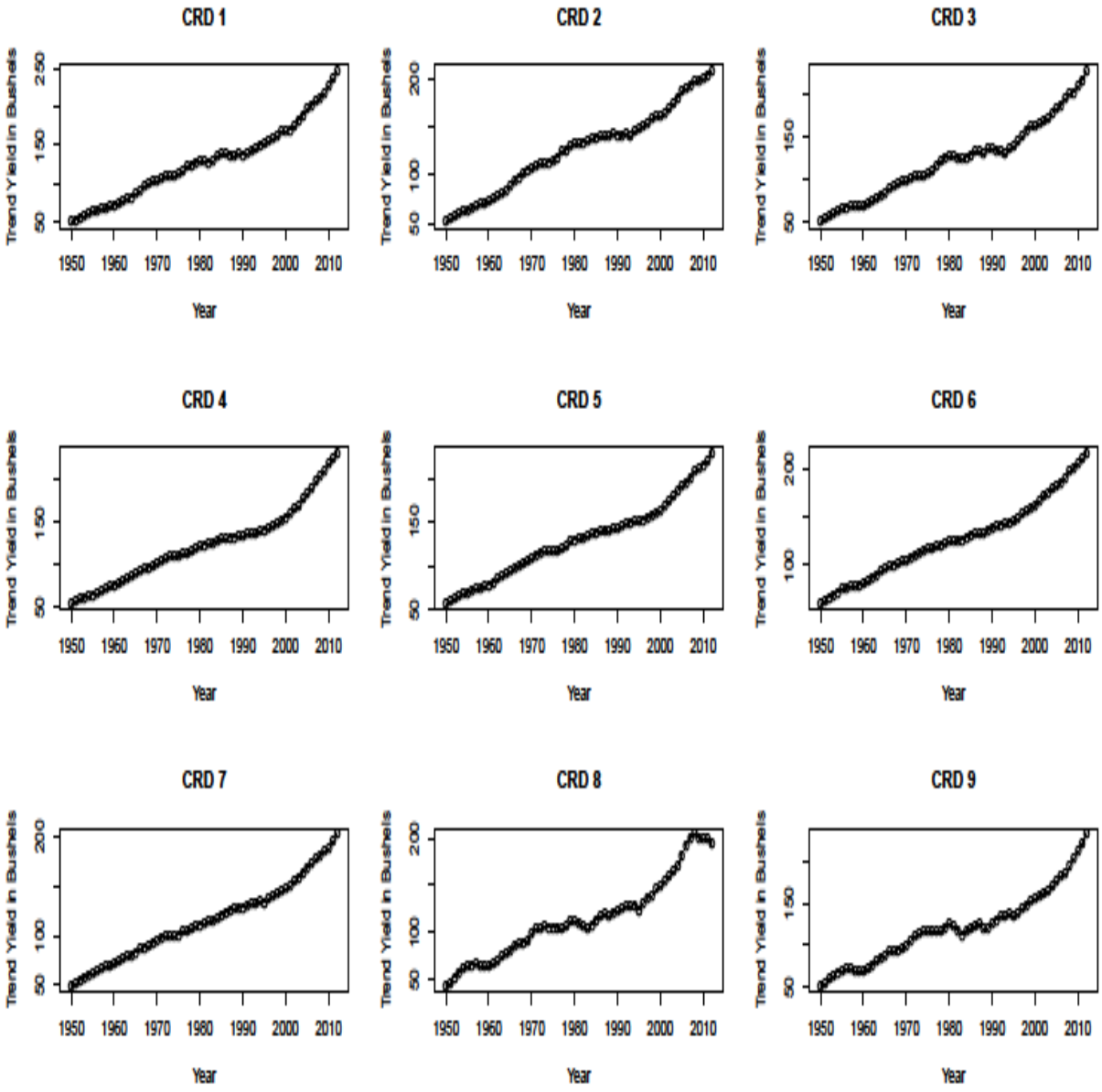

Figure 2.8: Corn yield trends in CRDs 1–9

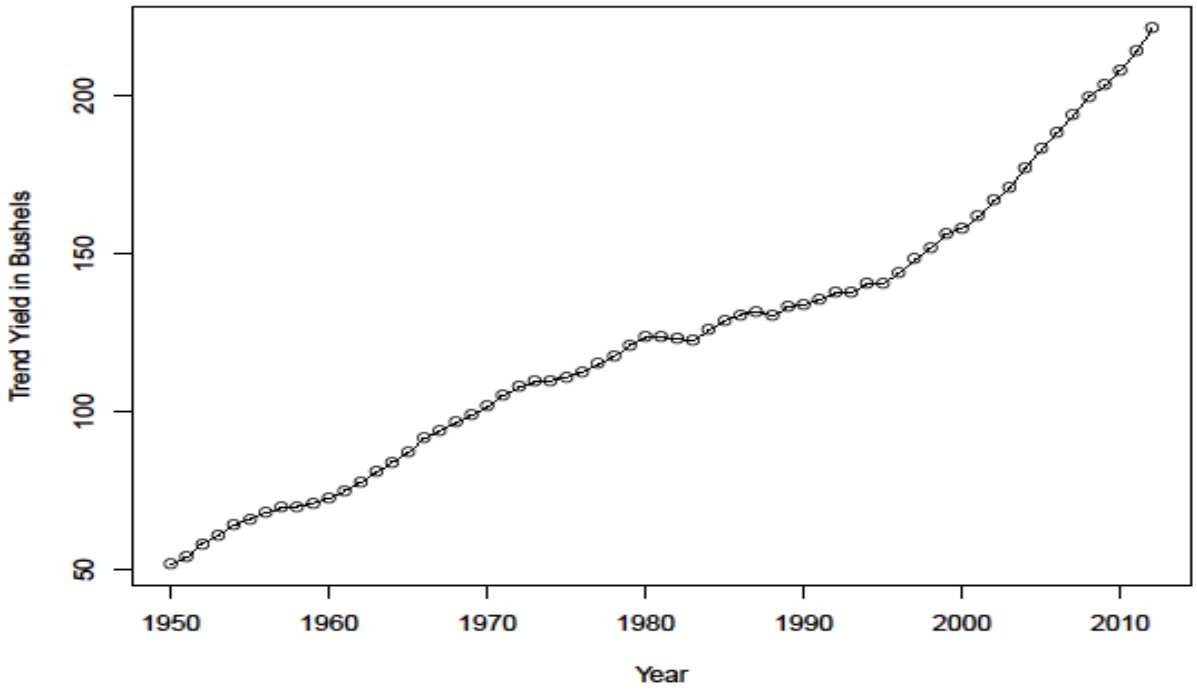

Figure 2.9: State of Iowa corn yield trend

Trend yield has increased by more than five bushels each year since 2008 in all CRDs except for CRD 8. There is a recent slight decrease for yield trend in the center of south Iowa (CRD 8). For the state as a whole trend yield has grown since the mid-1990s, and the growth speeds up since 2009.

The yield growth we show here is due to genetic gain and other variables such as disease, wind, management, and weather impacts that were not included in the model. Our initial explanation for the cross-CRD yield patterns was that there might be some excluded weather terms that explain patterns across the CRDs. We explored the possibility that an increase in excessively hot days occurred in the poorly performing regions, but this was not

borne out by the results. We also examined whether there was an increase in the number of rain events with more than two inches of rain in one event. Again, there was no statistically valid relationship.

2.6 Corn Yield Model Validation

The model can be applied to do both short- and long-term corn yield forecasts. The model is estimated using data up to 2012, and therefore, using the estimated results of parameters and state variables and the data of drought index, rainfall, and the number of the days that temperature exceeds the critical temperature, corn yield as of 2013 can be forecasted.

Let d, z, and n be the drought index, rainfall, and the number of the days that the maximum temperature exceeds the critical temperature used in forecasting yield, respectively. According to equations (2.1), (2.2), and (2.3) we have the following:

$$E(\ln \mathrm{y}_{\mathrm{T+1}} |y_{1:T}) = E(\theta_{T+1}|y_{1:T}) + \psi_1 d^2 \psi_2 n^2 + \psi_3 z_{jun}^2 + \psi_4 z_{\mathrm{Jun}}$$

$$+\psi_5 z_{jul}^2 + \psi_6 z_{\mathrm{Jul}} + \psi_7 z_{Aug}^2 + \psi_8 z_{\mathrm{Aug}} \tag{2.9}$$

$$E(\theta_{T+1}|y_{1:T}) = \theta_T + \beta_T \tag{2.10}$$

$$E(\beta_{T+1}|y_{1:T}) = \beta_T \tag{2.11}$$

Using actual weather data, we calculated corn yields for each CRD in the year 2013. For each group, we simulated three MCMC chains of corn yield with 100,000 iterations for each chain, using the MCMC chains of θ_T, β_T, and ψ_1 to ψ_8 obtained in section 5. We then calculated the posterior mean of corn yield for each CRD. The absolute value of the difference between the actual and posterior mean of calculated yields for each group are reported in Table 2.10.

The smallest difference between the calculated and actual corn yield is less than 5 bushels CRD 4 and CRD 8. The model under-estimate corn yield for CRD 4 and 7, and over-estimate corn yield for other CRDs. The calculated results for CRDs 2, 5 and 9 were large relative to the goodness of fit over the historic period. The 2013 crop year was an unusual one in that the state experienced drought in 2012 and again in 2013. See Figures 2.10 and 2.11 below. In developing the model we had tested for a drought on drought impact and the term was not significant. It seems likely that the poor performance of the model is due to a drought on drought impact in 2013. CRD 2 had the least amount of rainfall in 2012 and CRD 5 and 9 were the hardest hit in 2013. There is little we could have done to develop a model to predict 2013 given that we did not have two years of statewide drought in the period prior to 2013.

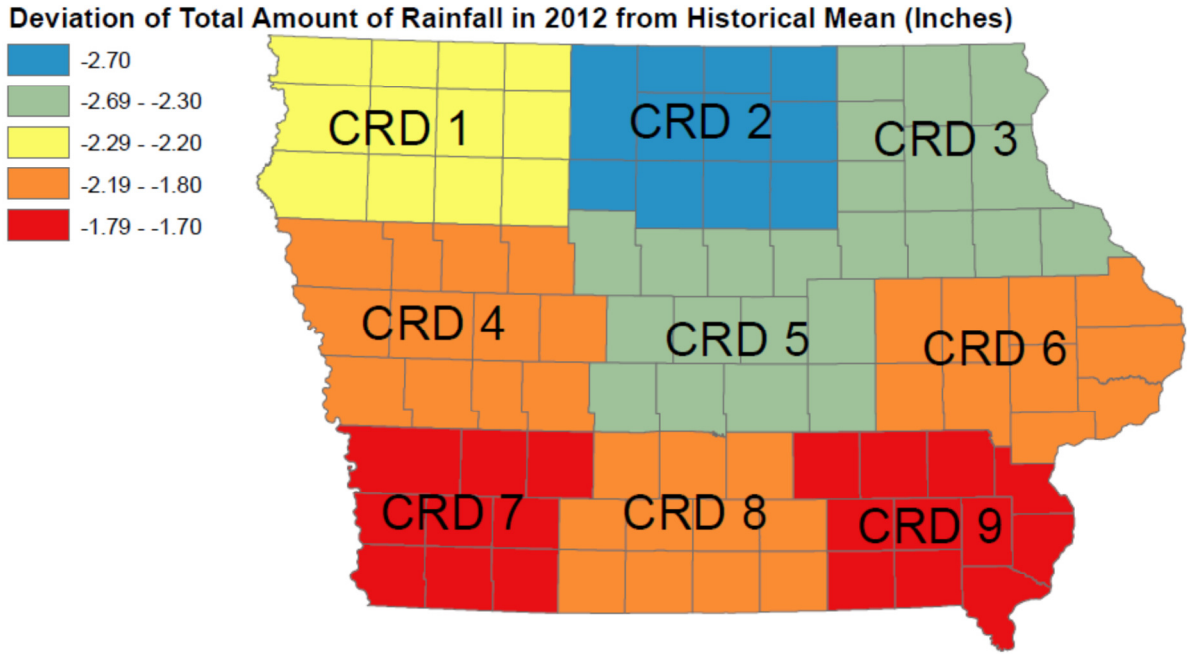

Figure 2.10: Deviation of amount of rainfall in 2012 from historical mean during corn growing season

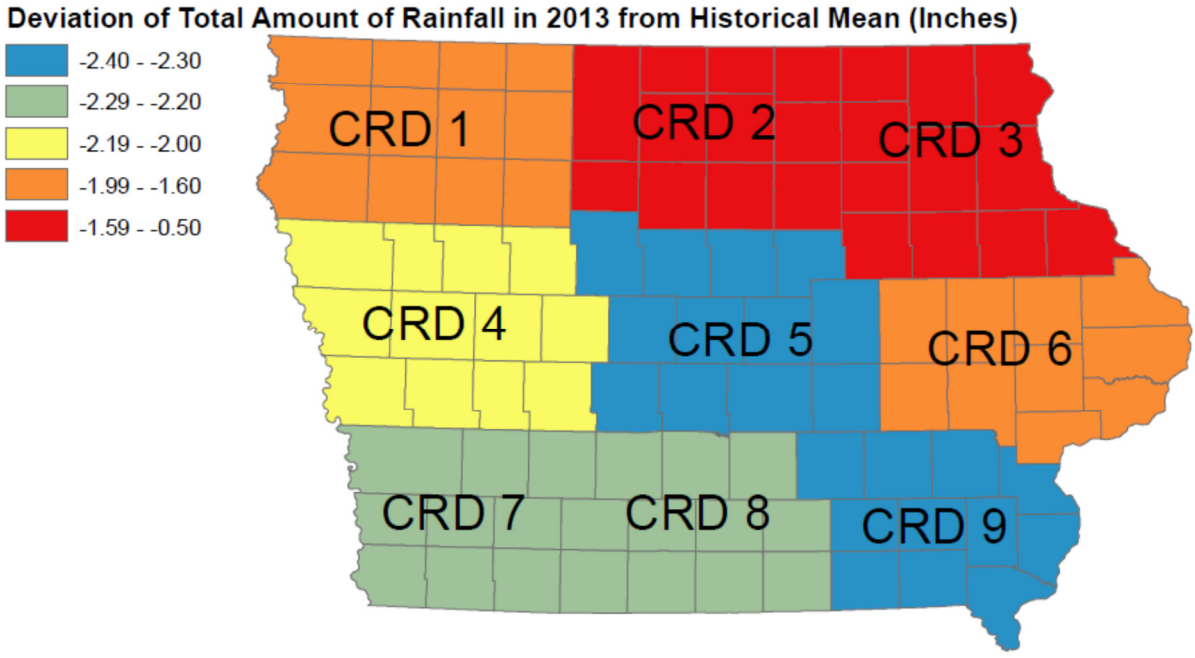

Figure 2.11: Deviation of amount of rainfall in 2013 from historical mean during corn growing season

2.7 Conclusion

Our results show that corn yield has a stochastic trend and that this trend has increased in bushel terms in recent years. We also find that high temperatures in July can damage corn yields. However in contrast to Schlenker and Roberts this critical temperature is relatively high, especially in areas of the state most suited for corn production. Schlenker and Roberts did test for regional differences in this critical temperature and did not find any support for regional differences in this value. The years 2012 and 2013 were unusual in that both had a high number of hot days in July and in that rainfall was below average in both years. The model did not predict yields in 2013 in areas of the state most impacted by low rainfall in 2012 and 2013. It seems possible that this was true because statewide drought in two consecutive years is very unusual. Corn yields are sensitive to rainfall in July even when one

controls for drought. The "optimal" amount of rainfall in July is 6.6 inches. Rainfall amounts above or below this amount can negatively impact on yields.

2.8 APPENDIX A

Table 2.1: Estimation results of ψ_1

CRD	Posterior Mean	2.5%	97.5%	5.0%	95.0%	Gelman-Rubin Test Statistics
CRD 1	-0.0105	-0.0135	-0.0075	-0.0130	-0.0080	1.000
CRD 2	-0.0106	-0.0143	-0.0068	-0.0137	-0.0074	1.000
CRD 3	-0.0049	-0.0093	-0.0005	-0.0086	-0.0012	1.000
CRD 4	-0.0128	-0.0160	-0.0096	-0.0155	-0.0101	1.000
CRD 5	-0.0084	-0.0113	-0.0054	-0.0108	-0.0059	1.000
CRD 6	-0.0093	-0.0128	-0.0058	-0.0122	-0.0064	1.000
CRD 7	-0.0113	-0.0155	-0.0072	-0.0148	-0.0079	1.000
CRD 8	-0.0130	-0.0191	-0.0070	-0.0181	-0.0080	1.000
CRD 9	-0.0085	-0.0132	-0.0037	-0.0125	-0.0045	1.000

Table 2.2: Estimation results of ψ_2

CRD	Posterior Mean	2.50%	97.50%	5%	95%	Gelman-Rubin Test Statistics
CRD 1	-0.0021	-0.0040	-0.0001	-0.0037	-0.0005	1.000
CRD 2	-0.0003	-0.0006	0.0001	-0.0006	0.0000	1.000
CRD 3	-0.0029	-0.0045	-0.0013	-0.0042	-0.0015	1.000
CRD 4	-0.0011	-0.0015	-0.0006	-0.0015	-0.0007	1.000
CRD 5	-0.0024	-0.0037	-0.0011	-0.0035	-0.0013	1.000
CRD 6	-0.0010	-0.0015	-0.0005	-0.0014	-0.0005	1.000

Table 2.3: Estimation results of ψ_2 (Continued)

CRD	Posterior Mean	2.50%	97.50%	5%	95%	Gelman-Rubin Test Statistics
CRD 7	-0.0007	-0.0009	-0.0004	-0.0009	-0.0004	1.000
CRD 8	-0.0007	-0.0010	-0.0004	-0.0010	-0.0004	1.000
CRD 9	-0.0015	-0.0022	-0.0008	-0.0021	-0.0010	1.000

Table 2.4: Estimation results of ψ_3

CRD	Posterior Mean	2.50%	97.50%	5%	95%	Gelman-Rubin Test Statistics
CRD 1	0.0013	-0.0060	0.0087	-0.0048	0.0075	1.000
CRD 2	0.0015	-0.0050	0.0079	-0.0039	0.0068	1.000
CRD 3	-0.0006	-0.0083	0.0071	-0.0070	0.0058	1.000
CRD 4	-0.0021	-0.0053	0.0010	-0.0047	0.0005	1.000
CRD 5	-0.0010	-0.0054	0.0033	-0.0047	0.0026	1.000
CRD 6	-0.0033	-0.0082	0.0016	-0.0074	0.0008	1.000
CRD 7	0.0013	-0.0020	0.0045	-0.0014	0.0040	1.000
CRD 8	-0.0042	-0.0110	0.0025	-0.0098	0.0013	1.000
CRD 9	-0.0047	-0.0114	0.0021	-0.0103	0.0010	1.000

Table 2.5: Estimation results of ψ_4

CRD	Posterior Mean	2.50%	97.50%	5%	95%	Gelman-Rubin Test Statistics
CRD 1	-0.0089	-0.0865	0.0685	-0.0736	0.0557	1.000
CRD 2	-0.0150	-0.0873	0.0571	-0.0752	0.0451	1.000
CRD 3	0.0022	-0.0809	0.0861	-0.0672	0.0720	1.000
CRD 4	0.0371	-0.0031	0.0774	0.0035	0.0707	1.000
CRD 5	0.0199	-0.0284	0.0685	-0.0204	0.0605	1.000
CRD 6	0.0485	-0.0095	0.1068	0.0000	0.0971	1.000
CRD 7	-0.0100	-0.0513	0.0312	-0.0444	0.0244	1.000
CRD 8	0.0484	-0.0257	0.1223	-0.0132	0.1101	1.000
CRD 9	0.0400	-0.0293	0.1095	-0.0181	0.0980	1.000

Table 2.6: Estimation results of ψ_5

CRD	Posterior Mean	2.50%	97.50%	5%	95%	Gelman-Rubin Test Statistics
CRD 1	-0.0106	-0.0173	-0.0039	-0.0162	-0.0050	1.000
CRD 2	-0.0046	-0.0109	0.0017	-0.0098	0.0007	1.000
CRD 3	-0.0028	-0.0086	0.0029	-0.0076	0.0020	1.000
CRD 4	-0.0090	-0.0143	-0.0037	-0.0134	-0.0045	1.000
CRD 5	-0.0033	-0.0077	0.0011	-0.0070	0.0004	1.000
CRD 6	-0.0028	-0.0078	0.0022	-0.0070	0.0014	1.000
CRD 7	-0.0066	-0.0094	-0.0038	-0.0089	-0.0043	1.000
CRD 8	-0.0078	-0.0119	-0.0038	-0.0112	-0.0044	1.000
CRD 9	-0.0058	-0.0115	-0.0001	-0.0105	-0.0010	1.000

Table 2.7: Estimation results of ψ_6

CRD	Posterior Mean	2.50%	97.50%	5%	95%	Gelman-Rubin Test Statistics
CRD 1	0.1140	0.0540	0.1741	0.0641	0.1640	1.000
CRD 2	0.0612	-0.0006	0.1231	0.0095	0.1128	1.000
CRD 3	0.0380	-0.0258	0.1020	-0.0150	0.0914	1.000
CRD 4	0.1141	0.0626	0.1656	0.0711	0.1571	1.000
CRD 5	0.0521	0.0065	0.0981	0.0140	0.0903	1.000
CRD 6	0.0481	-0.0085	0.1049	0.0008	0.0955	1.000
CRD 7	0.0975	0.0574	0.1377	0.0641	0.1309	1.000
CRD 8	0.1160	0.0591	0.1733	0.0686	0.1638	1.000
CRD 9	0.0802	0.0112	0.1497	0.0227	0.1381	1.000

Table 2.8: Estimation results of ψ_7

CRD	Posterior Mean	2.50%	97.50%	5%	95%	Gelman-Rubin Test Statistics
CRD 1	-0.0083	-0.0148	-0.0018	-0.0137	-0.0029	1.000
CRD 2	-0.0021	-0.0054	0.0013	-0.0049	0.0008	1.000
CRD 3	-0.0030	-0.0081	0.0022	-0.0073	0.0013	1.000
CRD 4	-0.0029	-0.0086	0.0028	-0.0077	0.0018	1.000
CRD 5	-0.0035	-0.0066	-0.0005	-0.0061	-0.0010	1.000
CRD 6	-0.0003	-0.0046	0.0041	-0.0039	0.0034	1.000
CRD 7	-0.0037	-0.0070	-0.0004	-0.0065	-0.0009	1.000
CRD 8	-0.0074	-0.0130	-0.0017	-0.0121	-0.0026	1.000
CRD 9	0.0002	-0.0068	0.0073	-0.0056	0.0061	1.000

Table 2.9: Estimation results of ψ_8

CRD	Posterior Mean	2.50%	97.50%	5%	95%	Gelman-Rubin Test Statistics
CRD 1	0.0873	0.0317	0.1427	0.0410	0.1335	1.000
CRD 2	0.0236	-0.0154	0.0621	-0.0088	0.0558	1.000
CRD 3	0.0303	-0.0252	0.0853	-0.0159	0.0763	1.000
CRD 4	0.0344	-0.0180	0.0868	-0.0093	0.0781	1.000
CRD 5	0.0366	0.0023	0.0708	0.0080	0.0652	1.000
CRD 6	0.0219	-0.0243	0.0684	-0.0166	0.0606	1.000
CRD 7	0.0490	0.0079	0.0902	0.0147	0.0834	1.000
CRD 8	0.0888	0.0247	0.1518	0.0354	0.1415	1.000
CRD 9	0.0048	-0.0684	0.0775	-0.0562	0.0653	1.000

Table 2.10: Estimation results of σ_ε^2, σ_μ^2 and σ_ω^2

CRD	Posterior Mean (σ_ε^2)	Posterior Mean (σ_μ^2)	Posterior Mean (σ_ω^2)	Gelman-Rubin Test Statistics (σ_ε^2)	Gelman-Rubin Test Statistics (σ_μ^2)	Gelman-Rubin Test Statistics (σ_ω^2)
CRD 1	0.0079	0.0017	0.0001	1.000	1.000	1.020
CRD 2	0.0078	0.0014	0.0001	1.000	1.001	1.007
CRD 3	0.0107	0.0028	0.0001	1.000	1.004	1.003
CRD 4	0.0075	0.0010	0.0001	1.000	1.003	1.009
CRD 5	0.0066	0.0011	0.0001	1.000	1.003	1.011
CRD 6	0.0101	0.0012	0.0001	1.000	1.006	1.014
CRD 7	0.0101	0.0012	0.0001	1.000	1.001	1.001
CRD 8	0.0189	0.0059	0.0003	1.001	1.001	1.004
CRD 9	0.0154	0.0045	0.0002	1.000	1.002	1.016

Table 2.11: The difference between actual and calculated corn yield

	Critical Temperature	Actual Corn Yield – Calculated Corn Yield
CRD 1	95°F	-16.6
CRD 2	88°F	-27.1
CRD 3	92°F	-5.2
CRD 4	92°F	3.4
CRD 5	95°F	-40.3
CRD 6	91°F	-15.3
CRD 7	90°F	5.3
CRD 8	89°F	-0.2
CRD 9	92°F	-55.5

2.9 APPENDIX B

The one-step-ahead corn yield forecasts can be defined as $f_t = E(\ln y_t \,|y_{1:t-1})$, where $E(\ln y_t \,|y_{1:t-1})$, can be obtained using equations (2.9) to (2.11). The forecast error is defined as follows:

$$e_t = \ln y_t - f_t \quad . \tag{2.12}$$

A time-series sample of e_t $(t = 1,\ldots,63)$ can be obtained from equation (2.12). To check whether the assumption about normality is reasonable or not, we need to check whether e_t is normally distributed, and whether e_t is identically independently distributed. Using the method stated in section 2.6, we simulated three MCMC chains for the yield forecast f_t and then calculated the corresponding errors, e_t, from equation (2.12), with 100,000 iterations for each chain. We then calculated the posterior means of e_t, which can be used to check the normality and independent assumptions. The QQ-plot is adopted to check

the normality of the forecast errors, and the Auto-Correlation Function (ACF) of e_t is calculated to check the autocorrelation. The results of QQ-plot and ACF are reported in Figures 2.12 and 2.13.

In Figure 2.12, the dashed lines are the 95% confidence interval of a normal distribution. According to Figure B1, at most, eight points are not included in the 95% confidence interval for the nine CRDs. This fact indicates that the assumption about normality, which was rejected by Moss and Shonkwiler (1993), is reasonable. When taking weather effect into consideration, normality cannot be rejected. It seems that weather removes the negatively skewed part of corn yield. This result is consistent with the suggestion made by Gallagher (1987). The ACF reported in Figure 2.13 is insignificant for almost all lags for all nine CRDs, which also indicates that the assumption about the independence of ε_t is reasonable.

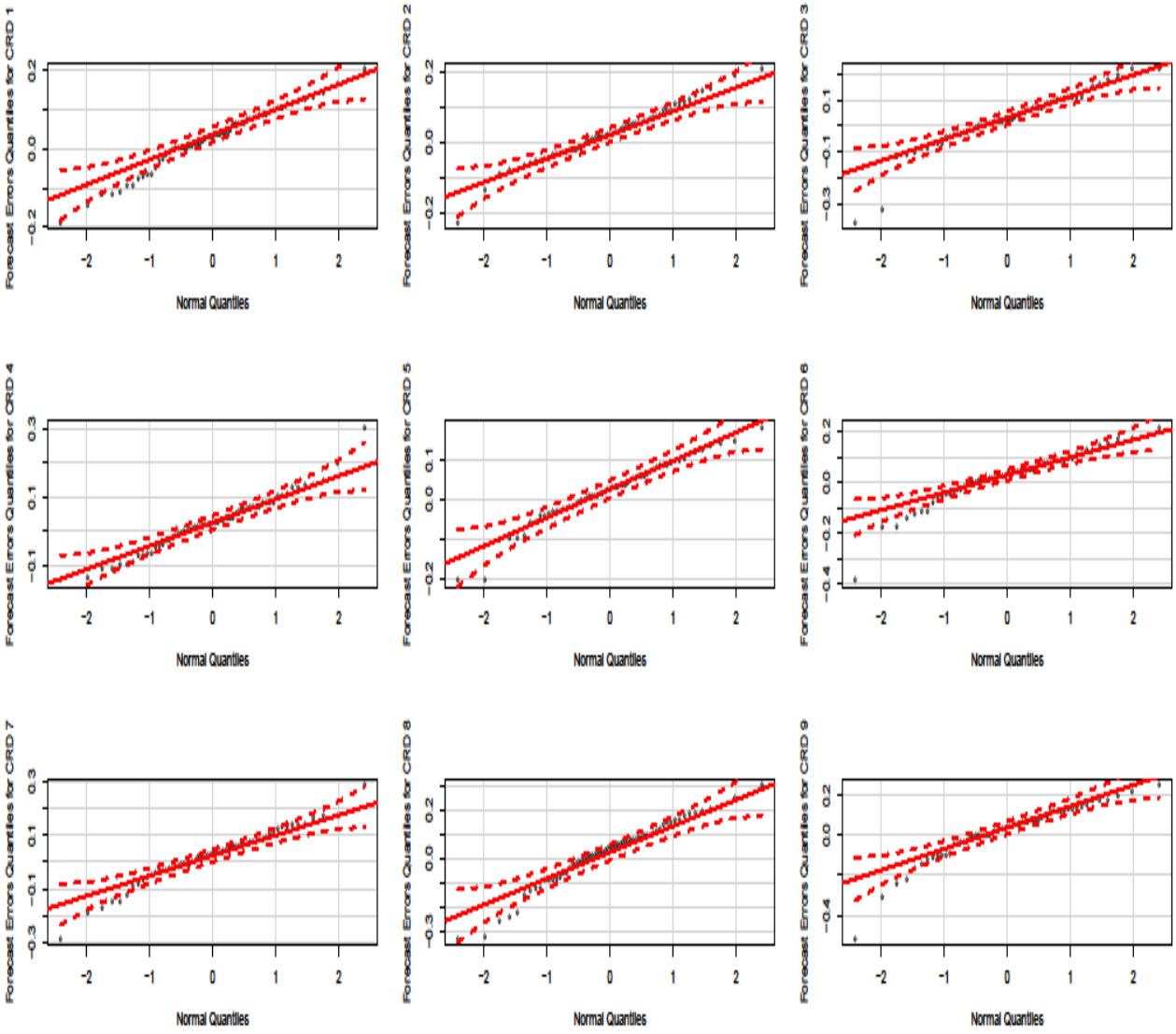

Figure 2.12: Normal QQ-plot for CRDs 1–9

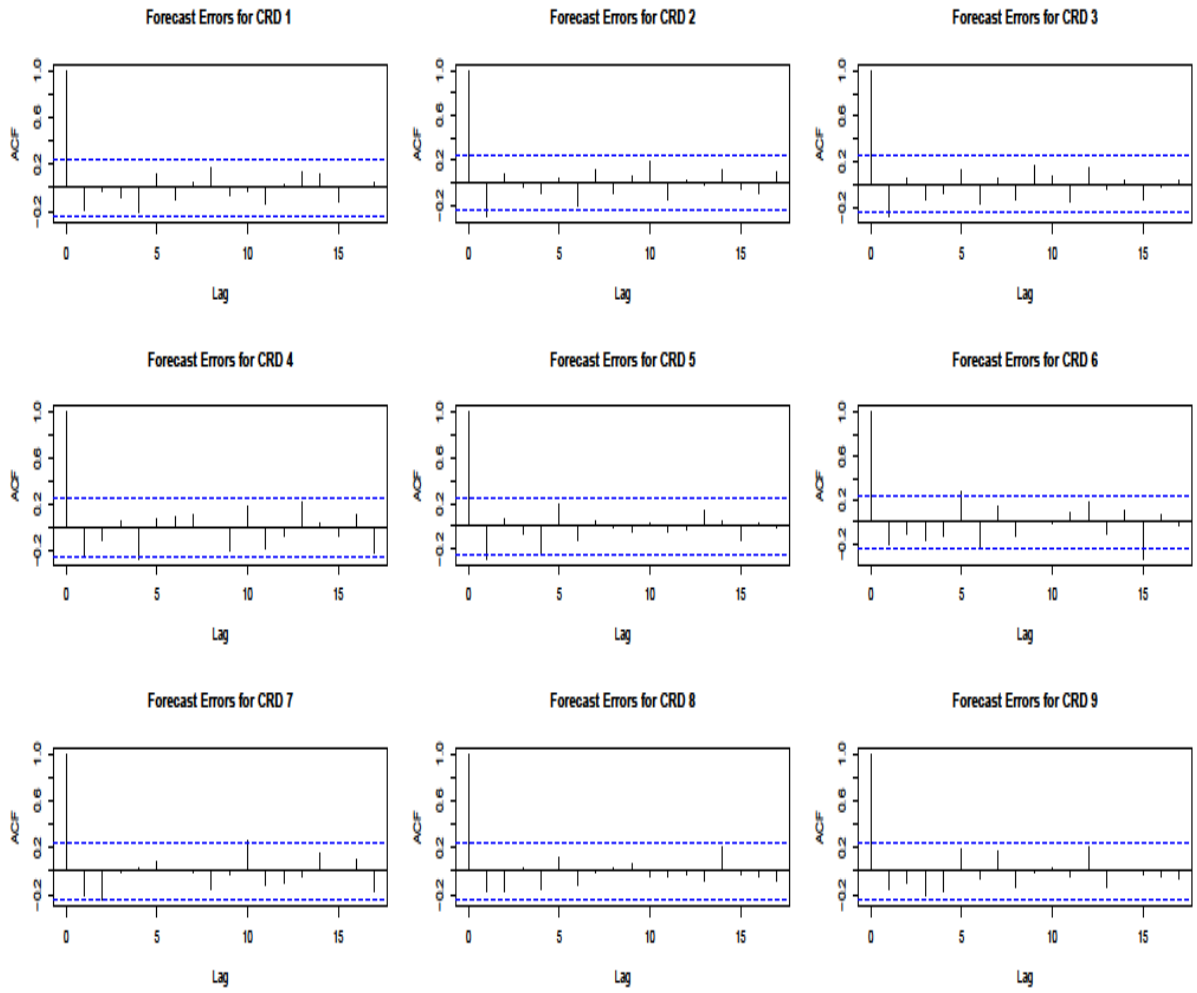

Figure 2.13: ACF for CRDs 1–9

CHAPTER 3. LONG-TERM CORN REVENUE INSURANCE

Abstract

This paper develops a long-term corn revenue insurance product that provides corn and soybean growers with yield or revenue protection for as long as five years into the future. It provides liability and indemnity formulas, sample premium rates and guarantees for a single producer. The method is calibrated so that in the first year, the premium rate is identical to the 75% premium rate that the producer would pay under the current single year insurance product. A commodity price model with mean reversion and seasonality in both the level of spot prices and their convenience yields is applied to generate long-run corn futures prices. A dynamic linear model with weather effects on corn yield is adopted to generate long-run corn yield forecasts. The historical correlation between corn yield and price is used to derive the corn revenue distribution. The premium rate is calculated according to the corn revenue distribution and the coverage level.

3.1 Introduction

Crop insurance, as it is currently structured, provides protection for only one crop year. But consider the risks faced by a farmer who plans to purchase land or machinery. This investment will require multiple years of earnings to repay. Producers who find themselves in this position should benefit from having a long-term revenue guarantee. One of the difficulties of providing long-term corn revenue insurance is the lack of long-term forecasts

of corn prices and yields. Modeling crop prices and yields has been a popular topic in the agricultural economics literature.

Kaldor (1939) pointed out that commodity markets are characterized by convenience yields. The theory of storage implies that convenience yields are negatively related to the inventory levels. Therefore, convenience yield is low when inventory is abundant, and it is high when inventory is scarce. Another important feature of commodity markets is mean reversion. Peterson, Ma, and Ritchey (1992), as well as Allen, Ma, and Pace (1994), found evidence that commodity cash prices are mean reverting. Schwartz (1997) constructed a two-factor model where convenience yield exhibits mean reversion and he found strong mean reversion in commodity prices. It is widely accepted that agricultural markets exhibit seasonality. By adding a deterministic seasonal component to the logarithm of commodity spot price, Sørensen (2002) introduced seasonality to agricultural commodity futures. Based on Schwartz (1997) and Sørensen (2002), Jin *et al*. (2012) constructed a two-factor model where both spot prices and convenience yields exhibit mean conversion and seasonality, so as to generate the long-term futures curve from existing futures prices. Also, they derived closed-form formulas for futures pricing which can be used to find futures prices with long maturity dates.

Crop yield is substantially affected by weather, especially temperature and rainfall. Foote and Bean (1951) were the first to suggest that crop yield distributions should depend on weather effects. Gallagher (1987) mentioned that weather could be one factor that causes a negatively skewed yield distribution. He suggested that crop yields are asymmetric and negatively skewed, and proposed a gamma distribution instead of a normal distribution to estimate soybean yields. Nelson and Preckel (1989) confirmed that the corn yield distribution

is negatively skewed and proposed a conditional beta distribution for corn yields. Nelson (1990) concluded that the beta distribution is better than the normal distribution for crop insurance premia calculation. Goodwin and Ker (1998) showed how a nonparametric kernel density can be used to estimate the corn yield density. They used an ARIMA process to estimate the mean yields for corn, and then used a nonparametric kernel smoother to estimate the deviations of corn yield from its mean.

Comparing the semi-parametric density estimator to the parametric density estimator and the nonparametric kernel density estimator, Ker and Coble (2003) concluded that the semi-parametric estimator with a normal distribution is more efficient than the other two estimators.

Recently, many researchers tried to capture how temperature and rainfall affect corn yield. Lobell and Asner (2003) suggested that corn yield decreases around 17% for each degree increment in temperature during the growing period. Deschênes and Greenstone (2007) also found that corn yield decreases in temperature and increases in rainfall. These two papers suggested that temperature and rainfall have a linear effect on corn yield. However, both Schlenker and Roberts (2006) and Schlenker and Roberts (2009) concluded that temperature has a nonlinear and asymmetric effect on corn yield. Increasing temperature improves corn yield at moderate levels, but it becomes seriously harmful for corn yield when it exceeds certain threshold. Using a two-knot linear spline model, Yu and Babcock (2011) found that corn yield is concave in both temperature and rainfall. The limitation of these papers is that they did not consider the interaction effect of temperature and rainfall. High temperature can evaporate rainfall. Therefore, temperature may offset or reinforce rainfall's effect on corn yields. Similarly, temperature may affect corn yield quite differently when

rainfall is at different levels. Based on these facts, this paper constructed a dynamic linear model taking drought, temperature and rainfall into consideration. Based on this dynamic linear model, long-term corn yield projections can be generated.

In this paper, we combine the price projection model from Jin *et al*. (2012) with a yield projection model of to examine the potential for multi-year crop insurance. We use the historical correlation between corn price and yield to generate the projected corn revenue insurance distribution. Iman and Conover (1982) introduced a method which rearranges the input variables so as to get the desired level of correlation. Following the Iman-Conover method, we rearrange corn price and yield draws so as to get the desired correlation between them. These correlated draws are then used to map out the corn revenue distribution.

The rest of this paper is organized as follows. In the next section, the long-term corn futures pricing model is introduced. In the third section, a long-term corn yield forecast model is provided. In the fourth section, the corn yield density estimator is described. In the fifth section, the corn revenue distribution is presented and the premium rate for corn revenue insurance is calculated. The sixth section concludes.

3.2 Long-Term Corn Futures Pricing Model

3.2.1 Corn Futures Pricing Model

It is widely accepted that commodity markets exhibit mean reversion and agricultural markets also exhibit seasonality. Jin *et al*. (2012) proved that a two-factor model where both spot price and convenience yield exhibit mean reversion and seasonality outperforms a model without seasonality and the model introduced by Schwartz (1997), where only convenience

yield exhibits mean reversion. Jin *et al*. (2012) also obtained closed-form futures pricing formulas which can be used to generate long-term corn futures prices. Therefore, we applied the two-factor model in Jin *et al*. (2012) to find the long-term corn futures prices.

Following Jin *et al*. (2012) , given convenience yield c_t as a constant, the corn spot price S_t is modeled as a geometric Brownian motion. That is:

$$dS_t = (\mu_s - c_t)S_t dt + \sigma_s S_t dz_s(t) \tag{3.1}$$

where $dz_s(t)$ is a Wiener process. Defining $x_t = \ln(S_t)$, and then by applying Ito's Lemma, we can get the stochastic process of x_t as follows:

$$dx_t = (\mu_x - c_t)dt + \sigma_x dz_x(t) \tag{3.2}$$

where $\mu_x \equiv \mu_s - \sigma_s^2/2$, $\sigma_x \equiv \sigma_s$ and $dz_x(t) \equiv dz_s(t)$.

When corn is relatively scarce, the corn price is high and its convenience yield is high, as well. Convenience yield is positively related to the spot price. Therefore, corn convenience yield c_t can be modeled as the sum of a linear function of the logarithm of its spot price $m_x x_t$ and an Ornstein-Uhlenbeck stochastic process y_t. We have:

$$c_t = y_t + m_x x_t \tag{3.3}$$

where the stochastic process of y_t is modeled as follows:

$$dy_t = (\mu_y - m_y y_t)dt + \sigma_y dz_y(t) \tag{3.4}$$

where $dz_y(t)$ is a Wiener process and $dz_x(t)dz_y(t) = \rho_{xy}dt$. Then, the corn spot price stochastic process can be written as:

$$dS_t = [\mu_s - y_t - m_x \ln(S_t)]S_t dt + \sigma_s S_t dz_s(t) \tag{3.5}$$

with $dz_s(t)dz_y(t) = \rho_{sy}dt$ and $\rho_{sy} \equiv \rho_{xy}$. Applying Ito's Lemma, we can get the Ornstein-Uhlenbeck stochastic process for the logarithm of the corn spot price:

$$dx_t = (\mu_x - y_t - m_x x_t)dt + \sigma_x dz_x(t) \tag{3.6}$$

Let r be the risk-free rate, and p_i for $i = s, y$ be the market price of risk for S_t and y_t respectively. In equilibrium, we have: $r + p_s = \mu_s(t)$. Therefore, the risk-neutral process of spot price can be rewritten as follows:

$$dS_t = [r - (y_t + m_x x_t)]S_t dt + \sigma_s S_t dz_s^Q(t) \tag{3.7}$$

According to Ito's Lemma, the corresponding risk-neutral process of dx_t can be written as:

$$dx_t = [r - \sigma_x^2/2 - (y_t + m_x x_t)]dt + \sigma_x dz_x^Q(t) \tag{3.8}$$

Similarly, the risk-neutral process of dy_t is:

$$dy_t = (\mu_y - m_y y_t - p_y)dt + \sigma_y dz_y^Q(t) \tag{3.9}$$

where $dz_x^Q(t)dz_y^Q(t) = \rho_{xy}dt$.

Seasonality is introduced into the model by allowing μ_x in equation (3.6) and μ_y in equation (3.9) to be a periodic deterministic function of time:

$$\mu_i(t) = \mu_{i,0} + \sum_{h=1}^{2} [\mu_{i,h,cos}\cos(2\pi ht)) + \mu_{i,h,sin}\sin(2\pi ht)] \tag{3.10}$$

where $i = x, y$ and $\mu_{i,0}$, $\mu_{i,h,cos}$ and $\mu_{i,h,sin}$ are constant seasonality parameters. If $\mu_{i,h,cos} = \mu_{i,h,sin} = 0$ for $h = 1,2$, then $\mu_i(t) = \mu_{i,0}$, and the model does not exhibit seasonality. The risk premium p_i where $i = s, y$ are also assumed to be a periodic deterministic function of time:

$$p_i(t) = p_{i,0} + \sum_{h=1}^{2} [p_{i,h,cos}\cos(2\pi ht)) + p_{i,h,sin}\sin(2\pi ht)] \tag{3.11}$$

where $i = s, y$ and $p_{i,0}$, $p_{i,h,cos}$ and $p_{i,h,sin}$ are constant seasonality parameters.

In this two-factor model, x_t and y_t are taken as the latent variables which can not be observed. The model can be simplified as follows:

$$\begin{pmatrix} dx_t \\ dy_t \end{pmatrix} \sim N\left(\begin{bmatrix} r - \sigma_x^2/2 - m_x x_t - y_t \\ \mu_y(t) - p_y(t) - m_y y_t \end{bmatrix} dt, \begin{bmatrix} \sigma_x^2 & \rho_{xy}\sigma_x\sigma_y \\ \rho_{xy}\sigma_x\sigma_y & \sigma_y^2 \end{bmatrix} dt \right)$$

According to Jin *et al*. (2012), the closed-form solution for the corn futures price at date t maturing at date T is:

$$\begin{aligned} F(t,T) &= E_t^Q[S(T)] \\ &= \exp[\kappa(t,T) + \delta(t,T)\omega(t) \end{aligned} \tag{3.12}$$

where $\omega(t) \equiv [x_t, y_t]'$, and $\kappa(t,T)$ and $\delta(t,T)$ are defined in Appendix A. Define $f_{t,T} \equiv \ln(F(t,T))$, then $f_{t,T}$ can be calculated as follows:

$$f_{t,T} = \kappa(t,T) + \delta(t,T)\omega(t) \tag{3.13}$$

Suppose we have a historical data set consisting of H $(H > 2)$ (logarithms of) futures prices with H different maturity dates. According to equation (3.13), and following Jin *et al*. (2012), we assume that all but two corn futures prices with distinct maturity dates are observed with normally distributed errors e_t. Then, the unobservable latent variables x_t and y_t can be calculated from the two futures prices which are perfectly correlated with the latent variables. Define $f_t^P \equiv [f_{t,T_1^P}^P, f_{t,T_2^P}^P,]'$ as the two perfectly correlated futures prices with maturity dates $[T_1^P, T_2^P]$. Similarly, define $f_t^{NP} \equiv [f_{t,T_1^{NP}}^P, f_{t,T_2^{NP}}^{NP}, \cdots, f_{t,T_{H-2}^{NP}}^{NP}]'$as the $(H-2)$ imperfectly correlated futures prices with maturity dates $[T_1^{NP}, T_2^{NP}, \cdots, T_{H-2}^{NP}]'$ respectively. Then,

$$f_{t,T^P}^P = \kappa(t,T^P) + \delta(t,T^P)\omega(t) \tag{3.14}$$

$$f_{t,T^{NP}}^{NP} = \kappa(t,T^{NP}) + \delta(t,T^{NP})\omega(t) + e_t \tag{3.15}$$

where $$\kappa(t,T^P) \equiv [\kappa(t,T_1^P),\kappa(t,T_2^P)]',$$

$$\delta(t,T^P) \equiv \begin{bmatrix} \delta_1(t,T_1^P) & \delta_2(t,T_1^P) \\ \delta_1(t,T_2^P) & \delta_2(t,T_2^P) \end{bmatrix},$$

$$\kappa(t,T^{NP}) \equiv [\kappa(t,T_1^{NP}),\kappa(t,T_2^{NP}),\cdots,\kappa(t,T_{H-2}^{NP})]', \text{ and}$$

$$\delta(t,T^{NP}) \equiv \begin{bmatrix} \delta_1(t,T_1^{NP}) & \delta_2(t,T_1^{NP}) \\ \cdot & \cdot \\ \cdot & \cdot \\ \cdot & \cdot \\ \delta_1(t,T_{H-2}^{NP}) & \delta_2(t,T_{H-2}^{NP}) \end{bmatrix}.$$

The errors e_t are assumed to be multivariate normally distributed, that is, $e_t \sim N(\underline{0}_{(H-2)\times 1}, \sigma_e^2 \Omega)$, where $\underline{0}_{(H-2)\times 1}$ is an $(H-2)$ vector of zeros, σ_e^2 is a scalar, $\boldsymbol{\Omega}$ is an $(H-2)\times(H-2)$ matrix with the i,jth element equal to $\rho^{|i-j|}$ and $\rho \in (-1,1)$.

3.2.2 Empirical Results for Corn Futures Price Model

The futures prices used to estimate corn future price model are the monthly mean settlement prices at the Chicago Mercantile Exchange (CME) from January 1995 to August 2012. The longest maturity in the corn futures sample is 48 months. Corn futures have only five maturity months: March, May, July, September and December. The risk-free rate is fixed at the 0% level. The Bayesian MCMC procedure introduced in Jin *et al*. (2012) is adopted to generate three MCMC chains for each parameter. Each chain is started at a different initial value and run for two million iterations. The first one million iterations are discarded as the burn-in period, and then we use the remaining one million iterations to test for convergence and make Bayesian posterior inference. We use Gelman-Rubin Diagnostics to test the convergence of the obtained MCMC chains. Estimation results for the corn futures pricing model are summarized in Table 3.1.

The Gelman-Rubin test statistics are reported in column 7 of Table 3.1. The MCMC chains converge very well for all of these parameters. According to Table 3.1, most of the parameters are significantly different from zero at the 0.025 level, whereas $\mu_{x,1,sin}$ and $p_{x,1,sin}$ are significantly different from zero at the 0.05 level. The correlation coefficient ρ is not significantly different from zero at standard levels, which indicates that the unobservable errors for the imperfectly correlated futures prices are uncorrelated. The mean reversion parameters m_x and m_y are estimated to be 0.0473 and 1.1476 respectively, supporting the assumption that corn spot price and convenience yield are mean reverting. The estimated seasonality parameters also provide strong evidence of seasonality in both corn spot price and convenience yield. Therefore, the corn market does exhibit mean reversion and seasonality in both spot price and convenience yield.

This paper considers a corn revenue insurance product that would provide protection for five years. Usually, crop insurance contracts use the average futures prices for a harvest time futures contract (in the case of corn, the contract is the December futures) during a month before planting (February) as the projected insurable price. To proceed, it is assumed that futures prices are lognormally distributed. For this analysis, it is assumed that the insurance product is made available in February 2012 and covers the $2012 - 2016$ crop years. For the price distributions, we need the means and implied volatilities of futures prices in

February 2012 for the December corn futures contracts maturing in December for the years 2012 to 2016. Given the current structure of the corn futures market, the contract with the longest time to maturity in February 2012 is the December 2014 corn futures contract at 34 months. Therefore, the required futures prices data are available for years 2012 to 2014.

However, the current futures market does not provide estimates for the prices in 2015 or 2016. The results from the Jin *et al*. (2012) model are used to construct those projections. The corn futures price data for years 2012 to 2014 are $5.68, $5.56 and $5.49 per bushel. The results from the Jin *et al*. (2012) model indicated the projected corn futures price for the December 2015 corn futures would be roughly 18 cents below the price for December 2014. Also, the December 2016 price would be approximately 34 cents below the December 2014 price. Therefore, the projected corn futures price for year 2015 is $5.31 per bushel and for year 2016 is $5.15 per bushel.

By including the mean reversion and seasonality to the spot price and convenience yield, option premia are significantly lower than for the Black-Scholes model (Jin (2011), Chapter 3). For the present work, the option pricing formula in Jin (2011) is adopted to calculate the at-the-money option premia.We then use the projected futures prices and the at-the-money option premia to calculate implied volatilities for futures prices in years 2012 to 2016. The calculated implied volatilities for these years are: 25.49%, 29.27%, 33.15%, 36.48% and 39.31% respectively. The implied volatility increases over time as there is more uncertainty and risk in future price movements.

3.3 Long Term Corn Yield Forecast Model

3.3.1 Dynamic Linear Model

The dynamic linear model was first used by Moss and Shonkwiler (1993) to estimate yield distribution with a stochastic trend. Moss and Shonkwiler (1993) found that corn yield has a non-stochastic trend under the assumption of normality. They tested for normality, and

claimed that the normality assumption is inappropriate. Using a hyperbolic sine transformation of normality for corn yield residuals, they found corn yield has a stochastic trend.

The weather factors included in the model are the number of days that temperature exceeds 93^oF in July, the monthly average rainfall from April to August, and the monthly average drought index from June to August. The model used the Palmer Modified Drought Index (PMDI), which is a long-term cumulative drought index. PMDI is negative under drought conditions and positive under wet conditions. The dynamic linear model was specified as follows:

$$q_t = \theta_t + \psi_1 d_t^2 + \psi_2 z_t^2 + \psi_3 z_t + \psi_4 z_t n_t + \varepsilon_t, \tag{3.16}$$

$$\theta_t = \theta_{t-1} + \beta_{t-1} + \nu_t, \tag{3.17}$$

$$\beta_t = \beta_{t-1} + \eta_t, \tag{3.18}$$

where $t = 1931,\cdots,2011$, q_t, d_t, z_t and n_t denote corn yield, drought index, rainfall and the number of days that temperature exceeds 93^oF respectively. This dynamic model allows for a stochastic yield trend which is represented by the state variables θ_t and β_t, where θ_t represents yield trend and β_t is the change of the yield trend. The stochastic part of the yield and state variables are represented by the error term ε_t, ν_t and η_t. We assume that the error terms are independently normally distributed: $\varepsilon_t \sim N(0, \sigma_\varepsilon^2)$, $\nu_t \sim N(0, \sigma_\mu^2)$ and $\eta_t \sim N(0, \sigma_\eta^2)$. The parameters ψ_1 to ψ_4 capture the weather effect. The state variables and parameters are estimated using the Gibbs sampling algorithm.

3.3.2 Yield Estimation Results

As an example, let us examine Lee County, Iowa. For the yield estimation, historical yield and weather data were collected from 1931 to 2011. The county-level corn yield data were collected from the National Agriculture Statistics Service (NASS), and were measured in bushels per acre. Corn yield is calculated as the total county-level production divided by acres harvested. County-level weather data were obtained from the National Oceanic and Atmospheric Administration (NOAA). The weather data include daily maximum temperature in July, measured in degrees Celsius; monthly drought indices from June to August; and monthly rainfall from April to August, measured in inches. The number of days that the temperature exceeds $93^{o}F$ was calculated from the daily temperature data.

The Bayesian MCMC procedure was adopted to generate three MCMC chains for each parameter of the yield model, and the detailed procedure is provided in Appendix B. Each chain was run for 200,000 iterations. We discarded the first 100,000 iterations as the burn-in period, and then used the remaining iterations to test for convergence and to make Bayesian posterior inference. Similar to the corn futures pricing model, we used the Gelman-Rubin Diagnostics to test the convergence of the obtained MCMC chains. The estimated results are reported in Table 3.2.

According to Table 3.2, σ_{μ}^{2} and σ_{η}^{2} are greater than zero, which indicates that corn yield in Lee county has a stochastic yield trend. All of the parameters are significantly different from zero at the 2.5% level. Parameter ψ_1 is negative, which indicates that both drought and wetness have negative effect on corn yield. Parameter ψ_4 indicates that the number of days that the temperature exceeds $93^{o}F$ in July has a negative effect on corn yield. It also suggests

that higher temperature together with higher rainfall reduces corn yield more severely. The estimates of ψ_2, ψ_3 and ψ_4 imply an asymmetric and concave relationship between rainfall and corn yield.

The posterior mean of the corn yield trend θ_t is shown in Figure 3.1, whereas the posterior mean of the change of corn yield trend β_t is depicted in Figure 3.2. According to Figure 3.2, the increase of the corn yield trend has declined since 2000. The posterior mean of the increase of the corn yield trend in 2011 is 0.33. The posterior mean of the corn yield trend in 2011 is 117.17. Combining these pieces of information, the corn yield forecasts before accounting for weather effects are 117.50, 117.83, 118.16, 118.49 and 118.82 bushels per acre for years 2012 to 2016, respectively. We used the mean of the historical weather data to build in the weather effect on the long-term yield forecast for years 2012 to 2016. The final corn yield forecasts for years 2012 to 2016 are 146.58, 146.91, 147.24, 147.57 and 147.90 bushels per acre, respectively.

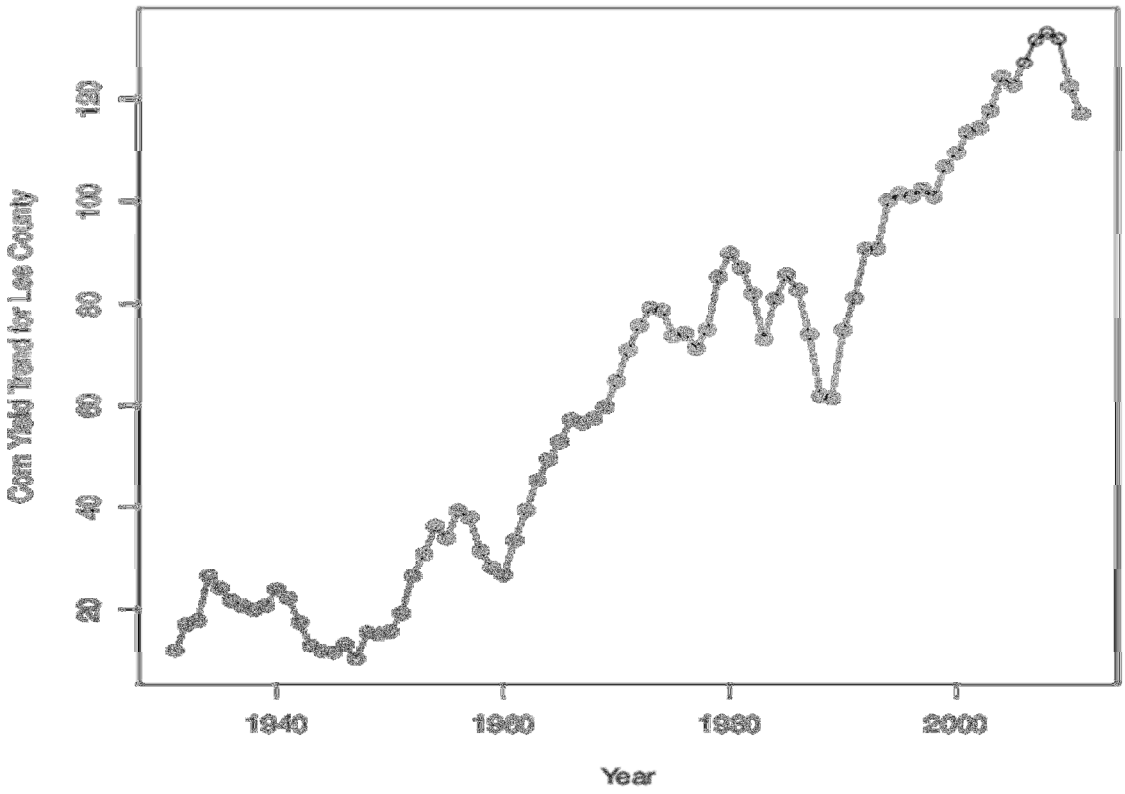

Figure 3.1: Posterior mean of corn yield trend for Lee County

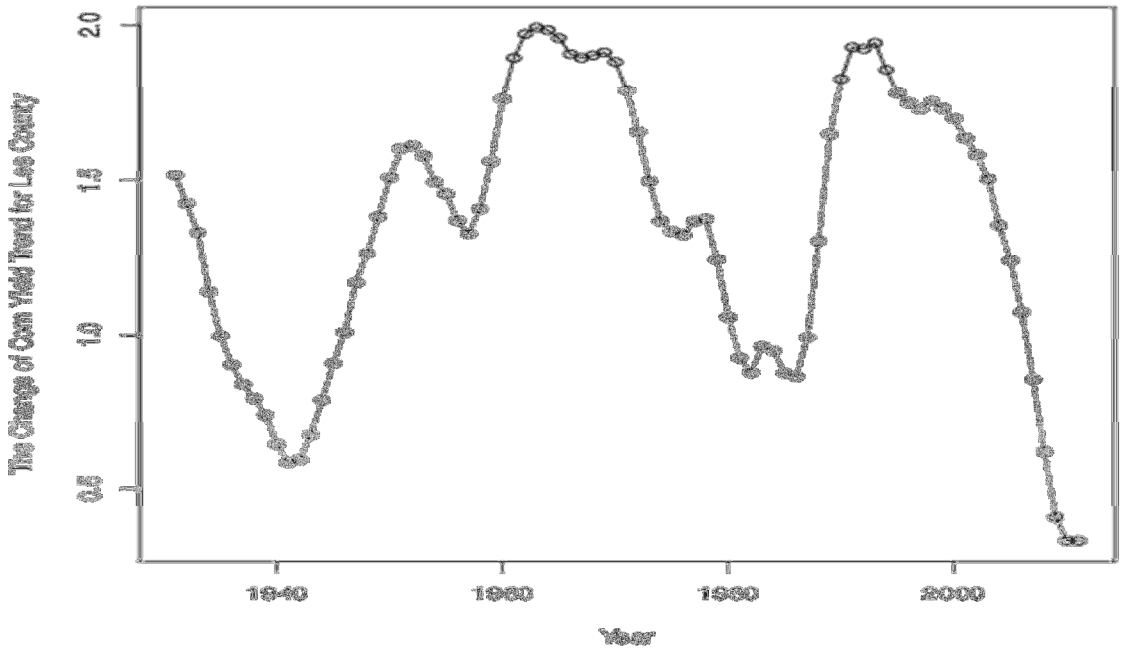

Figure 3.2: Posterior mean of the change of corn yield trend for Lee County

3.4 Semiparametric Corn Yield Distribution Estimator

The model outlined above provides an appropriate yield projection, but evaluating the potential insurance product also requires the distribution of potential yields around the estimated trends. Ker and Coble (2003) concluded that the semiparametric estimator with a normal distribution outperforms the parametric estimator and the standard nonparametric kernel estimator for yield distribution estimation. Therefore, the semiparametric estimator started with a normal distribution is adopted to estimate the conditional corn yield distribution for Lee county.

The semiparametric estimator is specified as follows:

$$d(x) = \frac{1}{nh}\sum_{i=1}^{n} \exp\left(-\frac{((e_i - x)/h)^2}{2}\right)\frac{\exp\left(-\frac{(x-\hat{\mu})^2}{2\hat{\sigma}^2}\right)}{\exp\left(-\frac{(e_i-\hat{\mu})^2}{2\hat{\sigma}^2}\right)}, \tag{3.19}$$

where h is the smoothing parameter which is called bandwidth, n is the number of yield observations, $\hat{\mu}$ and $\hat{\sigma}^2$ are the MLE estimates of the mean and variance of the normal distribution, respectively, and e_i is the detrended yield (defined as the difference between the actual yield data and the yield forecast obtained from the dynamic linear model). Here we used the standard normal kernel estimator, and the bandwidth h was selected according to the Silverman's rule of thumb. The estimated corn yield density for Lee county is shown in Figure 3.3, which is negatively skewed and has a hump.

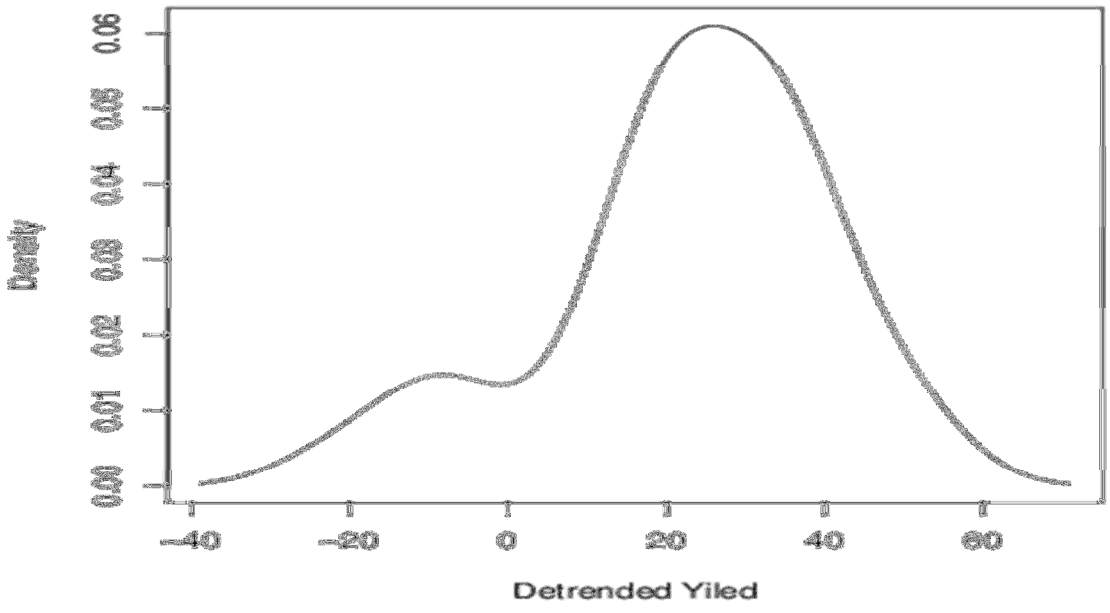

Figure 3.3: Corn yield density for Lee County

The density function (19) can be rewritten as follows:

$$d(x) = \frac{1}{nh}\sum_{i=1}^{n} \exp\left(-\frac{\left(x - \frac{\hat{\sigma}^2 e_i + h^2\hat{\mu}}{\hat{\sigma}^2 + h^2}\right)^2}{2\frac{\hat{\sigma}^2 h^2}{\hat{\sigma}^2 + h^2}}\right)\exp\left(\frac{(\hat{\sigma}^2 e_i + h^2\hat{\mu})^2}{2\hat{\sigma}^2 h^2(\hat{\sigma}^2 + h^2)} + \frac{(e_i - \hat{\mu})^2}{2\hat{\sigma}^2}\frac{\hat{\sigma}^2 e_i^2 + h^2\hat{\mu}^2}{2\hat{\sigma}^2 h^2}\right)$$

Denote $\mu_i = \frac{\hat{\sigma}^2 e_i + h^2\hat{\mu}}{\hat{\sigma}^2 + h^2}$, $\sigma^2 = \frac{\hat{\sigma}^2 h^2}{\hat{\sigma}^2 + h^2}$ and $\omega_i = \frac{1}{nh}\exp\left(\frac{(\hat{\sigma}^2 e_i + h^2\hat{\mu})^2}{2\hat{\sigma}^2 h^2(\hat{\sigma}^2 + h^2)} + \frac{(e_i - \hat{\mu})^2}{2\hat{\sigma}^2} - \frac{\hat{\sigma}^2 e_i^2 + h^2\hat{\mu}^2}{2\hat{\sigma}^2 h^2}\right)$.

Then $d(x) = \sum_{i=1}^{n} \omega_i \exp\left(-\frac{(x-\mu_i)^2}{2\sigma^2}\right)$ which is a mixture of n normal distributions with different means (μ_i) and same variance(σ^2), where $\omega_i's$ are the weights. The weights ω_i can be normalized as $\widehat{\omega}_i = \frac{\omega_i}{\sum_{i=1}^{n}\omega_i}$. Therefore, by drawing a sample from these normal distributions with probability $\widehat{\omega}_i$'s, we can get a sample for the density function (3.19).

3.5 Corn Revenue Insurance

In the preceding sections, we obtained the projected futures prices and corn yields that would determine the guarantee for a multi-year revenue insurance product. We also constructed samples from the yield distribution. In addition, we required samples from the futures price distribution. As was stated before, futures prices are assumed to be lognormally distributed, based on the projected price and the implied volatility. Denoting μ and σ^2 as the mean and variance of the lognormal distribution, respectively, they were estimated as:

$$\mu = \ln(P_p) - \sigma^2/2, \tag{3.20}$$

$$\sigma^2 = \ln(1 + V^2), \tag{3.21}$$

where P_p is the projected price, and V is the implied volatility. The projected prices, yield forecasts, and implied volatilities are reported in Table 3.3. The distribution of the logarithm of futures prices can thus be obtained for each year.

The final piece needed is the correlation structure between corn prices and yields. We used the historical correlation between corn price and yield to construct the corn revenue distribution. The historical correlation was calculated as:

$$\rho_{p,y} = \frac{\sum_i (P_{h,i} - P_{p,i})(Q_{h,i} - Q_{f,i})}{\sqrt{\sum_i (P_{h,i} - P_{p,i})^2 \sum_i (Q_{h,i} - Q_{f,i})^2}}, \tag{3.22}$$

where $i = 1976, \cdots, 2011$. $P_{h,i}$ and $Q_{h,i}$ are corn harvest price and yield in year i. $P_{p,i}$ is the projected corn price in year i. $Q_{f,i}$ is the corn yield forecast for year i. For each year, we took the December corn futures price in February as the projected price, and the December corn futures prices in October as the harvest price. Corn yield one-step ahead forecasts were obtained from the dynamic linear model in section 3.3, and the means of the historical weather data were used.

3.5.1 Corn Revenue Insurance at the County Level

According to section 3.3, weather factors such as temperature, rainfall, and the number of days that temperature exceeds $93^o F$ substantially affect corn yield. An increase in the covariance of rainfall, temperature, and drought index may cause a decrease in the mean of corn yield and an increase in yield variability, which substantially affects the premium rates of crop insurance products. Therefore, in the construction of a multi-year revenue insurance product, we incorporate the variability of these weather factors to calculate the premium rate.

We used the semiparametric method described in section 3.4 to estimate the distributions of rainfall, drought index, and number of days that temperature exceeds 93^oF. We then collected 100,000 samples for rainfall, drought index, number of days that temperature exceeds 93^oF, and detrended corn yield from their distributions, denoting these samples as z_i, d_i, n_i and y_i $(i = 1, \dots, 100{,}000)$, respectively. Also, the variability of the two state variables (σ_μ^2 and σ_η^2) was included in the premium calculation. We collected 100,000 samples for v_t and η_t from their estimated normal distributions, denoting these sample as v_i and η_i $(i = 1, \dots, 100{,}000)$, respectively. Following the Iman-Conover method, we rearranged all of these samples so as to impose the historical correlation between the weather factors. Then, for each year from 2012 to 2016, we obtained 100,000 samples of corn yields (q_i) from these rearranged samples and the forecasted yield trend $(trend_t, t = 2012, \dots, 2016)$. For example, the 100,000 samples for corn yield in 2012 were obtained from the equation: $q_i = trend_{2012} + y_{i'} + \psi_1 d_{i'}^2 + \psi_2 z_{i'}^2 + \psi_3 z_{i'} + \psi_4 z_{i'} n_{i'} + v_{i'} + \eta_{i'}$, where i' indicates the reordered i.

We take Lee County as an example to illustrate how the premium rate is calculated at the county level. The historical correlation between corn price and yield for Lee County is -0.37. For years 2012 to 2016, the price samples were generated from their lognormal distributions. Using the Iman-Conover method, we imposed the historical correlation -0.37 between corn price and yield. The revenue sample can be computed from these two rearranged samples. The densities of county level corn revenue per acre based on the simulated samples for year 2012 to 2016 are shown in Figure 3.4.

Prices are lognormally distributed for years 2012 to 2016, and corn yield is negatively skewed. Since the correlation between price and yield is -0.37, it does not totally offset the skewness of price and yield, the corn revenue distribution looks like a lognormal distribution. The revenue distribution shifts to the left over time, because the expected price decreases over time, while the yield increases very slowly.

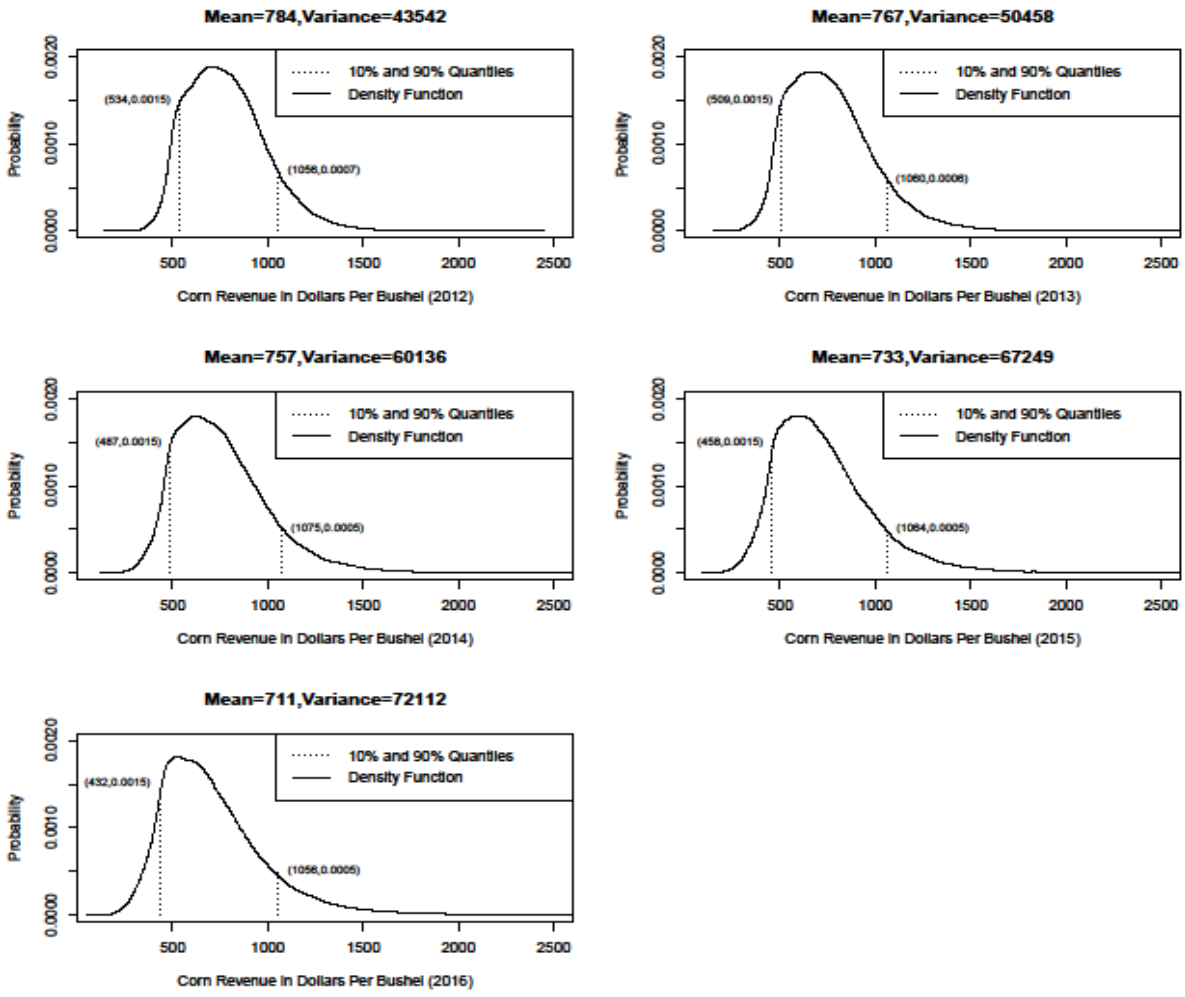

Figure 3.4: Density of corn revenue in dollars per acre for years 2012 to 2016

The liability (R_g) for corn revenue insurance is calculated from the following equation:

$$R_g = C_l \times P_p \times Q_f \tag{3.23}$$

where C_l is the coverage level which range from 65% to 90%, and Q_f is the corn yield forecast. The liability for each year at each coverage level is reported in Table 3.4. For each coverage level, the liability decreases over time because of the decrease in expected price.

We consider the situation in which farmers get their indemnity at the end of each year. The total indemnity (I) for each year is calculated as follows:

$$I = E(R_g - P_h \times Q_h | R_g > P_h \times Q_h), \tag{3.24}$$

where P_h is the corn harvest price, and Q_h is the corn harvest yield. The Loss Cost Ratio (LCR) is calculated as in the following equation:

$$LCR = I/R_g. \tag{3.25}$$

The simulated LCR is reported in Table 3.5.

According to Table 3.5, the higher coverage level has higher loss-cost ratio for each insured year. Also, for each coverage level, the loss-cost ratio increases over time. When the coverage level is higher, a higher revenue is insured; therefore, a higher premium must be paid. Uncertainty and risk increase with the time elapsed between the policy is purchased and the insured year, which requires a higher premium for policies with longer maturities. The current GRP rates for Lee County in 2012 are 0.0661, 0.0795, 0.0963, 0.1175 and 0.1369 for coverage levels ranging from 70% to 90%, respectively. On average, the premium rates computed from our model are lower than the GRP rates by 0.0489.

3.5.2 Corn Revenue Insurance at the Farm Level

For this analysis, we have assumed that the farm-level yield has the same mean but a higher variance than the county-level yield. In doing this, we enlarged the variance of the estimated yield distribution in section 3.4, while keeping its mean unchanged. Denote by σ_f^2 and σ_c^2 as the variance of farm- and county-level yields, respectively. Then, the relationship between σ_f^2 and σ_c^2 can be defined as $\sigma_f = k\sigma_c$. We solve for k where the farm level yield protection premium rate matches the current RMA yield protection premium rate at the 75% coverage level.

Using Lee County as an example, k was computed to be 1.94. That is, the standard deviation of the farm-level yield is 94% higher than the standard deviation of the county-level yield. The densities of farm-level corn revenue per acre based on the simulated samples for years 2012 to 2016 are depicted in Figure 3.5.

Since farm-level yield shares the same mean with the county-level yield, the liability for each year at each coverage level at the farm level is also the same as for the county level. In the case where farm level yields are different than the county, farm level yields will be calculated using the county level projection adjusted to maintain the same yield difference, measured in bushels per acre between the farm APH and the county. For example if the farm APH is five bushels less than the county in in 2013, then the farm level projected yield will be five bushels less than the projected county yield in 2018.

The loss-cost ratio for each year at each coverage level at the farm level is reported in Table 3.6. The current RP rates for Lee County in 2012 are 0.0738, 0.0954, 0.1208, 0.1502

and 0.1834 for coverage levels from 65% to 85%, respectively. On average, the premium rates computed from our model are lower than the RP rates by 0.0472.

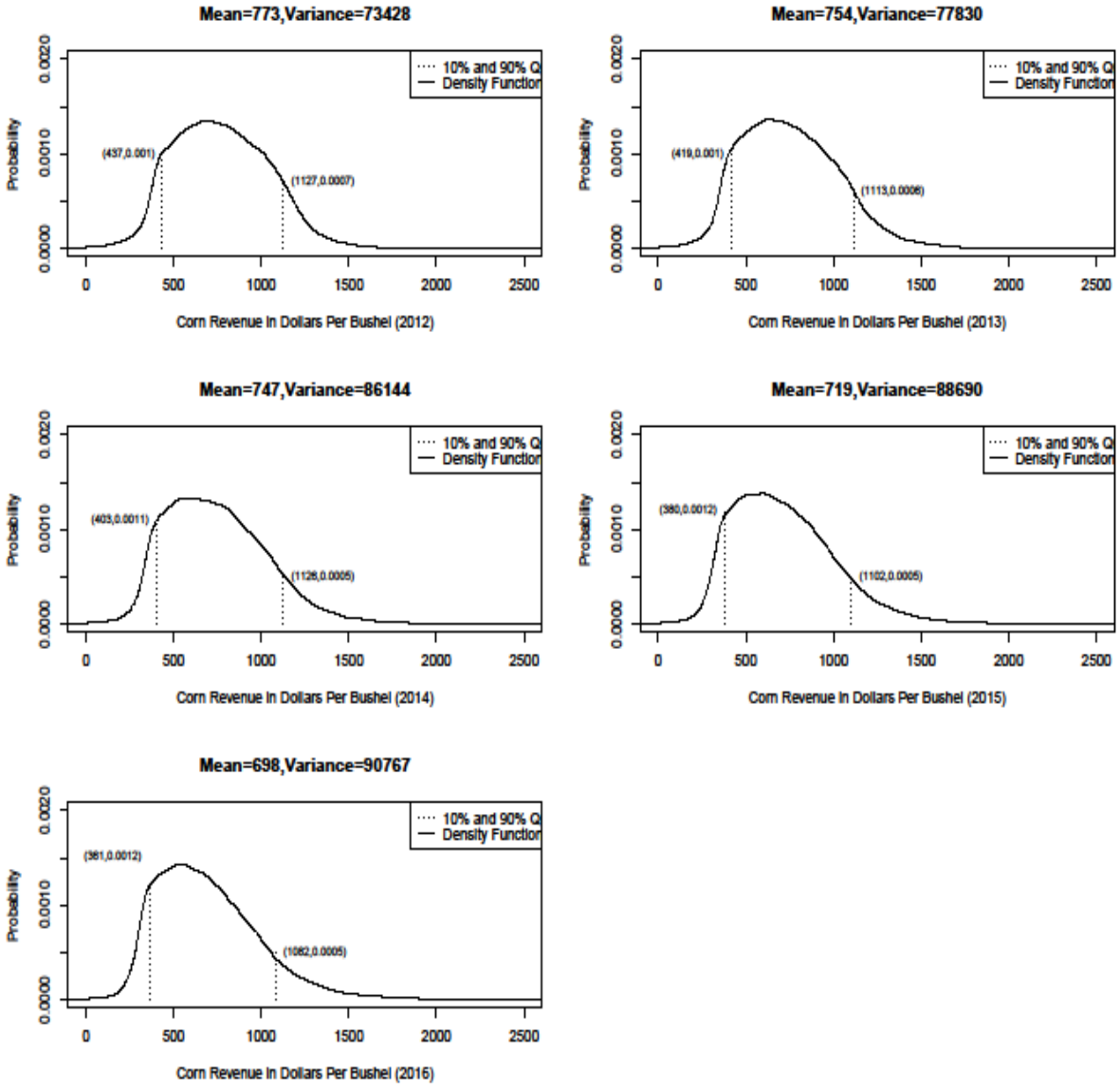

Figure 3.5: Histogram of farm level corn revenue in dollars per acre for years 2012 to 2016

Comparing Table 3.6 to Table 3.5, the loss-cost ratio at the farm level is higher than at the county level. Since the yield at the farm level is much riskier than at the county level, the insurance company will charge more to compensate for this risk. The percentage change between the farm- and county-level premium rates are reported in Table 3.7. For each coverage level, the percentage change decreases across years. The percentage changes for 2016 are sizably less than those for 2012. One possible reason is that both farm- and county-level yields have similar uncertainty in the distant future. Therefore, the difference between farm- and county-level premium rates are smaller for the year 2016.

3.6 Conclusion

This paper proposed a methodology to construct a long-term corn revenue insurance contract at both the county and farm levels. We adopted the long-term futures pricing model in Jin *et al*. (2012) to compute long-term corn futures prices, and calculated the volatility of futures price according to Jin (2011). Long-term corn yield forecasts were obtained using the dynamic linear model. A semiparametric estimator was adopted to estimate corn yield distributions. Following the Iman-Conover method, we rearranged corn price and yield samples so as to get the desired correlations. We then used the rearranged corn price and yield samples to construct the corn revenue distribution. Finally, premium rates were calculated from the resulting corn revenue distribution. The premium rates computed in our model are calibrated to equal the current 75% corresponding RMA rates at the farm level.

3.7 APPENDIX A

The definitions for $\kappa(t,T)$ and $\delta(t,T)$ are as follows:

$$\delta_1(t,T) = \exp(m_x(t-T)), \tag{3.26}$$

$$\delta_2(t,T) = \frac{\exp(m_x(t-T))-\exp(m_y(t-T))}{m_x-m_y}, \tag{3.27}$$

$$\begin{aligned}
\kappa(t,T) = {} & \frac{r-\sigma_x^2/2}{m_x}(\exp(m_x(t-T))-1) \\
& + \frac{\mu_{y,0}-p_{y,0}}{m_x-m_y}\left[\frac{1}{m_x}(\exp(m_x(t-T))-1) - \frac{1}{m_y}(\exp(m_y(t-T))-1)\right] \\
& + \sum_{h=1}^{2} \frac{\mu_{y,h,cos}-p_{y,h,cos}}{m_x-m_y}\left(\frac{1}{m_x^2+4\pi^2h^2} - \frac{1}{m_y^2+4\pi^2h^2}\right) \\
& \times \{m_x[\exp(m_x(t-T))\cos(2\pi ht) - \cos(2\pi hT)] \\
& + 2\pi h[\exp(m_x(t-T))\sin(2\pi ht) - \sin(2\pi hT)]\} \\
& + \sum_{h=1}^{2} \frac{\mu_{y,h,sin}-p_{y,h,sin}}{m_x-m_y}\left(\frac{1}{m_x^2+4\pi^2h^2} - \frac{1}{m_y^2+4\pi^2h^2}\right) \\
& \times \{m_x[\exp(m_x(t-T))\sin(2\pi ht) - \sin(2\pi hT)] \\
& + 2\pi h[\exp(m_x(t-T))\cos(2\pi ht) - \cos(2\pi hT)]\} \\
& - \frac{1}{2}\left\{\left[\frac{\sigma_x^2}{2m_x} + \frac{\rho_{xy}\sigma_x\sigma_y}{m_x(m_x-m_y)} + \frac{\sigma_y^2}{2m_x(m_x-m_y)^2}\right] \times [\exp(2m_x(t-T))-1]\right. \\
& - \left[\frac{2\rho_{xy}\sigma_x\sigma_y}{m_x^2-m_y^2} + \frac{2\sigma_y^2}{(m_x+m_y)(m_x-m_y)^2}\right] \times [\exp((m_x+m_y)(t-T))-1] \\
& \left. + \frac{\sigma_y^2}{2m_y(m_x-m_y)^2}[\exp(2m_y(t-T))-1]\right\}
\end{aligned} \tag{3.28}$$

3.8 APPENDIX B

Table 3.1: Estimation Results for Corn Futures Pricing Model

Parameters	Mean	2.5%	97.5%	5.0%	95.0%	Gelman-Rubin Test Statistics
m_x	0.0473	0.0371	0.0566	0.0345	0.0549	1.0113
m_y	1.1476	1.0734	1.2267	1.0722	1.2063	1.0022
σ_x	0.2621	0.2481	0.2772	0.2501	0.2746	1.0003
σ_y	0.2203	0.2052	0.2367	0.2070	0.2333	1.0002
ρ_{xy}	0.7172	0.6763	0.7547	0.6849	0.7508	1.0020
$\mu_{x,0}$	-0.0771	-0.0894	-0.0649	-0.0874	-0.0669	1.0002
$\mu_{x,1,cos}$	0.1847	0.1683	0.2011	0.1709	0.1983	1.0000
$\mu_{x,2,cos}$	-0.0406	-0.0558	-0.0254	-0.0532	-0.0277	1.0013
$\mu_{x,1,sin}$	0.0146	-0.0020	0.0312	0.0006	0.0285	1.0025
$\mu_{x,2,sin}$	0.0457	0.0263	0.0651	0.0292	0.0615	1.0014
$\mu_{y,0}$	-0.4588	-0.5335	-0.3804	-0.5170	-0.3598	1.0210
$\mu_{y,1,cos}$	-0.5976	-0.6560	-0.5389	-0.6467	-0.5479	1.0068
$\mu_{y,2,cos}$	0.7467	0.5645	0.9249	0.6035	0.9042	1.0148
$\mu_{y,1,sin}$	0.2079	0.1408	0.2738	0.1543	0.2655	1.0013
$\mu_{y,2,sin}$	0.9522	0.7037	1.1904	0.7460	1.1611	1.0030
$p_{x,0}$	-0.0427	-0.0552	-0.0300	-0.0533	-0.0322	1.0001
$p_{x,1,cos}$	0.1847	0.1683	0.2011	0.1709	0.1983	1.0000
$p_{x,2,cos}$	-0.0406	-0.0558	-0.0254	-0.0532	-0.0277	1.0013
$p_{x,1,sin}$	0.0146	-0.0020	0.0312	0.0006	0.0285	1.0025

Note: The four columns with 2.5%, 5.0%, 95.0% and 97.5% are the percentiles of the posterior probability band.

Table 3.2: Estimation Results for Corn Futures Pricing Model (Continued)

Parameters	Mean	2.5%	97.5%	5.0%	95.0%	Gelman-Rubin Test Statistics
$p_{y,0}$	-0.1331	-0.1534	-0.1139	-0.1498	-0.1170	1.0011
$p_{y,1,cos}$	0.1569	0.1306	0.1828	0.1355	0.1790	1.0029
$p_{y,2,cos}$	0.5299	0.3745	0.6801	0.3997	0.6628	1.0051
$p_{x,1,sin}$	0.1577	0.1337	0.1817	0.1379	0.1782	1.0014
$p_{x,2,sin}$	-0.2994	-0.4168	-0.1820	-0.4001	-0.2061	1.0111
ρ	-0.0004	-0.0395	0.0385	-0.0332	0.0325	1.0012
σ_e^2	0.0010	0.0009	0.0011	0.0009	0.0010	1.0000

Note: The four columns with 2.5%, 5.0%, 95.0% and 97.5% are the percentiles of the posterior probability band.

Table 3.3: Estimation Results for Corn Yield Forecast Model

Parameters	Mean	2.5%	97.5%	Gelman-Rubin Test Statistics
σ_ε^2	201.53	81.19	339.96	1.002
σ_μ^2	94.36	7.47	271.11	1.004
σ_η^2	1.33	0.01	7.51	1.009
ψ_1	-0.63	-1.06	-0.20	1.000
ψ_2	-1.95	-3.38	-0.49	1.000
ψ_3	18.48	7.23	29.50	1.000
ψ_4	-0.63	-0.84	-0.40	1.003

Note: The three columns with 2.5%, and 97.5% are the percentiles of the posterior probability band.

Table 3.4: Projected Price, Yield Forecast and Implied Volatility

	2012	2013	2014	2015	2016
projected price	5.68	5.56	5.49	5.31	5.15
yield forecast	146.58	146.91	147.24	147.57	147.90
implied volatility	25.49%	29.27%	33.15%	36.48%	39.31%

Table 3.5: Liability in Dollars Per Acre

	2012	2013	2014	2015	2016
65%	540.98	530.54	525.41	509.49	495.51
70%	582.60	571.35	565.83	548.68	533.63
75%	624.21	612.16	606.25	587.88	571.74
80%	665.83	652.97	646.66	627.07	609.86
85%	707.44	693.78	687.08	666.26	647.98
90%	749.06	734.59	727.50	705.45	686.09

Table 3.6: Loss Cost Ratio for Each Coverage Level at the County Level

	2012	2013	2014	2015	2016
65%	0.0010	0.0140	0.0203	0.0263	0.0322
70%	0.0194	0.0250	0.0328	0.0400	0.0472
75%	0.0321	0.0392	0.0484	0.0566	0.0649
80%	0.0477	0.0561	0.0665	0.0755	0.0845
85%	0.0660	0.0754	0.0867	0.0962	0.1058
90%	0.0866	0.0968	0.1086	0.1186	0.1283

Table 3.7: Loss Cost Ratio for Each Coverage Level at the Farm Level

	2012	2013	2014	2015	2016
65%	0.0466	0.0502	0.0548	0.0602	0.0642
70%	0.0605	0.0651	0.0706	0.0769	0.0813
75%	0.0760	0.0815	0.0878	0.0949	0.0999
80%	0.0931	0.0994	0.1062	0.1140	0.1196
85%	0.1114	0.1184	0.1256	0.1340	0.1400
90%	0.1308	0.1383	0.1458	0.1547	0.1610

Table 3.8: Percentage Change Between The Farm and County Level Premium Rates

	2012	2013	2014	2015	2016
65%	366.00%	258.57%	169.95%	128.90%	99.38%
70%	211.86%	160.40%	115.24%	92.25%	72.25%
75%	136.76%	107.91%	81.40%	67.67%	53.93%
80%	95.18%	77.18%	59.70%	50.99%	41.54%
85%	68.79%	57.03%	44.87%	39.29%	32.33%
90%	51.04%	42.87%	34.25%	30.44%	25.49%

3.9 APPENDIX C

We use the conjugate priors for the state variables and parameters. The conjugate prior for θ_0, β_0 and ψ_i where $i = 1,\ldots,4$ is normal distribution $N(0,100)$. We choose the variance of the prior to be 100 so as to reasonably diffuse the prior. The conjugate prior for σ_ε^2, σ_μ^2

and σ_ω^2 is uniform distribution $U(0,1000)$. Similarly, 1000 is chosen so as to reasonably diffuse the prior of the variances.

To simplify the writing, denote X_t as follows:

$$X_t = \psi_1 d_t^2 + \psi_2 z_t^2 + \psi_3 z_t + \psi_4 z_t n_t \tag{3.29}$$

Then, the likelihood function can be written as follows:

$$\begin{aligned} L(\cdot) &= f(y_{1:T}|\theta_{0:T}, \beta_{0:T}, \sigma_\varepsilon^2, \sigma_\mu^2, \sigma_\omega^2, \psi_1, \ldots, \psi_4, n_{1:T}, d_{1:T}) \\ &= \prod_{t=1}^{T} f(y_t|\theta_{0:T}, \beta_{0:T}, \sigma_\varepsilon^2, \sigma_\mu^2, \sigma_\omega^2, \psi_1, \ldots, \psi_4, n_{1:T}, d_{1:T}) \\ &= (2\pi\sigma_\varepsilon^2)^{-\frac{T}{2}} \exp\left(-\frac{1}{\sigma_\varepsilon^2}\sum_{t=1}^{T} (y_t - \theta_t - X_t)^2\right) \end{aligned} \tag{3.30}$$

The conditional posterior distributions are derived according to the conjugate priors and the likelihood function. The conditional posterior distributions of the three variance parameters are as follows:

$$\sigma_\varepsilon^2|y_{1:T}, \theta_{0:T}, \beta_{0:T}, \sigma_\mu^2, \sigma_\omega^2, X_{1:T} \sim IG\left(\frac{T}{2} - 1, \left(\frac{1}{2}\sum_{t=1}^{T} (y_t - \theta_t - X_t)^2\right)^{-1}\right) \tag{3.31}$$

$$\sigma_\mu^2|y_{1:T}, \theta_{0:T}, \beta_{0:T}, \sigma_\varepsilon^2, \sigma_\omega^2, X_{1:T} \sim IG\left(\frac{T}{2} - 1, \left(\frac{1}{2}\sum_{t=1}^{T} (\theta_t - \theta_{t-1})^2\right)^{-1}\right) \tag{3.32}$$

$$\sigma_\omega^2|y_{1:T}, \theta_{0:T}, \beta_{0:T}, \sigma_\varepsilon^2, \sigma_\mu^2, X_{1:T} \sim IG\left(\frac{T}{2} - 1, \left(\frac{1}{2}\sum_{t=1}^{T} (\beta_t - \beta_{t-1})^2\right)^{-1}\right) \tag{3.33}$$

Therefore, based on these three conditional posterior distribution, we can draw samples for σ_ε^2, σ_μ^2 and σ_ω^2. Following the Kalman Filter introduced in Campagnoli et al. (2009), the conditional posterior distribution of θ_T, β_T and ψ_i $(i = 1, \ldots, 4)$ can be obtained. Then, by using a forward filtering backward sampling (FFBS) algorithm, we can draw sample for θ_t,

β_t $(t = 1, \ldots, T)$ and ψ_i $(i = 1, \ldots, 4)$. This FFBS method came from Carter and Kohn (1994), FrühwirthSchnatter (1994) and Jong and Shephard (1995).

The steps to draw samples are as follows:

• Step 1: choose initial values for $\sigma_\varepsilon^{2[0]}$, $\sigma_\mu^{2[0]}$, $\sigma_\omega^{2[0]}$, θ_0, β_0 and ψ_i $(i = 1, \ldots, 4)$.

• Step 2: using the prior distribution for θ_0, β_0 and ψ_i $(i = 1, \ldots, 4)$, together with the initial values in step 1, run the Kalman Filter.

• Step 3: using forward filtering backward sampling (FFBS) algorithm to get the sample of $\theta_{0:T}^{[j]}$, $\beta_{0:T}^{[j]}$ and $\psi_i^{[j]}$ $(i = 1, \ldots, 4)$.

• Step 4: calculate $X_{1:T}^{[j]}$

• Step 5: draw $\sigma_\varepsilon^{2[j]}$ using equation (3.31)

• Step 6: draw $\sigma_\mu^{2[j]}$ using equation (3.32)

• Step 7: draw $\sigma_\omega^{2[j]}$ using equation (3.33)

• step 8: substitute for the values of $\sigma_\varepsilon^{2[j]}$, $\sigma_\mu^{2[j]}$ and $\sigma_\omega^{2[j]}$ in Step 1, and repeat Steps $1 - 8$ for 200,000 iterations. In the first step, we chose three different initial values for $\sigma_\varepsilon^{2[0]}$, $\sigma_\mu^{2[0]}$ and $\sigma_\omega^{2[0]}$ so as to generate three different MCMC chains.

CHAPTER 4. THE IMPACT OF CLIMATE CHANGE ON IOWA CORN YIELD

Abstract

This paper estimates the impact of projected climate change on corn yields in Iowa. The climate projection data includes sixteen unique combinations of carbon emissions scenarios and global climate models. Climate impact scenarios are based on projected changes in daily maximum temperature in July and the amount of rainfall from June to August. Controlling for the uncertainty in yield projection, results indicate that projected climate change will cause a reduction of corn yield by 1%–35% depending on the area of the state and the climate change scenario with a statewide average of 10%. Controlling for uncertainty in climate projection and allowing for uncertainty in yield projections, results show that projected climate change reduces Iowa corn yield by seven to twenty nine percent with an average of 9%.

4.1 Introduction

4.1.1 Related Literature

The 4th Intergovernmental Panel on Climate Change (IPCC) report indicates that the 100-year trend in temperature during 1906 to 2005 was 0.14°C higher than the trend from 1901 to 2000. Additionally, the 5th IPCC reports conclude that the global average near-surface temperatures have increased since the nineteenth century, and that the decades in the 2000s are the warmest on record. These studies also suggest there will be a warmer

environment in decades to come. Crop production critically depends on weather factors such as temperature, the amount of rainfall and drought. This paper uses an estimated corn yield model to predict how climate change will impact corn yields in Iowa.

Corn, as a major staple grain, accounts for 95.4% of the total feed grain production in the United States as of 2014. With the bio-fuel boom in last decade, more than half of the corn production has been used as feedstock to ethanol production and the usage of corn in ethanol production in 2014 is more than four times as in 2003.[5] Globally, the demand for animal protein has also increased dramatically at the same time due to rapid growth in developing countries. If future climate change causes damages to corn production, the resulting cost to society will be significant.

Schlenker and Robert (2009) predict that climate change will result in a decline of US crop yields (corn, soybean and cotton) by 30%–46% under the slowest climate warming scenario, and a reduction of crop yields by 63%–82% under the most rapid climate warming scenario before the end of the century. In Schlenker and Robert (2009), the critical temperature effect on crop yields is additive and substitutable over the whole growing season. They define the growing season of corn to be March to August.

In this paper, the weather variables included in the yield projection model consist of the number of days that the maximum temperature exceeds certain critical value in July, and a measurement of moisture content in the soil and amount of rainfall during June to August. We include temperature in July because it emerged as a critical month in our earlier work and it is a very important stage of corn development. According to the historical temperature

[5] See http://www.ers.usda.gov/topics/crops/corn/background.aspx Access on 2/1/2015

data, the daily average temperature was above normal in 27 out of 31 days in July of 2012. 2012 was the 3rd warmest July in the past 140 years.[6] The extremely hot and dry weather in 2012 caused the lowest state average corn yield in last 10 years.[7]

Schlenker and Robert's do not separate the temperature effect on corn yield according to the different growing stages. In their model the impact of a one day exposure to 100°F on corn yield in July has the same effect as in March.

4.1.2 Previous Work

According to the analysis on corn yield trend and the observed trend in temperature, Lobell and Asner (2003) conclude that each one-degree increment in temperature during corn growing period will cause corn yield decreases by roughly 17%. Deschênes and Greenstone (2007) obtain a similar conclusion that corn yield decreases with temperature and increase with rainfall. In addition, they find that climate change will bring a 4% (based on 2002) increment in the profit of agricultural sector.

Both Schlenker and Robert (2009) and Yu and Babcock (2011) find a steep non-linear decline in county-level corn yields at temperature above certain threshold. Schlenker and Roberts (2009) concludes the threshold is 84°F. Yu and Babcock (2011) use the county-level monthly mean temperature and rainfall from June to August as explanatory variables, and found corn yield in the state of Iowa decreases with temperatures below 72.9°F, and decreases for temperatures above 75.6°F. Note that Yu and Babcock critical temperature

---

[6] See http://www.iowaagriculture.gov/climatology/weatherSummaries/2012/pms201207.pdf

[7] See http://www.extension.iastate.edu/agdm/crops/pdf/a1-14.pdf

results are not comparable with ours because we use the number of days above a critical temperature for the growing season and not a monthly mean temperature.

Elmore and Taylor (2011) indicate that 93°F is the critical temperature for corn yield based on the agronomic reasons that link high temperatures to reduced yield. They state that high temperatures induce leaf rolling which slows down plant development and therefore reduces corn yields. In addition, four or more consecutive days with a maximum temperature exceeding 93°F reduces corn yield over and above the loss computed from leaf rolling.

The results in chapter 2 support Schlenker and Robert's (2009) finding of a non-linear temperature response with steep declines above a critical temperature, but the results show that this critical temperature is much higher than 84°F. In contrast to Schlenker and Roberts, their results show that this critical temperature changes across the state with higher critical temperatures occurring in the areas with the greatest reported suitability for corn production. This cross-sectional variability suggests that producers will in fact have the opportunity to adjust genetics and management to offset the impact of higher temperatures.

The climate projections for Iowa that we use here indicate that the 70-year linear trend in the July daily maximum temperature during 2030 to 2099 will be almost twice as high as the 70-year linear trend during 1960 to 2029. These models also indicate that the amount of rainfall in July and August will be relatively unchanged.

4.2 The Corn Yield Model

The dynamic linear model as stated in chapter 2 is applied to do yield forecast. The weather factors included in the model are the number of days that temperature exceeds certain critical value in July, average monthly total rainfall in corn growing periods (June–

August) and monthly average drought index from June to August. The model used the Palmer Drought Severity Index (PDSI), a long-term cumulative drought index. PDSI is negative under drought conditions and positive under wet conditions. The dynamic linear model is specified as follows.

$$\ln y_t = \theta_t + \psi_1 d_t^2 + \psi_2 n_t^2 + \psi_3 {z_{Jun}}_t^2 + \psi_4 {z_{Jun}}_t + \psi_5 {z_{Jul}}_t^2 + \psi_6 {z_{Jul}}_t + \psi_7 {z_{Aug}}_t^2 + \psi_8 {z_{Aug}}_t + \varepsilon_t \quad (4.1)$$

$$\theta_t = \theta_{t-1} + \beta_{t-1} + \nu_t \quad (4.2)$$

$$\beta_t = \beta_{t-1} + \omega_t \quad (4.3)$$

where t denotes time, y_t, d_t, and n_t denote corn yield, drought index, and the number of days that the maximum temperature exceeds a certain threshold, respectively. ${z_{Jun}}_t$, ${z_{Jul}}_t$, and ${z_{Aug}}_t$ represent the amount of total rainfall during the month of June to August, respectively. The state variables θ_t and β_t are introduced to capture the stochastic trend in corn yield. The stochastic part of yield and state variables are represented by the error terms ε_t, ν_t, and η_t. The error terms are assumed to be identically and independently normally distributed: $\varepsilon_t \sim N(0, \sigma_\varepsilon^2)$, $\nu_t \sim N(0, \sigma_\mu^2)$, and $\omega_t \sim N(0, \sigma_\omega^2)$. The parameters $(\psi_1, \ldots, \psi_8)$ are introduced to capture weather effects. Using a Bayesian-based Kalman filter, this dynamic linear model recursively updates the information of the two state variables. The state variables and parameters are estimated using a Gibbs sampling algorithm.

4.2.1 Data Collection

The model was estimated in the Crop Reporting District (CRD) level to avoid county level anomalies. The state of Iowa consists of nine CRDs, with each CRD including

approximately 11 counties. County-level corn yield data in the state of Iowa are collected from the National Agriculture Statistics Service (NASS) for the years 1950–2012.

County-level weather data including daily maximum temperature (TMAX) in July and total monthly precipitation (TPCP) from June to August was collected from the National Oceanic and Atmospheric Administration (NOAA). The number of days the maximum temperature exceeds each critical value is then calculated from the collected daily temperature data. All the counties in the state of Iowa are matched with at least one weather station. For the counties with multiple stations, we use the average weather data for all stations included in the county. Where data is missing of certain years for some counties, we use the weather data collected from their neighboring counties. The PDSI is available from NOAA at the CRD level.

4.2.2 Estimation Results

Schlenker and Robert (2009) suggest a critical temperature of 84°F for corn yield, and Elmore and Taylor (2011) indicate that critical temperature for corn yield is 93°F. The model was estimated using different critical temperatures ranging from 84°F to 95°F with 1°F increments—twelve critical values in total. Therefore, there are twelve models to be estimated. The Akaike information criterion (AIC) is applied to choose the best model for each CRD.

We apply the Bayesian Markov Chain Monte Carlo (MCMC) method described in section 2.3 of Chapter 2 to estimate parameters in each model. Figure 4.1 below provides the result of the critical temperature selected by the AIC measure. Tables 2.1 to 2.9 show the

estimation results of the parameters from the model with the critical temperature chosen by the AIC and data set of 1950–2012.[8]

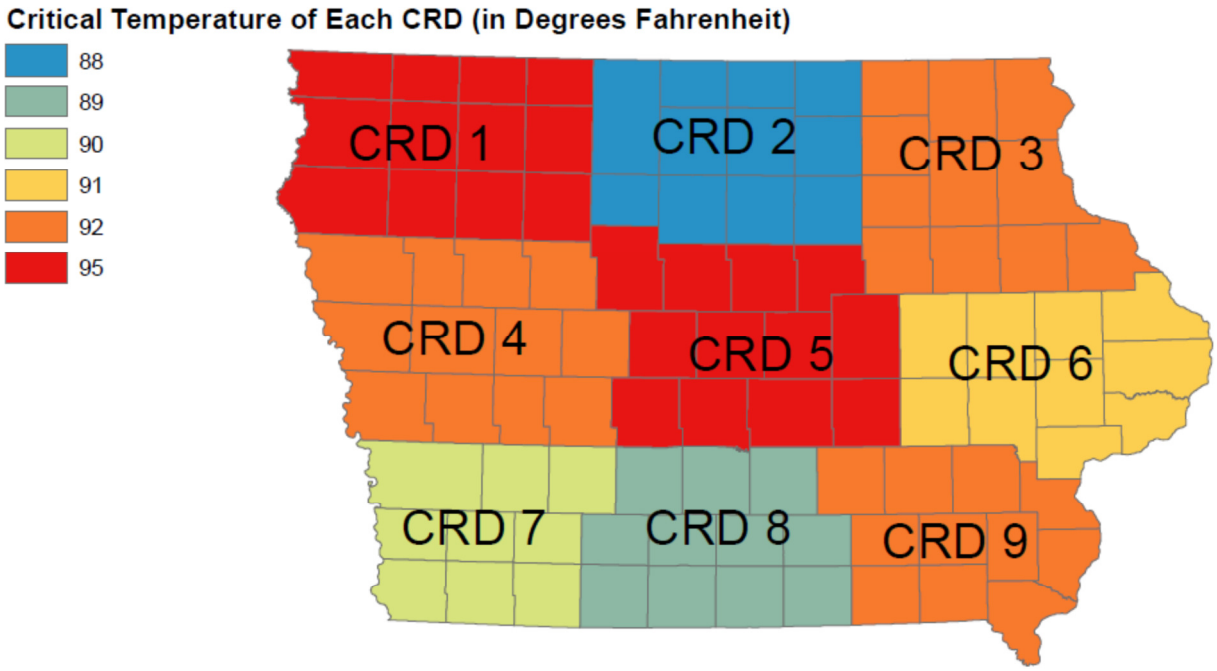

Figure 4.1: Critical temperature for each CRD selected by AIC

4.3 Analysis and Plots for Climate Projections

Climate projection for weather perils for crop yield is examined. Several uncertainties are inherent in projections of future climate, including the trajectory of radiative forcing (i.e., greenhouse gas emissions scenarios), the climate model structure, and the spatial resolution of the climate model. Thus, a single climate projection of future climate is inadequate for determining the expected response of a climate variable. We address climate projection

[8] Estimation results of other runs provided upon request.

variability from all sources by using projections from: (*a*) different greenhouse gas emissions scenarios; (*b*) different global climate models; and (*c*) empirical transfer functions that translate from the coarse global model grid (1.0–2.5 degree latitude-longitude grid) to a 12 km grid (Stoner et al. 2012). The ensemble consists of seven projections spanning three emissions scenarios and eight global climate models. The climate projection data applied in this paper includes 16 unique combinations of the three emissions scenarios and eight global climate models. We evaluate change in daily maximum temperature and April–August rainfall. The number of grid points in the climate projection for Iowa will be approximately 1,650. Each grid point is a time series for 1960 to 2099 of daily temperature and precipitation. We do not use this ensemble to evaluate PDSI, because key variables are absent in the data that would result in spurious increase in drought (Bruke et al. 2006).

The change of the ensemble average is the expected climate change under the assumption that individual model errors are independent (Lambert and Boer 2001; Meehl et al. 2007). Daily maximum temperature in July is used in the corn yield model. The ensemble mean of projected statewide daily maximum temperature in July is reported in Figure 4.2 (blue line). The statewide daily maximum temperature in July shows a significant increase trend. The 70-year linear trend for 2030–2099 is almost twice as the 70-year linear trend in 1960–2029. The 70-year linear trend from 2030 to 2099 is around 1.3 times the 140-year linear trend from 1960 to 2099. Figure 4.2 provides a credible band of the statewide daily maximum temperature as well. The credible band expends with time, which is consistent with Figure 4.3, where the standard deviation of ensemble daily maximum temperature shows a significant increase trend.

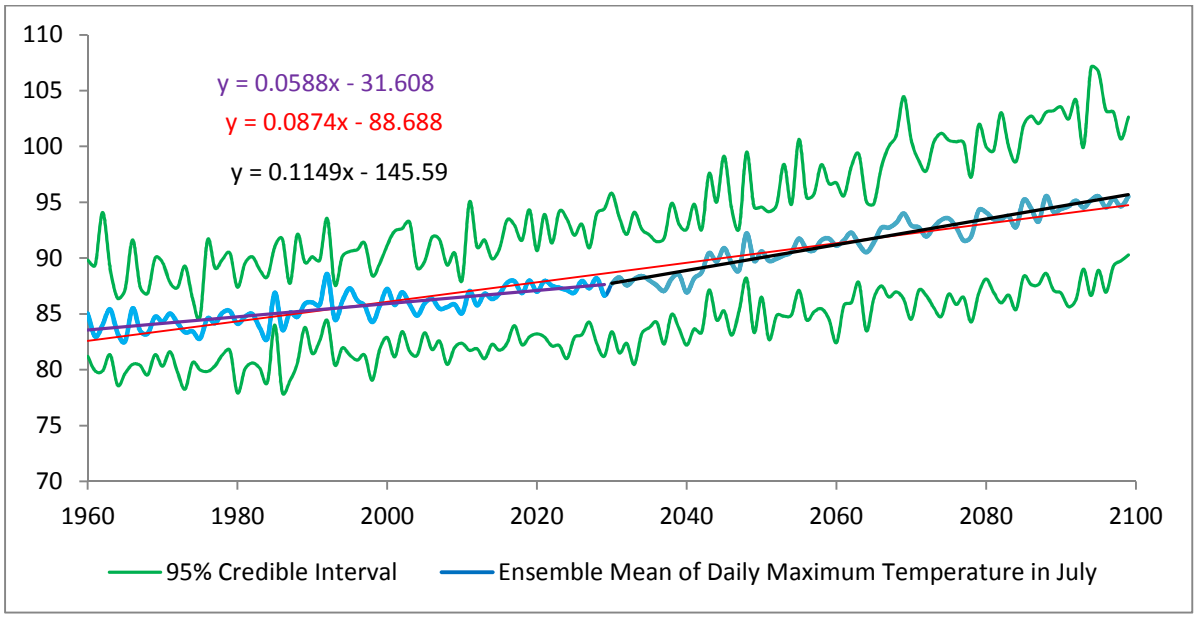

Figure 4.2: Statewide projected maximum temperature in July

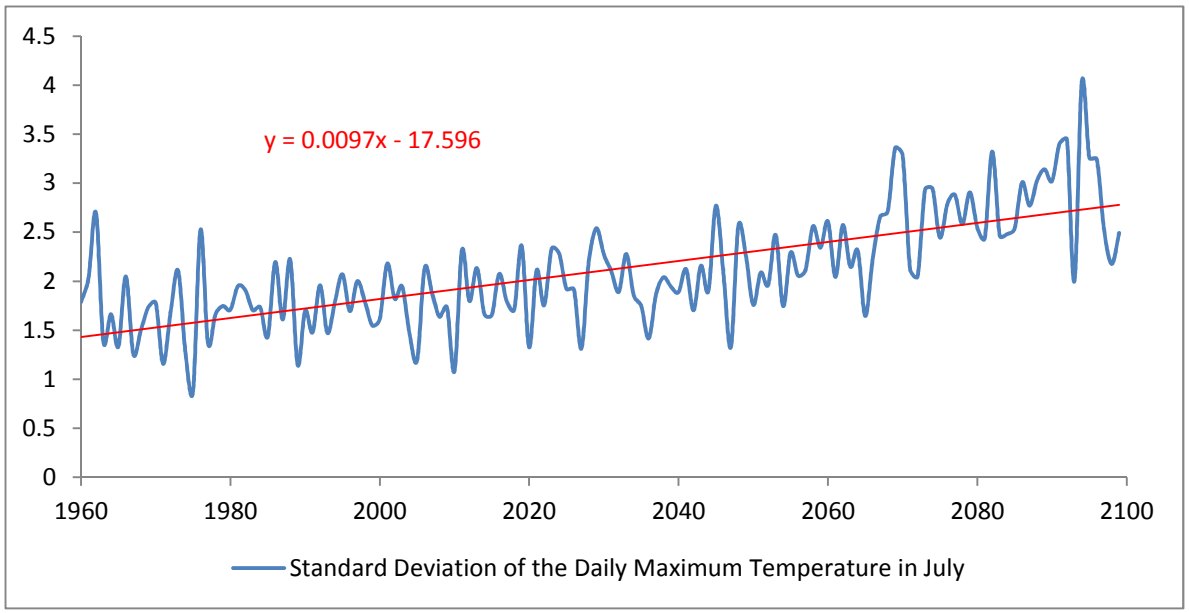

Figure 4.3: Standard deviation of ensemble daily maximum temperature in July

According to the AIC selection results, the average statewide critical daily maximum temperature in July is around 92°F. Therefore, the numbers of days that maximum temperature exceeds 92°F in July was calculated based on the projected temperature. The ensemble mean of the number of days that maximum temperature exceeds 92°F in Iowa during July is reported in Figure 4.4. The 70-year linear trend from 2030 to 2099 is nearly 2.5 times of the 70-year linear trend from 1960 to 2029. The 140-year linear trend from 1960 to 2099 is around 1.8 times the 70-year linear trend from 1960 to 2029. According to Figure 4, the credible band of the number of days that maximum temperature exceeds 92°F in July expands with time. Figure 4.5 indicates an obvious increase trend of the standard deviation of the number of days that maximum temperature exceeds 92°F, which also indicates that weather is more likely to fluctuate in the future.

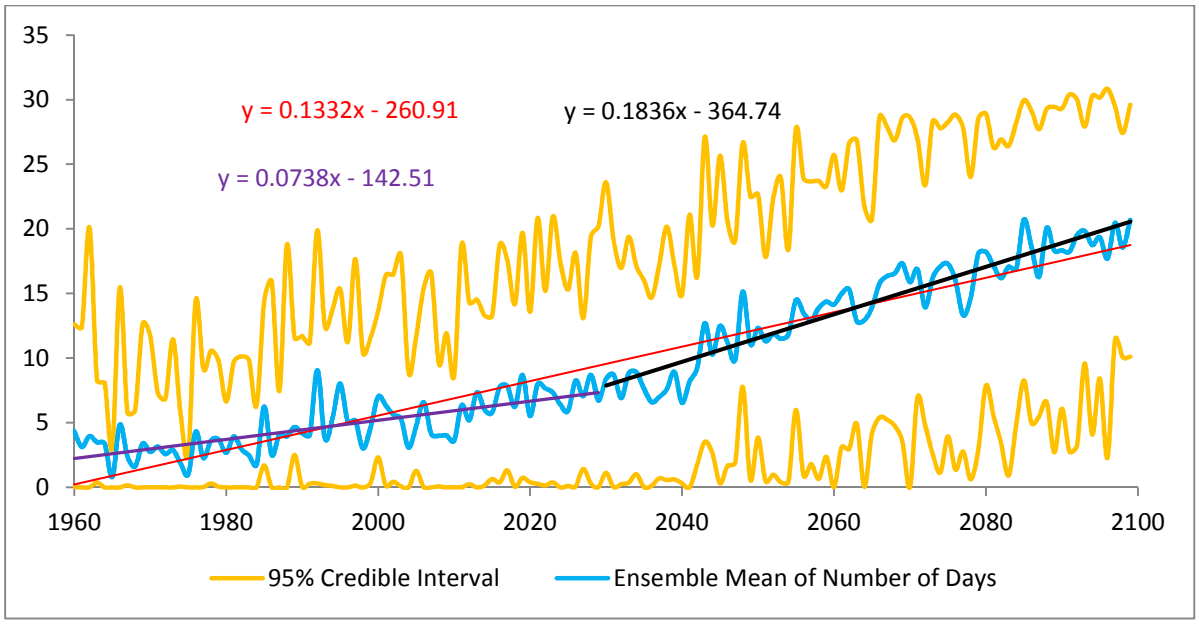

Figure 4.4: Statewide average of the number of days that maximum temperature exceeds 92°F in July

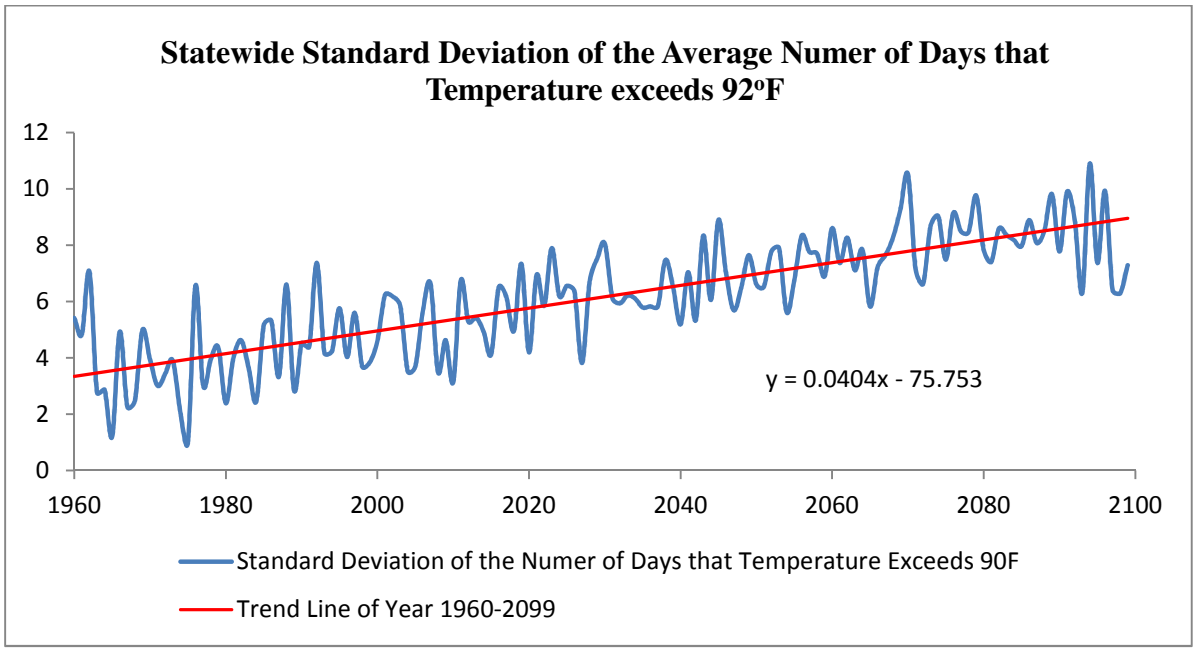

Figure 4.5: Statewide standard deviation of the number of days that temperature exceeds 92°F

Using a regional climate process model to downscale global climate model data, Diffenbaugh et al. (2012) finds an increment in growing degree days above 29°C as early as the mid-2020s. Our results are consistent but emphasize the most yield damaging days are likely to increase under climate warming.

Statewide rainfall is calculated annually for spring (May–June) and summer (July–August) for each climate projection. The ensemble average spring rainfall shows a clear increase in the number of years spring rainfall exceeds 11.8 inches during 2013–2100 (Figure 4.6). In fact, this threshold is not eclipsed during 1960–2000. The notable result for summer is that the no discernible increase is evident in the extremes. Together, the spring and summer results mean that damaging spring rainfall is expected to increase while damaging summer dry conditions are no less frequent.

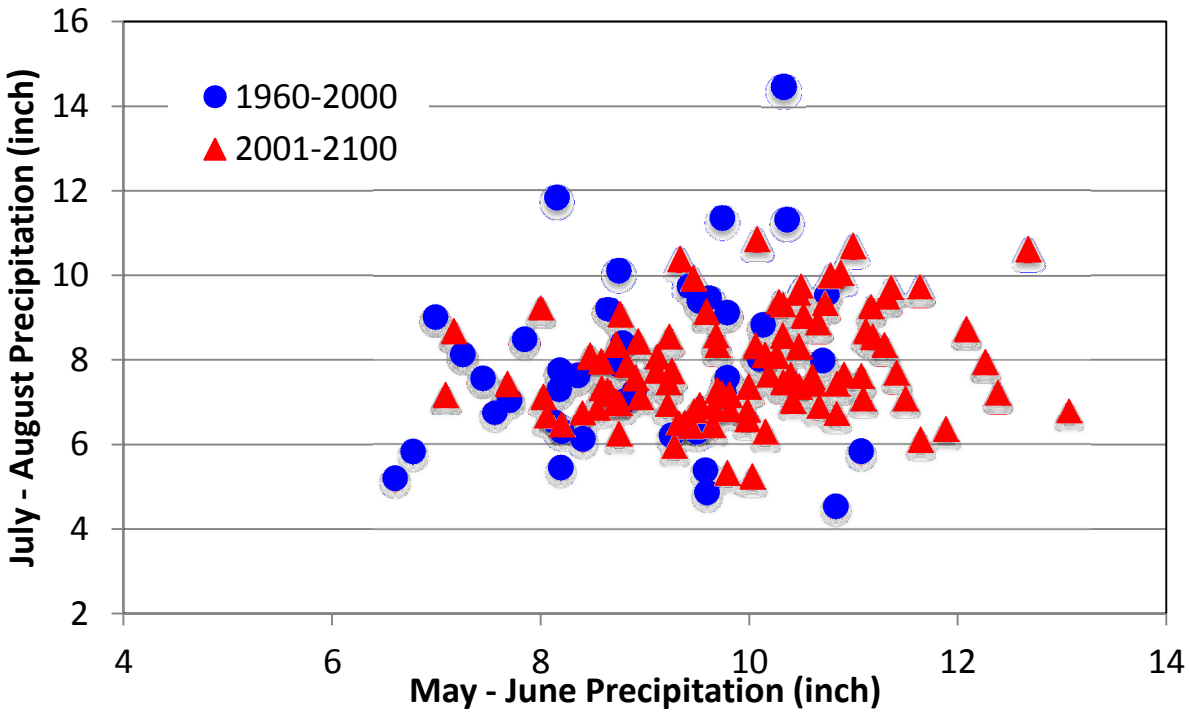

Figure 4.6: Climate projection ensemble average spring (May–June)

Statewide total amount of rainfall during the corn growing period (June–August) is reported in Figures 4.7–4.8. The ensemble average of rainfall does not show a clear trend. However, a clear increase trends are found in the standard deviation of rainfall in June-August. Unlike temperature, change in ensemble mean of rainfall is not obvious (Figure 4.7). The ensemble standard deviation is calculated to represent ensemble variability (Figure 4.8). Over time, the ensemble standard deviation increases. In fact, the 70-year linear trend of 2030–2099 is more than four times that of the 70-year linear trend of 1960–2029 for the standard deviation of July rainfall.

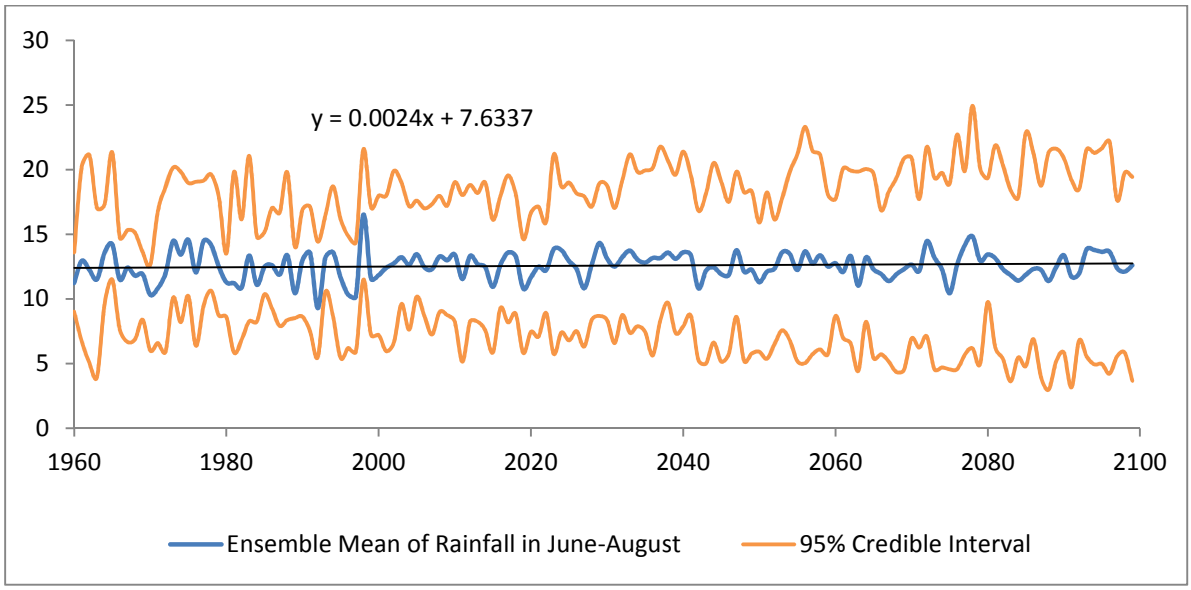

Figure 4.7: Statewide ensemble mean of rainfall in June–August

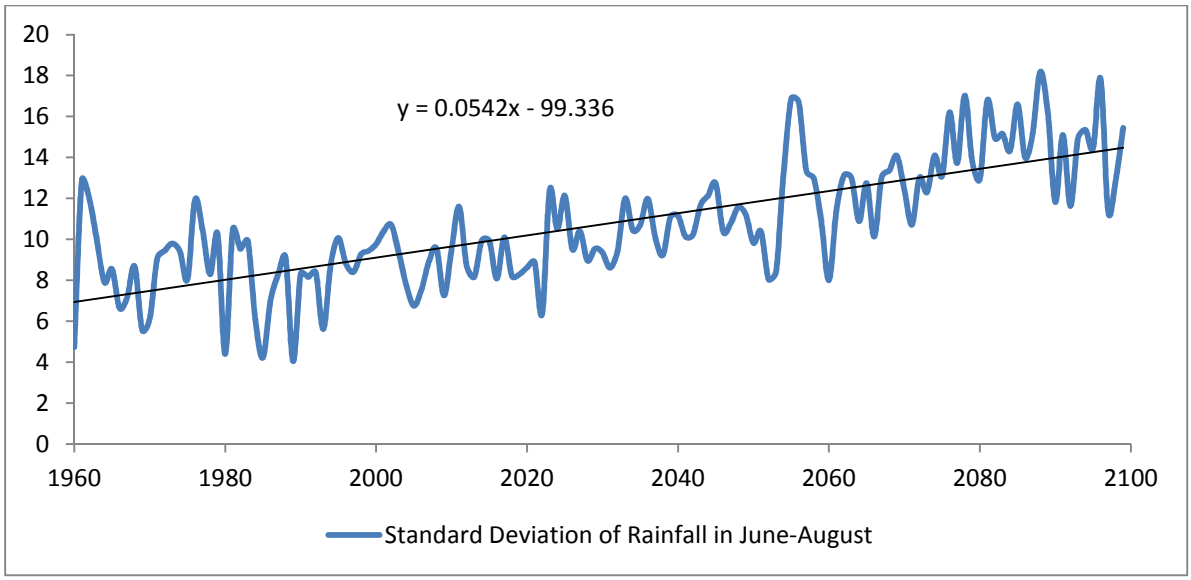

Figure 4.8: Standard deviation of rainfall in June-August

4.4 The Impact of Climate Change on Corn Yield

The yield model introduced in section 4.2 can be applied to do both short- and long-term corn yield projections. Combining the estimated results from yield model and the projection of rainfall and the number of the days that the maximum temperature exceeds the critical temperature in section 3, the impact of climate change can be projected.

Let d, z, and n be the drought index, rainfall, and the number of the days that the maximum temperature exceeds the critical temperature used in projecting corn yield, respectively. According to equations (4.1), (4.2), and (4.3) we have the following:

$$E(y_{T+1}|y_{1:T}) = E(\theta_{T+1}|y_{1:T}) + \psi_1 d^2 + \psi_2 n^2 + \psi_3 z_{Jun}^2 + \psi_4 z_{Jun} + \psi_5 z_{Jul}^2 + \psi_6 z_{Jul} + \psi_7 z_{Aug}^2 + \psi_8 z_{Aug} \quad (4.5)$$

$$E(\theta_{T+1}|y_{1:T}) = \theta_T + \beta_T \quad (4.6)$$

$$E(\beta_{T+1}|y_{1:T}) = \beta_T \ . \quad (4.7)$$

Using the mean of historical weather data in the last thirty years, corn yield as of 2015 can be projected. Since a significant change in the amount of rainfall during corn growing season is not found, the paper focuses on the impact of the projected temperature on corn yield. Using projected weather data in section 4.3 and the estimation result in section 4.2, we are able to predict the impact of climate change on corn yield for each CRD in the state of Iowa by the end of this century.

4.4.1 The Impact of Climate Change on Corn Yield According to the Uncertainty of Climate Projection

For each of the 16 combinations of the emission scenario and global climate model, we chose the last thirty years projected data (2070-2099) of the daily maximum temperature in

each July and mapped it into county level data. The bootstrap method was applied to generate 10,000 sample of the daily maximum temperature, and take it as the sample of the daily maximum temperature as of July, 2099. Based on the estimated critical temperatures in section 4.2, the number of days that the maximum temperature exceeds critical value was calculated for each county. The CRD level sample of the number of days that the maximum temperature exceeds critical value can be obtained by averaging the county level data within the CRD. Therefore, a total of 16 distributions of the number of days that the maximum temperature exceeds critical value can be generated for each CRD based on the projected climate data.

Applying the sample of the number of days that the maximum temperature exceeds critical value to equation (4.5), a sample of predicted corn yield can be generated, holding all others the same as in 2015 yield projection. Comparing to the projected 2015 corn yield, the impact of the projected climate change as of the projected 2015 corn yield can be calculated. We do this for each CRD and each generated distribution of the number of days that the maximum temperature exceeds critical value. The 95% confidence interval of the impact of climate change for each CRD is reported in Figure 4.9, and the circle indicates the mean.

Figure 4.9 shows variation across the 16 distributions with respect to the impact of the number of days that the maximum temperature exceeds the CRD specific critical value. Therefore, climate impact results presented here include climate model uncertainty as well as yield model uncertainty.

Schlenker and Roberts (2009) show a steep non-linear decline in county-level corn yields at temperatures above 84°F. They also point out that the projected climate change will

result in a reduction of US corn yields of 30–46% under one climate model and 63–82% under a second climate model. This shows that they also have climate model uncertainty.

As can be seen in Figure 4.9, the impact of climate change on corn yield is as high as 35% in CRD 3 and 9. This is in the lower range provided by Schlenker and Roberts (2009). In the other seven CRDs, our results indicate that the projected climate change causes a reduction of corn yield by 0–25%. Averaging across the nine CRDs, climate change causes a decline of corn yield by 10%. In general, the estimated impact of climate change on corn yield is much lower than the results from Schlenker and Roberts (2009). Next we present several alternative versions of our model in an attempt to understand why our results differ so much from Schlenker and Roberts.

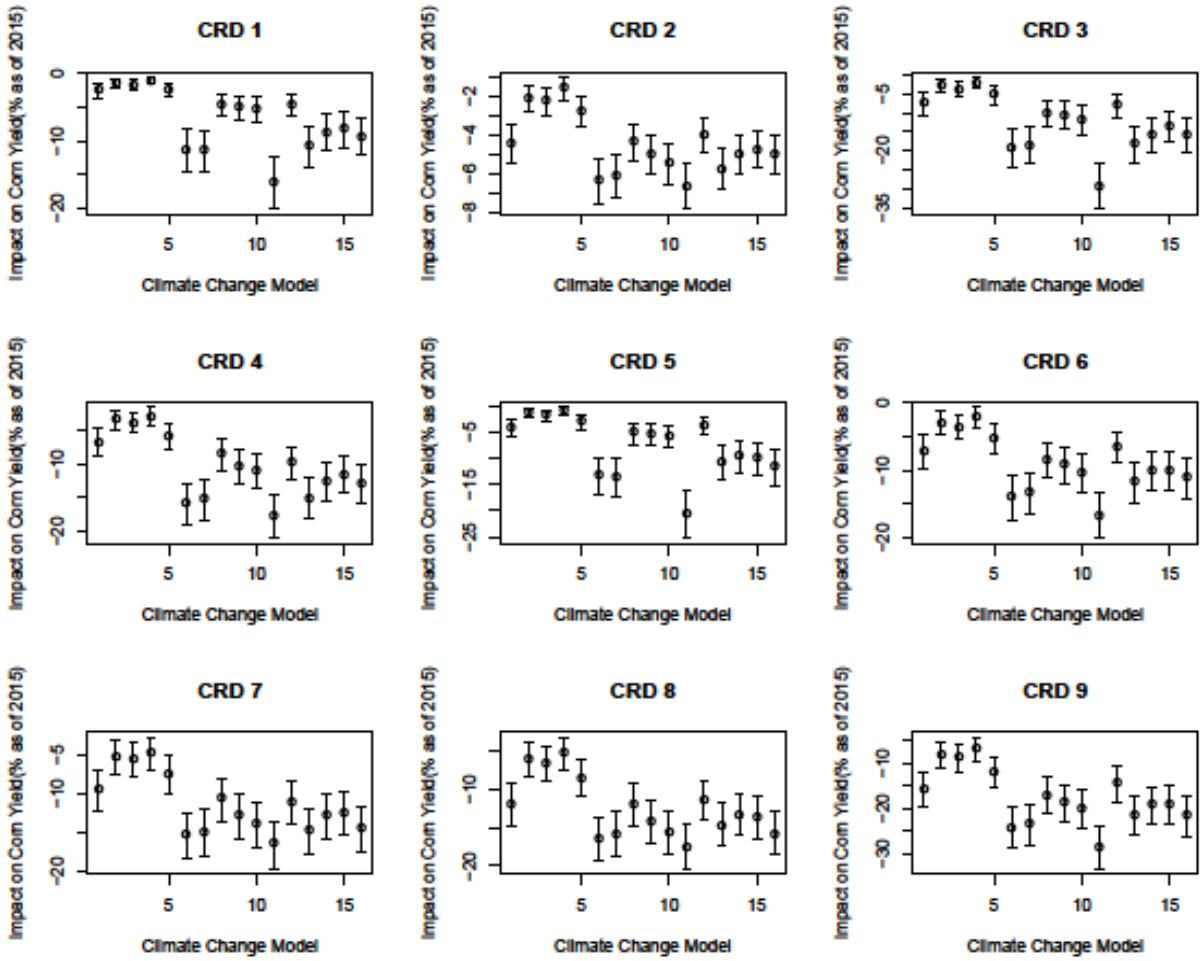

Figure 4.9: The impact of projected climate change on corn yield under the uncertainty of climate projection

Alternative 1: Holding the Critical Temperature At 84°F

Figure 4.10 shows the climate change results using the same critical temperature of 84°F for all CRDs as in Schlenker and Roberts (2009). These results show much smaller climate change results as those obtained when a CRD specific critical temperature is used in the yield model. The logic here is that temperatures above 84°F do not cause a large impact on yields in Iowa. Therefore the coefficient on the critical temperature term is very small.

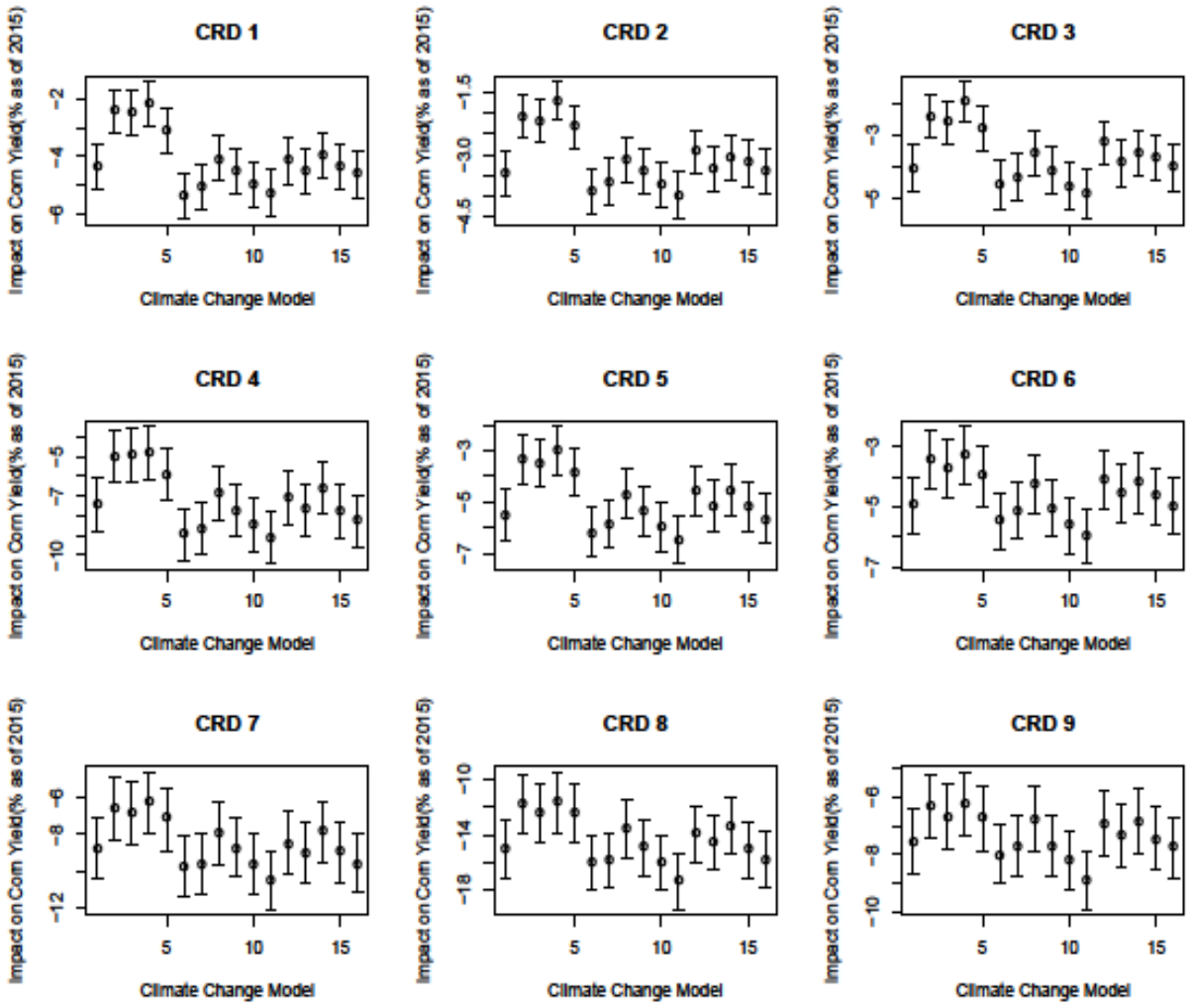

Figure 4.10: The impact of projected climate change on corn yield with a critical temperature of 84°F

Alternative 2: Using the Level of Yields instead of the Log of Yields

Figure 4.11 provides climate change results when we use level of yield instead of log yield in the corn yield model. Comparing to Figure 9, climate change has a much smaller impact on corn yield using level of yield. The average impact of climate change on corn yield is around 5%, which is half of its impact using the log of yield.

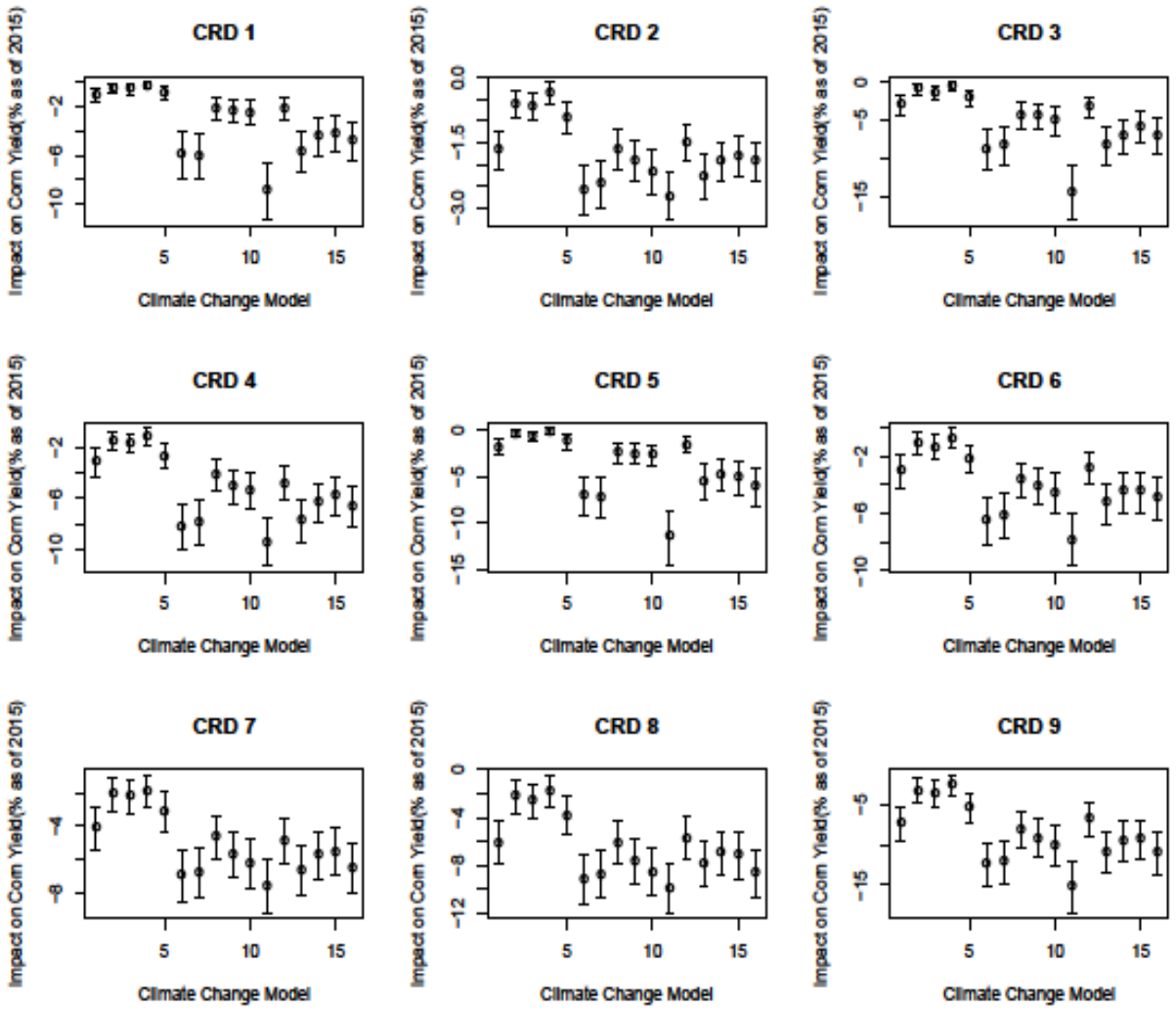

Figure 4.11: The impact of projected climate change on corn yield using level of yield

Alternative 3: A Quadratic Time Trend with Constant Yield Growth

Figure 4.12, presents the climate change results from a yield model that includes a quadratic form of time trend, holding the functional form of weather variables the same. This model drops the stochastic yield growth term. We include this scenario because Schlenker and Roberts include a quadratic time term and estimate and assume constant yield growth.

Again, the projected impact of climate change is smaller than the results from Schlenker and Roberts (2009). Only in CRD 3, does the 95% confidence interval of climate change effect have an overlap with Schlenker and Roberts (2009).

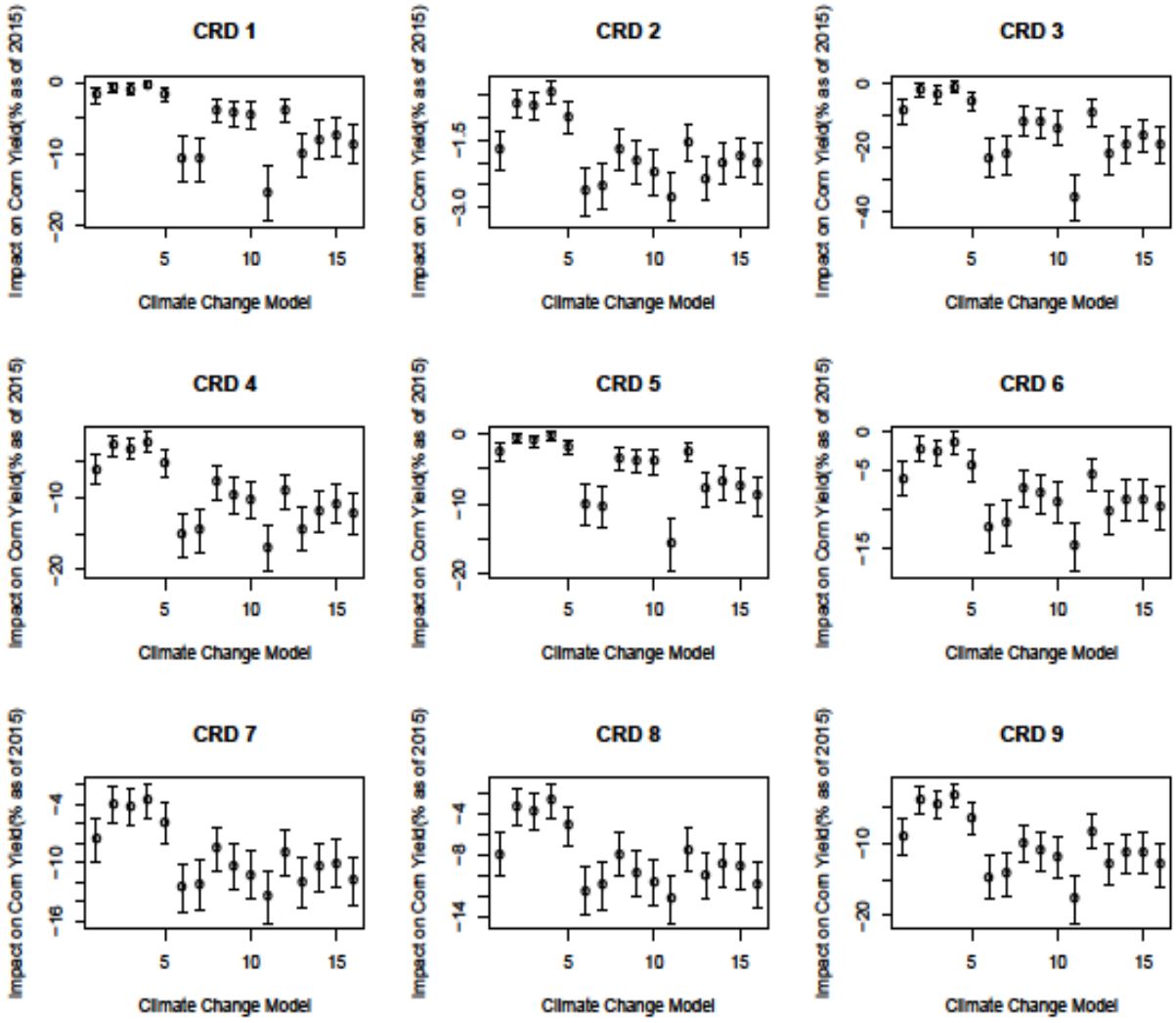

Figure 4.12: The impact of projected climate change on corn yield using quadratic of time trend

Alternative 4: Excluding the Drought Term

Our yield model includes a quadratic term reflecting long-term drought, which is not included in Schlenker and Roberts. We dropped the term of drought, and run the yield model for CRD 1, 4 and 9. The coefficient of the number of days that the maximum temperature exceeds critical value turns out to remain unchanged. The estimated impact of climate change (Figure 4.13) is slightly larger for CRD 1 and 9 than for the base model shown in Figure 4.9.

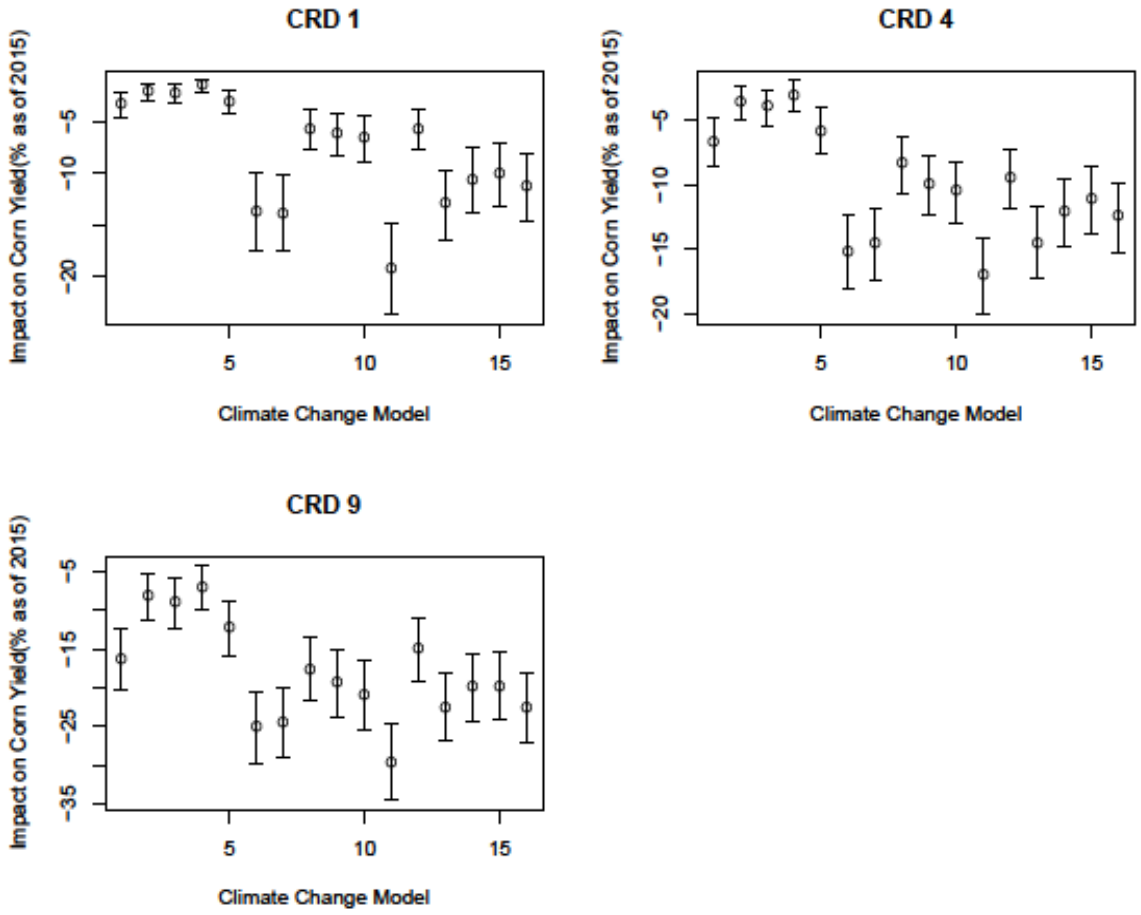

Figure 4.13: The impact of projected climate change on corn yield excluding the measurement of drought

Alternative 5: Using a Season Long Critical Temperature

Another reason that may cause the difference is that we use the temperature in July and capture the impact of extremely high temperature, while Schlenker and Roberts (2009) use the temperature during March to August. We removed the terms of drought and the stochastic yield growth, and included the seasonal long critical temperature (June–August), holding the functional form of weather variables the same. These results are shown in Figure 4.14. The estimated impact of climate change is slightly larger for CRD 1 and 4 than for the base model shown in Figure 4.9.

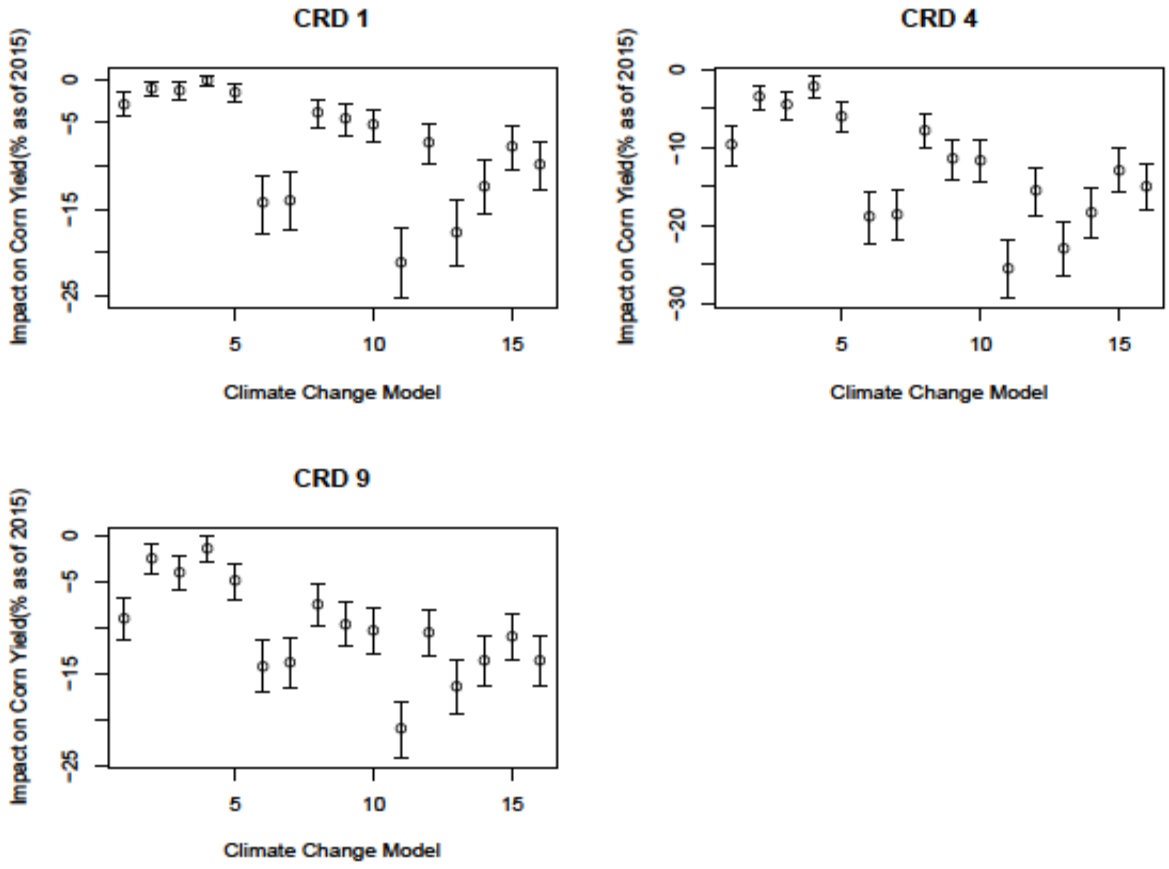

Figure 4.14: The impact of projected climate change on corn yield using corn growing season temperature

We are puzzled as to why our climate change impacts are so much greater than in Schlenker and Roberts. Their model is based on parameters estimated for the entire country and it is possible that parts of the US outside the Corn Belt will see a larger climate impact on corn yields.

4.4.2 The Impact of Climate Change on Corn Yield According to the Uncertainty of Yield Projection Model

Instead of introducing the uncertainty of climate projection, we introduce the uncertainty of yield projection to predict the impact of climate change on corn yield. Keeping the number of days that maximum temperature exceeds critical value at the mean of the generated samples, a sample of corn yield can be generated according to the Bayesian MCMC chains of the parameters estimated in yield model[9], holding all others the same as in 2015 yield projection. The 95% confidence interval of the impact of climate change for each CRD is reported in Figure 4.15, and the circle indicates the mean. The predicted impact of climate change on corn yield is around -7%–29% when we remove the uncertainty of climate projection. Averaging across the state of Iowa, climate change is predicted to result in a reduction of corn yield by 9%, which is very close to the result with uncertainty of climate projection.

[9] Refer to Appendix A for the detailed information about the Bayesian MCMC chains.

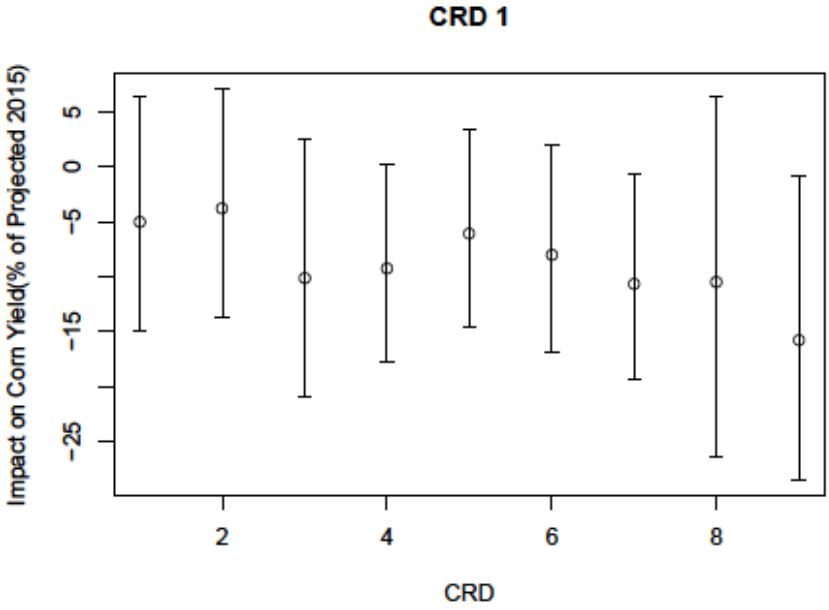

Figure 4.15: The impact of projected climate change on corn yield under the uncertainty of yield projection

4.5 Conclusion

Climate models predict a significant increase in the daily maximum temperatures in July, which is a critical month for growth in corn plants. Controlling for the uncertainty of yield projection, our results show that the projected climate change causes a reduction of corn yield by as much as 35% in Crop Reporting District 3 and 9. The statewide average impact is 10%. Controlling for the uncertainty of climate projection and introducing the uncertainty of yield projection, our results show that the projected climate change reduces Iowa corn yield by as much as 29%, with a statewide average of 9%. These results are much lower than in Schlenker and Roberts (2009). We tried several alternative versions of our model to determine if we could find a model that provided results closer to Schlenker and Roberts and we were unable to do so. These alternative models accounted for as many of the differences

between our model and Schlenker and Roberts as was possible for us to implement. It is difficult to explain why our climate change results are so much smaller than theirs. On a more positive note our results suggest that the impact of climate change on corn yields in Iowa will likely not be catastrophic.

REFERENCES

Allen, M.T., C.K. Ma, and R.D. Pace. 1994. "Over-Reations in US Agricultural Commodity Prices." *Journal of Agricultural Economics* 45:240–251.

Campagnoli, P., S. Petrone, G. Petris, G. Petris, S. Petrone, and P. Campagnoli. 2009. "Dynamic Linear Models." In *Dynamic Linear Models with R*. pp. 31–84. New York: Springer.

Carter, C.K., and R. Kohn. 1994. "On Gibbs Sampling for State Space Models." *Biometrika* 81: 541–553.

Deschênes, O., and M. Greenstone. 2007. "The Economic Impacts of Climate Change: Evidence from Agricultural Output and Random Fluctuations in Weather." *The American Economic Review* 97: 354–385.

Diffenbaugh, N.S., T.W. Hertel, M. Scherer, and M. Verma. 2012. "Response of Corn Markets to Climate Volatility under Alternative Energy Futures." *Nature Climate Change* 2(7): 514–518.

Elmore, R. and E.Taylor. 2011. "Corn and 'A Big Long Heat Wave on the Way'." Iowa Integrated Crop Management Newsletter Iowa State University.

Foote, R.J., and L.H. Bean. 1951. "Are Yearly Variations in Crop Yields Really Random?" *Journal of Agricultural Economic Resources* 3: 23–30.

Frühwirth-Schnatter, S. 1994. "Data Augmentation and Dynamic Linear Models." *Journal of Time Series Analysis* 15: 183.

Gallagher, P. 1987. "U.S. Soybean Yields: Estimation and Forecasting with Nonsymmetric Disturbances." *American Journal of Agricultural Economics* 69: 796–803.

Goodwin, B.K., and A.P. Ker. 1998. "Nonparametric Estimation of Crop Yield Distributions: Implications for Rating Group-Risk Crop Insurance Contracts." *American Journal of Agricultural Economics* 80: 139–153.

Harri, Ardian K.H.C., Cumhur Erdem, and T.O. Knight. 2009. "Crop Yield Distributions: A Reconciliation of Previous Research and Statistical Tests for Normality." *Review of Agricultural Economics* 31(1): 163–182.

Iman, R.L., and W.J. Conover. 1982. "A Distribution-free Approach to Inducing Rank Correlation Among Input Variables." *Communications in Statistics - Simulation and Computation* 11:311–334.

Jin, N. 2011. "Three essays on commodity futures and options markets." Seasonality; 2012-04-27; 3494162; 920123196; 66569; n/a; Social sciences; Mean reversion; English; Commodity futures; 9781267154354; 64556771; 0505: Economics; Options markets; Jin, Na; Copyright ProQuest, UMI Dissertations Publishing 2011; Options pricing models; 2011; 2580039101; M1: Ph.D.; M3: 3494162.

Jin, N., S. Lence, C. Hart, and D. Hayes. 2012. "The Long-Term Structure of Commodity Futures." *American Journal of Agricultural Economics*, pp. .

Jong, P.D., and N. Shephard. 1995. "The Simulation Smoother for Time Series Models." *Biometrika* 82: 339–350.

Just, R.E., and Q. Weninger. 1999. "Are Crop Yields Normally Distributed? " *American Journal of Agricultural Economics* 81: 287–304.

Kaylen, M.S., and S.S. Koroma. 1991. "Trend, Weather Variables, and the Distribution of U.S. Corn Yields." *Review of Agricultural Economics, Oxford University Press on behalf of Agricultural & Applied Economics Association* 1991 13: 249–258.

Kaldor, N. 1939. "Speculation and Economic Stability." *The Review of Economic Studies* 7:pp. 1–27.

Ker, A.P., and K. Coble. 2003. "Modeling Conditional Yield Densities." *American Journal of Agricultural Economics* 85:pp. 291–304.

Lambert, S.J., and G.J. Boer 2001. "CMIP1 Evaluation and Inter-comparison of Coupled Climate Models." *Climate Dynamics* 17: 83–106.

Lobell, D.B., and G.P. Asner. 2003. "Climate and Management Contributions to Recent Trends in U.S. Agricultural Yields." *Science* 299: 1032.

Marra, M.C., N.E. Piggott, and B.K. Goodwin. 2012. "The Impact of Corn Rootworm Protected Biotechnology Traits in the United States." *AgBioForum* 15(2): 217–230.

Mallory, M.L., S.H. Irwin, and D.J. Hayes. 2012. "How Market Efficiency and the Theory of Storage Link Corn and Ethanol Markets." *Energy Economics* 34: 2157–2166.

Meehl, G.A., T.F. Stocker, W.D. Collins, P. Friedlingstein, A.T. Gaye, J.M. Gregory, A. Kitoh, R. Knutti, J.M. Murphy, A. Noda, S.C.B. Raper, I.G. Watterson, A.J. Weaver and Z.-C. Zhao. 2007. "Global Climate Projections." In *Climate Change 2007: The*

Physical Science Basis, edited by S. Solomon, D. Qin, M. Manning, Z. Chen, M. Marquis, K.B. Averyt, M. Tignor and H.L. Miller. New York: Cambridge University Press.

Menz, K.M., and P. Pardey. 1983. "Technology and U.S. Corn Yields: Plateaus and Price Responsiveness." *American Journal of Agricultural Economics, Oxford University Press on behalf of the Agricultural & Applied Economics Association* 1983 65: 558–562.

Moss, C.B., and J.S. Shonkwiler. 1993. "Estimating Yield Distributions with a Stochastic Trend and Nonnormal Errors." *American Journal of Agricultural Economics* 75: 1056–1062.

NRC. 2010. "Advancing the Science of Climate Change." National Research Council. The National Academies Press, Washington, DC, USA.

Nelson, C.H. 1990. "The Influence of Distributional Assumptions on the Calculation of Crop Insurance Premia." *North Central Journal of Agricultural Economics* 12: 71–78.

Nelson, C.H., and P.V. Preckel. 1989. "The Conditional Beta Distribution as a Stochastic Production Function." *American Journal of Agricultural Economics* 71: 370–378.

NRC. 2010. "Advancing the Science of Climate Change." National Research Council. The National Academies Press, Washington, DC, USA.

Peterson, R.L., C.K. Ma, and R.J. Ritchey. 1992. "Dependence in commodity prices." *Journal of Futures Markets* 12:429–446.

Schlenker, W., and M.J. Roberts. 2009. "Nonlinear Temperature Effects Indicate Severe Damages to U.S. Crop Yields under Climate Change." *Proceedings of the National Academy of Sciences* 106: 15594–15598.

Schwartz, E.S. 1997. "The Stochastic Behavior of Commodity Prices: Implications for Valuation and Hedging." *The Journal of Finance* 52:pp. 923–973.

Sørensen, C. 2002. "Modeling Seasonality in Agricultural Commodity Futures." *Journal of Futures Markets* 22:393–426.

Stoner, A.M.K., K. Hayhoe, X. Yang, and D.J. Wuebbles. 2012. "An Asynchronous Regional Regression Model for Statistical Downscaling of Daily Climate Variables." *International Journal of Climatology* 33(11): 2473–2494 doi: 10.1002/joc.3603

Tannura, M.A., S.H. Irwin, and D.L. Good. 2008. "Weather, Technology, and Corn and Soybean Yields in the U.S. Corn Belt." Marketing and Outlook Research Report 2008–01. Department of Agricultural and Consumer Economics, University of Illinois at

Urbana-Champaign, February 2008.

World Bank. 2013. "Turn Down the Heat: Climate Extremes, Regional Impacts, and the Case for Resilience." A report for the World Bank by the Potsdam Institute for Climate Impact Research and Climate Analytics. Washington, D.C.

Yu, T., and B.A. Babcock. 2011. "Estimating Non-linear Weather Impacts on Corn Yield—A Bayesian Approach." *www.card.iastate.edu* 11: 522.